UNIVERSITY OF CRETE

DEPARTMENT OF CHEMISTRY

POSTGRADUATE PROGRAMME ENVIRONMENTAL SCIENCES AND ENGINEERING

LABORATORY OF CLINICAL MICROBIOLOGY AND MICROBIAL PATHOGENESIS – MEDICAL SCHOOL, UNIVERSITY OF CRETE

MASTER THESIS

WASTEWATER AS A PROGNOSTIC TOOL OF THE SPREADING OF SARS-COV-2 WITHIN THE COMMUNITY – PHYSICOCHEMICAL DATA AS PARAMETERS OF CORRECT RECORDING

ARETI KOKKINOMAGOULA

Head Professor: Anna Psaroulaki

Supervising Professor: Maria Kanakidou

HERAKLION 2024

ΠΑΝΕΠΙΣΤΗΜΙΟ ΚΡΗΤΗΣ

ΤΜΗΜΑ ΧΗΜΕΙΑΣ
ΠΡΟΓΡΑΜΜΑ ΜΕΤΑΠΤΥΧΙΑΚΩΝ ΣΠΟΥΔΩΝ ΕΠΙΣΤΗΜΕΣ ΚΑΙ ΜΗΧΑΝΙΚΗ ΠΕΡΙΒΑΛΛΟΝΤΟΣ

ΕΡΓΑΣΤΗΡΙΟ ΚΛΙΝΙΚΗΣ ΜΙΚΡΟΒΙΟΛΟΓΙΑΣ ΚΑΙ ΜΙΚΡΟΒΙΑΚΗΣ ΠΑΘΟΓΕΝΕΣΗΣ – ΙΑΤΡΙΚΗ ΣΧΟΛΗ ΠΑΝΕΠΙΣΤΗΜΙΟΥ ΚΡΗΤΗΣ

ΜΕΤΑΠΤΥΧΙΑΚΟ ΔΙΠΛΩΜΑ ΕΙΔΙΚΕΥΣΗΣ

ΤΑ ΛΥΜΑΤΑ ΩΣ ΕΡΓΑΛΕΙΟ ΠΡΟΓΝΩΣΗΣ ΤΗΣ ΕΞΑΠΛΩΣΗΣ ΤΟΥ SARS-COV-2 ΣΤΗΝ ΚΟΙΝΟΤΗΤΑ – ΦΥΣΙΚΟΧΗΜΙΚΑ ΔΕΔΟΜΕΝΑ ΩΣ ΠΑΡΑΜΕΤΡΟΙ ΟΡΘΗΣ ΑΠΟΤΥΠΩΣΗΣ

ΑΡΕΤΗ ΚΟΚΚΙΝΟΜΑΓΟΥΛΑ

Υπεύθυνη Καθηγήτρια: Άννα Ψαρουλάκη

Επιβλέπουσα Καθηγήτρια: Μαρία Κανακίδου

ΗΡΑΚΛΕΙΟ 2024

Εξεταστική Επιτροπή (αλφαβητικά)

Μαρία Κανακίδου

Καθηγήτρια Υπολογιστικής Χημείας Περιβάλλοντος. Τμήμα Χημείας, ΠΚ

Ευάγγελος Σακκαλής

Διευθυντής Ερευνών, Ινστιτούτο Πληροφορικής – ΙΤΕ

Άννα Ψαρουλάκη

Αναπληρώτρια Καθηγήτρια Μικροβιολογίας, Τμήμα Ιατρικής, ΠΚ (Υπεύθυνη)

ΕΥΧΑΡΙΣΤΙΕΣ

Έχοντας πλέον ολοκληρώσει την μεταπτυχιακή μου εργασία, θα ήθελα να ευχαριστήσω από καρδιάς την υπεύθυνη Καθηγήτριά μου, κ. Άννα Ψαρουλάκη, για την ευκαιρία που μου έδωσε να εργαστώ στο Εργαστήριο Κλινικής Μικροβιολογίας και Μικροβιακής Παθογένεσης στην Ιατρική Σχολή του Πανεπιστημίου Κρήτης, καθώς και για την καθοδήγηση και υποστήριξη που μου παρείχε καθ' όλη τη διάρκεια των μεταπτυχιακών μου σπουδών. Ευχαριστώ επίσης θερμά την υπεύθυνη Καθηγήτριά μου από το Τμήμα Χημείας, κ. Μαρία Κανακίδου, για τη διαθεσιμότητα και τη βοήθεια που μου παρείχε καθ' όλη τη διάρκεια των σπουδών μου. Ακόμα, θα ήθελα να ευχαριστήσω τον κ. Ευάγγελο Σακκαλή, Διευθυντή Ερευνών στο Ινστιτούτο Πληροφορικής του ΙΤΕ και την ομάδα του, για την άψογη συνεργασία στο κομμάτι της υπολογιστικής επεξεργασίας δεδομένων της παρούσας έρευνας, καθώς και για την προθυμία του να είναι μέλος της εξεταστικής μου επιτροπής και να αξιολογήσει τη μεταπτυχιακή μου εργασία.

Ένα μεγάλο ευχαριστώ από καρδιάς οφείλω επίσης στον Δρ. Δημοσθένη Χοχλάκη, Ερευνητή στο Εργαστήριο Κλινικής Μικροβιολογίας, για την καθοδήγηση και την αμέριστη υποστήριξή του όλα αυτά τα χρόνια.

Επίσης, ευχαριστώ την κ. Αναστασία Κουτσολιούτσου προϊσταμένη του γραφείου Περιβαλλοντικής Υγείας στον Εθνικό Οργανισμό Δημόσιας Υγείας, και συντονίστρια του Εθνικού Δικτύου Επιτήρησης του SARS-CoV-2 στα λύματα.

Ευχαριστώ πολύ την κ. Μαρία Μαλλιαρού, βιοπληροφορικό στο Εργαστήριο Κλινικής Μικροβιολογίας και Μικροβιακής Παθογένεσης, για τη βοήθεια της στην επεξεργασία και αποτύπωση των αποτελεσμάτων.

Θέλω επίσης να ευχαριστήσω πολύ τον κ. Γιώργο Τζεδάκη, συνεργάτη του κ. Ευάγγελου Σακκαλή στο Ινστιτούτο Υπολογιστικών Επιστημών του ΙΤΕ, για τη στατιστική ανάλυση των αποτελεσμάτων και την άψογη συνεργασία.

Επιπλέον, ευχαριστώ τον κ. Βαγγέλη Δολαψάκη και την κ. Κρυσταλλία Σηφακάκη από τη Δημοτική Επιχείρηση Ύδρευσης και Αποχέτευσης (ΔΕΥΑ) Ηρακλείου, καθώς και τις κυρίες Κοτσιφάκη και Καλησπέρη από τη ΔΕΥΑ Χανίων για τη συλλογή και αποστολή των δειγμάτων και των συνοδευτικών εγγράφων και κυρίως για την άψογη συνεργασία τους.

Ευχαριστώ επίσης όλους τους εργαζόμενους των Κινητών Μονάδων Υγείας για την παραλαβή των δειγμάτων και τη μεταφορά τους στο χώρο του Εργαστηρίου Κλινικής Μικροβιολογίας.

Ένα πολύ μεγάλο ευχαριστώ σε όλα τα μέλη του Εργαστηρίου Κλινικής Μικροβιολογίας για το όμορφο κλίμα, τις φιλικές σχέσεις που έχουμε αναπτύξει και την πολύπλευρη υποστήριξή τους.

Τέλος, θέλω να ευχαριστήσω από καρδιάς τους γονείς μου, που είναι πάντα δίπλα μου, και τις πιο κοντινές μου φίλες, που είναι στο πλευρό μου στο πέρασμα του χρόνου και με στηρίζουν σε κάθε μου βήμα.

ΧΡΗΜΑΤΟΔΟΤΗΣΗ

Η παρούσα εργασία χρησιμοποίησε δεδομένα τα οποία αποκτήθηκαν μέσω του Εθνικού Δικτύου Επιτήρησης του SARS-CoV-2 στα λύματα το οποίο χρηματοδοτείται από τον ΕΟΔΥ. Για την χρήση των δεδομένων αυτών, χορηγήθηκε η σχετική άδεια από τον ΕΟΔΥ.

ΒΙΟΓΡΑΦΙΚΟ ΣΗΜΕΙΩΜΑ

Αρετή Κοκκινομαγουλά

Προσωπικές πληροφορίες

Ηλεκτρονική διεύθυνση: kokareti@gmail.com, chemp1109@edu.chemistry.uoc.gr

Ημερομηνία γέννησης: 12/09/1997

Εθνικότητα: Ελληνική

Εκπαίδευση

Μεταπτυχιακό Δίπλωμα Ειδίκευσης – Επιστήμες και Μηχανική Περιβάλλοντος

[03/2021 – Τρέχουσα]

Πανεπιστήμιο Κρήτης - Τμήμα Χημείας

Πτυχίο Χημείας

[2014 - 2020]

Πανεπιστήμιο Κρήτης - Τμήμα Χημείας

Τίτλος διατριβής: Προσδιορισμός επιπέδων Parabens και Triclosan (ενδοκρινικοί οργανικοί ρύποι) σε δείγματα λυμάτων στην περιοχή Ηρακλείου - *Εργαστήριο Τοξικολογίας και Ιατροδικαστικής Χημείας - Ιατρική Σχολή Πανεπιστημίου Κρήτης*.

Πτυχίο πιάνου

[2004 – 2019]

Ωδείο Χρωμάτων – Ηράκλειο Κρήτης

Εκπαιδευτικά Προγράμματα και Επιμόρφωση

Βραχυπρόθεσμη Επιστημονική Αποστολή (STSM) - Ευρωπαϊκή Συνεργασία στην Επιστήμη και την Τεχνολογία (COST)

[13/03/23 – 17/03/23]

Πανεπιστήμιο της La Laguna – Τμήμα Χημείας – Εργαστήριο Εφαρμοσμένης Αναλυτικής Χημείας, Τενερίφη, Κανάρια Νησιά, Ισπανία

Τίτλος αποστολής: Απομόνωση και χαρακτηρισμός μικροπλαστικών από δείγματα λυμάτων

Εργαστηριακές πρακτικές:

- Απομόνωση μικροπλαστικών (επεξεργασία δειγμάτων και διήθηση)
- Παρατήρηση μικροπλαστικών σε στερεομικροσκόπιο για μορφολογικό χαρακτηρισμό (σχήμα, χρώμα, μέγεθος)
- Χαρακτηρισμός μικροπλαστικών κατά σύνθεση (με χρήση φασματοσκοπίας υπερύθρου μετασχηματισμού Fourier)

Επιστημονικοι/τεχνικοι υπευθυνοι περιβαλλοντικης διαχειρισης, υγειας και ασφαλειας επιχειρησεων (σύμφωνα με το πρότυπο ISO/IEC 17024)

[11/11/2021 – 12/01/2022]

Ένωση Ελλήνων Χημικών

- Περιβαλλοντική διαχείριση και βιωσιμότητα
- Περιβάλλον και παραγωγή
- Περιβαλλοντικός έλεγχος
- Καλές πρακτικές περιβαλλοντικής διαχείρισης
- Υγεία και ασφάλεια στην εργασία (πρότυπο ISO 45001)
- Βασικές αρχές εργατικού δικαίου
- Εφαρμογή της αρχής της μη διάκρισης
- Βασικές αρχές επιχειρηματικής λειτουργίας με έμφαση στην καινοτομία, το περιβάλλον, τη βιωσιμότητα και την ανάπτυξη νέων προϊόντων και υπηρεσιών

Εργασιακή Εμπειρία

Χημικός

[31/05/2021 – Τρέχουσα]

Εργαστήριο Κλινικής Μικροβιολογίας και Παθογένεσης - Ιατρική Σχολή Πανεπιστημίου Κρήτης

Καθήκοντα:

- Φυσικοχημική ανάλυση δειγμάτων λυμάτων, εμφιαλωμένων και πόσιμων υδάτων (προσδιορισμός ιόντων, pH, αγωγιμότητας) με φασματοφωτομετρία, ατομική απορρόφηση, τιτλοδότηση
- Μικροβιολογική και χημική ανάλυση του Sars-CoV-2 σε δείγματα λυμάτων
- Εκχύλιση RNA ιού και ποσοτικοποίηση με αλυσιδωτή αντίδραση πολυμεράσης (PCR)

Χημικός ΕΟΔΥ

[13/12/2021 – 30/09/2022]

Εθνικός Οργανισμός Δημόσιας Υγείας, Εργαστήριο Κλινικής Μικροβιολογίας και Μικροβιακής Παθογένεσης - Ιατρική Σχολή Πανεπιστημίου Κρήτης

Καθήκοντα:

- Εκτέλεση αναλύσεων Μοριακής Βιολογίας για την ανίχνευση του SARS-CoV-2 σε κλινικά δείγματα (RT-PCR)
- Προετοιμασία περαιτέρω για γονιδιωματική ανάλυση του ιού με Whole Genome Sequencing (WGS)

Καθηγήτρια Χημείας

[10/2022 – 05/2023]

Φροντιστήριο Μαθημάτων Δευτεροβάθμιας Εκπαίδευσης, Ηράκλειο Κρήτης

Καθηγήτρια πιάνου

[2019 – Τρέχουσα]

Ωδείο Χρωμάτων, Ηράκλειο Κρήτης, Ελλάδα

Δίκτυα και Συμμετοχές

Ευρωπαϊκή Συνεργασία στην Επιστήμη και την Τεχνολογία (COST)

Συμμετοχή στη δράση COST PRIORITY CA20101 - Plastics Monitoring Detection Remediation Recovery

Ομάδες Εργασίας:

- Επιπτώσεις και κίνδυνοι για την ανθρώπινη υγεία και το περιβάλλον που σχετίζονται με N/MP
- Παρακολούθηση και δειγματοληψία Μικροπλαστικών
- Όργανα, μοντελοποίηση, αξιολόγηση δεδομένων, λογισμικό και αναλυτικές διαδικασίες

Δημοσιεύσεις και αφίσες σε Συνέδρια

1. The monitoring of Sars-CoV-2 in sample of raw wastewater from four municipal wastewater treatment facilities of Crete as a time tool forecast. D. Chochlakis, V. Sandalakis, A. Xylouri, C. Kotsifaki, D. Kalisperi, C. Vogiatzi, K. Sifakaki, E. Martimianaki, A. Kokkinomagoula, M. O. Daskalaki, A. Koutsolioutsou, A. Psaroulaki. Hellenic Congress of Public Health. 28/2-2/3/22, Athens, Greece. https://www.free-spirit.gr/uploads/files/pan_syn_dimosias_ygeias_28-02-2022_fp.pdf.
2. Microbiological and Chemical monitoring of Sars-cov-2 in untreated wastewater samples from five Municipal WASTE-WATER TREATMENT PLANTS of Crete: some initial remarks. D. Chochlakis, V. Sandalakis, A. Xylouri, N. Kounalakis, C. Petroulaki, D. Marinopoulou, A. Kokkimagoula, E. Ouranou, M. Pitsaki, A. Psaroulaki. 7th International Conference on Industrial & Hazardous Waste Management. 27-30 July, 2021, Chania, Crete. http://hwm-conferences.tuc.gr/program-new/
3. Determination of emerging pollutants with possible endocrine action in Greek wastewater treatment samples. E. I. Iatrou, Z. Pournara, A. Kokkinomagoula, M.

Tzatzarakis, A. Tsatsakis. 7th International Conference on Industrial & Hazardous Waste Management. 27-30 July, 2021, Chania, Crete. http://hwm-conferences.tuc.gr/program-new/

4. Microbiological and chemical monitoring of SARS-CoV-2 in untreated wastewater samples from four municipal wastewater treatment plants of Crete and the role of wastewater on forecasting human cases: some initial remarks. A. Kokkinomagoula* (Heraklion, Greece), D. Chochlakis, V. Sandalakis, A. Xylouri, C. Petroulaki, D. Marinopoulou, E. Ouranou, M. Koureas, A. Psaroulaki. 32nd European Congress of Clinical Microbiology and Infectious Diseases (ECCMID). 23-26 April 2022, Lisbon, Portugal. https://markterfolg.de/ESCMID/Final_Programme_2022/#page=222
5. The effect of chemical elements and ions on the presence of Legionella in water systems. Dimosthenis Chochlakis, Areti Kokkinomagoula, Vassilios Sandalakis, Christos Panoulis, Xanthi Andrianou, Maria Keramarou, Spyros Pergantis, Anna Psaroulaki. 10th International Conference on Legionella. 20-24 September 2022, Yokohama, Japan. http://legionella2021.umin.jp/pdf/poster_session.pdf
6. Application of Culturomics and Whole Genome Sequencing for the detection of antibiotic resistance genes in novel bacteria isolated from Wastewater Treatment sites. E.Ouranou, M. Malliarou, A. Ntoula, E. Makridaki, N. Thalassinaki, N.Tsamandouras, A.Kokkinomagoula, A. Psaroulaki, D. Chochlakis. International Conference on One Health Antimicrobial Resistance (ICOHAR). 18-20 April 2023, Copenhagen, Denmark. https://www.icohar.org/fileadmin/files/2023/icohar2023/pdf/ALL_ABSTRACTS-_updated.pdf

Γλώσσες

Ελληνικά: Μητρική Γλώσσα

Αγγλικά: C2 – Certificate of Proficiency in English – University of Michigan

Γερμανικά: B2 – Goethe Institut

CURRICULUM VITAE

Areti Kokkinomagoula

Personal Information

E-mail: kokareti@gmail.com , chemp1109@edu.chemistry.uoc.gr

Date of birth: 12/09/1997

Nationality: Greek

Education

MSc in Chemistry – Environmental Science and Engineering

[03/2021 – Current]

University of Crete - Department of Chemistry

BSc in Chemistry

[2014 – 2020]

University of Crete - Department of Chemistry

Thesis title: Determination of Parabens and Triclosan levels (endocrine disrupting organic pollutants) in wastewater samples in the area of Heraklion - *Laborarory of Toxicology and Forensic Chemistry - Medical School, University of Crete.*

Piano Degree

[2004 – 2019]

Conservatory of Colours – Heraklion, Crete, Greece

Educational Programmes and Training

Short-Term Scientific Mission (STSM) - European Cooperation in Science and Technology (COST)

[13/03/23 – 17/03/23]

University of La Laguna - Department of Chemistry - Applied Analytical Chemistry Laboratory, Tenerife, Canary Islands, Spain

Mission title: Isolation and characterization of microplastics from wastewater samples

Laboratory practices:

- Isolation of microplastics (sample treatment and filtration)

- Inspection of microplastics under stereomicroscope for morphological characterization (shape, color, size)
- Characterization of microplastics by composition (using Fourier-Transform Infrared spectroscopy)

Seminar on Corporate Environmental Management, Health and Safety (according to ISO/IEC 17024 Standard)

[11/11/2021 – 12/01/2022]

Association of Greek Chemists

- Environmental management and sustainability
- Environment and production
- Environmental control
- Good environmental management practices
- Health and safety at work (ISO 45001 standard)
- Basic principles of labor law
- Application of the principle of non-discrimination
- Basic principles of business operations with an emphasis on innovation, the environment, sustainability, and the development of new products and services

Work experience

Chemist

[31/05/2021 – Current]

Laboratory of Clinical Microbiology and Pathogenesis - Medical School, University of Crete

Duties:

- Physico-chemical analysis of wastewater samples (pollutants, ions, pH etc.) by spectrophotometry, atomic absorption, titration
- Microbiological and chemical analysis of Sars-CoV-2 in untreated wastewater samples
- Virus RNA extraction and quantification by Polymerase Chain Reaction (PCR)

Chemist – National Public Health Organization

[13/12/2021 – 30/09/2022]

National Public Health Organization, Laboratory of Clinical Microbiology and Microbial Pathogenesis - University of Crete School of Medicine

Duties:

- Performing Molecular Biology analyzes for the detection of SARS-CoV-2 in clinical samples (RT-PCR)

- Further preparation for genomic analysis of the virus by Whole Genome Sequencing (WGS)

Chemistry Teacher

[10/2022 – 05/2023]

Secondary Education Private School, Heraklion, Crete, Greece

Piano Teacher

[2019 – Current]

Conservatory of Colors, Heraklion, Crete, Greece

Networks and Memberships

European Cooperation in Science and Technology (COST)

Membership in COST PRIORITY action CA20101 - Plastics Monitoring Detection Remediation Recovery

Working Groups:

- Impacts and risks on human health and environment related to N/MPs
- Monitoring and sampling Microplastics
- Instrumentation, modelling, data evaluation, software and analytical procedures

Publications and posters in Conferences

1. The monitoring of Sars-CoV-2 in sample of raw wastewater from four municipal wastewater treatment facilities of Crete as a time tool forecast. D. Chochlakis, V. Sandalakis, A. Xylouri, C. Kotsifaki, D. Kalisperi, C. Vogiatzi, K. Sifakaki, E. Martimianaki, A. Kokkinomagoula, M. O. Daskalaki, A. Koutsolioutsou, A. Psaroulaki. Hellenic Congress of Public Health. 28/2-2/3/22, Athens, Greece. https://www.free-spirit.gr/uploads/files/pan_syn_dimosias_ygeias_28-02-2022_fp.pdf.
2. Microbiological and Chemical monitoring of Sars-cov-2 in untreated wastewater samples from five Municipal WASTE-WATER TREATMENT PLANTS of Crete: some initial remarks. D. Chochlakis, V. Sandalakis, A. Xylouri, N. Kounalakis, C. Petroulaki, D. Marinopoulou, A. Kokkimagoula, E. Ouranou, M. Pitsaki, A. Psaroulaki. 7th International Conference on Industrial & Hazardous Waste Management. 27-30 July, 2021, Chania, Crete. http://hwm-conferences.tuc.gr/program-new/
3. Determination of emerging pollutants with possible endocrine action in Greek wastewater treatment samples. E. I. Iatrou, Z. Pournara, A. Kokkinomagoula, M. Tzatzarakis, A. Tsatsakis. 7th International Conference on Industrial & Hazardous Waste Management. 27-30 July, 2021, Chania, Crete. http://hwm-conferences.tuc.gr/program-new/

4. Microbiological and chemical monitoring of SARS-CoV-2 in untreated wastewater samples from four municipal wastewater treatment plants of Crete and the role of wastewater on forecasting human cases: some initial remarks. A. Kokkinomagoula* (Heraklion, Greece), D. Chochlakis, V. Sandalakis, A. Xylouri, C. Petroulaki, D. Marinopoulou, E. Ouranou, M. Koureas, A. Psaroulaki. 32nd European Congress of Clinical Microbiology and Infectious Diseases (ECCMID). 23-26 April 2022, Lisbon, Portugal. https://markterfolg.de/ESCMID/Final_Programme_2022/#page=222
5. The effect of chemical elements and ions on the presence of Legionella in water systems. Dimosthenis Chochlakis, Areti Kokkinomagoula, Vassilios Sandalakis, Christos Panoulis, Xanthi Andrianou, Maria Keramarou, Spyros Pergantis, Anna Psaroulaki. 10th International Conference on Legionella. 20-24 September 2022, Yokohama, Japan. http://legionella2021.umin.jp/pdf/poster_session.pdf
6. Application of Culturomics and Whole Genome Sequencing for the detection of antibiotic resistance genes in novel bacteria isolated from Wastewater Treatment sites. E.Ouranou, M. Malliarou, A. Ntoula, E. Makridaki, N. Thalassinaki, N.Tsamandouras, A.Kokkinomagoula, A. Psaroulaki, D. Chochlakis. International Conference on One Health Antimicrobial Resistance (ICOHAR). 18-20 April 2023, Copenhagen, Denmark. https://www.icohar.org/fileadmin/files/2023/icohar2023/pdf/ALL_ABSTRACTS-_updated.pdf

Language Skills

Greek: Mother Language

English: C2 – Certificate of Proficiency in English – University of Michigan

German: B2 – Goethe Institut

ΠΕΡΙΛΗΨΗ

Η νόσος COVID-19 (Corona Virus Disease 2019), και ο αιτιολογικός της παράγοντας, ο κορονοϊός SARS-CoV-2 καταγράφηκαν για πρώτη φορά στην Κίνα στα τέλη του 2019 και εξαπλώθηκε ταχύτατα σε όλο τον πλανήτη, προκαλώντας την πανδημία COVID-19 . Κατά τη διάρκεια της πανδημίας, η παρακολούθηση του ιικού φορτίου αλλά και των παραλλαγών του κορονοιού στα λύματα (ανίχνευση και ποσοτικοποίηση του RNA του SARS-CoV-2 και προσδιορισμός παραλλαγών) συνέβαλε σημαντικά στην επιδημιολογική επιτήρηση της νόσου COVID-19. Την περίοδο της πανδημίας, οι μεθοδολογίες Επιδημιολογίας με βάση τα λύματα (Wastewater-based epidemiology) εξελίχθηκαν ταχύτατα σε ένα συμπληρωματικό εργαλείο επιτήρησης για την COVID-19, ενώ σήμερα εφαρμόζονται και για άλλα θέματα δημόσιας υγείας.

Ενώ οι κλινικές διαγνωστικές δοκιμές σε ατομικό επίπεδο για τη νόσο COVID-19 παραμένουν σε εξέλιξη, από μόνες τους δεν παρέχουν έναν αξιόπιστο δείκτη κινδύνου για την υγεία στην κοινότητα. Δεδομένου ότι τα άτομα σε διάφορες καταστάσεις μόλυνσης από τον COVID-19 μπορούν να αποβάλλουν το RNA του SARS-CoV-2 μέσω των κοπράνων, η επιδημιολογική μελέτη μέσω των λυμάτων, θεωρήθηκε μια πιο ολιστική προσέγγιση.

Πολλοί παράγοντες, ωστόσο, μπορούν να επηρεάσουν την ανάκτηση RNA από τα λύματα, εμποδίζοντας την επιδημιολογική σημασία του. Τα χαρακτηριστικά των λυμάτων όπως το pH, η αγωγιμότητα, η συγκέντρωση αιωρούμενων στερεών κ.λπ., καθώς και τα εποχιακά χαρακτηριστικά όπως τα γεγονότα βροχοπτώσεων, έχει βρεθεί ότι έχουν πιθανή επίδραση στην ανάκτηση του RNA του SARS-CoV-2 από τα λύματα.

Έχουν διεξαχθεί διάφορες μελέτες σε αυτό το πλαίσιο και αρκετές παράμετροι έχουν χρησιμοποιηθεί για την ερμηνεία και/ή την κανονικοποίηση της τελικής συγκέντρωσης RNA. Μερικοί από τους πιο συνηθισμένους παράγοντες κανονικοποίησης περιλαμβάνουν το ρυθμό ροής εισροής, τον πληθυσμό που εξυπηρετείται από τις εγκαταστάσεις επεξεργασίας λυμάτων, τα ιόντα αμμωνίου και ορθοφωσφορικών, την αγωγιμότητα των λυμάτων και το pH, παράγοντες που μπορούν επίσης να χρησιμοποιηθούν για την ερμηνεία των αποτελεσμάτων.

Για αυτήν τη μελέτη λάβαμε δείγματα λυμάτων σε ένα ευρύ χρονικό πλαίσιο, το οποίο περιελάμβανε βασικά κοινωνικά και πανδημικά ορόσημα και παρεμβάσεις. Συγκεκριμένα, η μελέτη περιλαμβάνει την περίοδο κατά την οποία εφαρμόστηκαν αυστηρά μέτρα παρέμβασης (π.χ. lockdown, υποχρεωτική κάλυψη προσώπου, διαδικτυακά μαθήματα κ.λπ.) και η σταδιακή

αφαίρεσή τους, καθώς και η έναρξη των εμβολιασμών και η εμφάνιση διαφορετικών παραλλαγών του ιού.

Από τον Φεβρουάριο του 2021 έως σήμερα, συλλέγονταν δείγματα λυμάτων τρεις φορές την εβδομάδα από δύο σταθμούς επεξεργασίας λυμάτων που βρίσκονται στο νησί της Κρήτης (Χανιά και Ηράκλειο), που μας έδιναν συνολικά έξι (6) δείγματα σε εβδομαδιαία βάση. Περίπου 2-6 L σύνθετα δείγματα συλλέγονταν μέσω αυτόματων δειγματοληπτών σε μια περίοδο 24 ωρών. Συνολικά, αναλύθηκαν 781 δείγματα για τις ανάγκες της παρούσας μελέτης.

Η παρούσα μελέτη είχε ως στόχο την επίτευξη των ακόλουθων στόχων: (1) ανίχνευση και ποσοτικοποίηση του γενετικού υλικού SARS-CoV-2 σε δύο WWTP που βρίσκονται στην Κρήτη, Ελλάδα, (2) προσδιορισμός της πιθανής σχέσης μεταξύ των κρουσμάτων COVID-19 και των συγκεντρώσεων RNA του SARS-CoV-2 στα λύματα, (3) ενίσχυση της κατανόησης της σχέσης μεταξύ των φυσικοχημικών χαρακτηριστικών των λυμάτων και της ανάκτησης και ποσοτικοποίησης του ιού και (4) αξιολόγηση του αντίκτυπου της καραντίνας και των περιοριστικών μέτρων κατά τη διάρκεια της πανδημίας, τόσο στα ανθρώπινα κρούσματα όσο και στο ιικό φορτίο των λυμάτων, λαμβάνοντας υπόψη ταυτόχρονα την επίδραση των μαζικών εμβολιασμών και των παραλλαγών στα πρότυπα αποβολής του ιού. Οι γνώσεις που αποκτήθηκαν κατά τη διάρκεια αυτής της πανδημίας και η χρήση της επιδημιολογίας μέσω των λυμάτων, είναι πολύτιμες για τη μελλοντική διαχείριση των αναδυόμενων και περίπλοκων απειλών για τη δημόσια υγεία.

Λέξεις κλειδιά: Επιδημιολογική Μελέτη Λυμάτων, SARS-CoV-2, COVID-19, Δημόσια Υγεία, Επιστήμες Περιβάλλοντος.

ABSTRACT

The disease COVID-19 (Corona Virus Disease 2019), and its causative agent, the SARS-CoV-2 coronavirus, were first recorded in China at the end of 2019 and spread rapidly throughout the planet, causing the COVID-19 pandemic. During the pandemic, the monitoring of the viral load as well as the variants of the coronavirus in wastewater (detection and quantification of SARS-CoV-2 RNA and identification of variants) contributed significantly to the epidemiological surveillance of the COVID-19 disease. During the pandemic, Wastewater-based Epidemiology methodologies quickly evolved into a complementary surveillance tool for COVID-19, while today they are also applied to other public health issues.

While individual-level clinical diagnostic testing for COVID-19 remains ongoing, it alone does not provide a reliable indicator of health risk within community. Given that individuals in various COVID-19 infection states can shed SARS-CoV-2 RNA through feces, WBE was considered a more holistic approach.

Numerous factors, however, can influence RNA recovery from wastewater, hindering its epidemiological significance. Wastewater characteristics such as pH, conductivity, Suspended Solids concentration, etc., as well as seasonal characteristics such as rainfall events, have been found to have possible influence on the recovery of SARS-CoV-2 RNA from wastewater.

Various studies have been carried out in this context and quite a few parameters have been used to interpret and/or normalize the final RNA concentration. Some of the most usual normalization factors include the influent flow rate, the population served by Wastewater Treatment Plants (WWTPs), ammonium and orthophosphate ions, wastewater conductivity and pH, which can also be used for the interpretation of the results.

For this study we received wastewater samples during a broad time frame, which included key societal and pandemic milestones and interventions. Specifically, the study encompasses the period, during which, strict intervention measures (e.g., lockdowns, mandatory face coverings, online lessons, etc.) and their gradual removal were implemented, as well as the start of vaccinations and the emergence of different variants.

From February of 2021 until today, wastewater samples have been collected three times a week from two WWTPs located in the island of Crete, Greece (Chania and Heraklion), which gave us a total of six (6) samples on a weekly basis. Approximately 2-6 L composite samples were collected via autosamplers over a 24-hour period. In total, 781 samples were analyzed for the needs of the current study.

The current study aimed to achieve the following objectives: (1) detect and quantify SARS-CoV-2 genetic material in two WWTPs located in Crete, Greece, (2) establish a potential link between Corona Virus Disease - 19 (COVID-19) cases and SARS-CoV-2 RNA concentrations in wastewater, (3) enhance understanding of the relationship between the physico-chemical characteristics of the wastewater and viral recovery and quantification and (4) assess the impact of in-house and community restrictions during the pandemic, on both human cases and wastewater viral load, considering the effect of mass vaccinations and variants on viral shedding

patterns. The insights gained during this pandemic and the use of WBE is valuable for future management of emerging and challenging public health threats.

Keywords: Wastewater-Based Epidemiology, SARS-CoV-2, COVID-19, Public Health, Environmental Sciences.

ABBREVIATIONS

APHA: American Public Health Association

BOD: Biochemical Oxygen Demand

BSL: Biosafety Level

CDC: Centers for Disease Control and Prevention

CoA: Certificate of Analysis

COD: Chemical Oxygen Demand

COVID-19: Corona Virus Disease-19

CT: Threshold Cycle

DI water: Deionized water

ECDC: European Center for Disease Prevention and Control

EMR: Electromagnetic Radiation

ML: Machine Learning

PEG: Polyethylene glycol precipitation

PMMoV: Pepper Mild Mottle Virus

RT-PCR: Real-Time Polymerase Chain Reaction

SARS: Severe Acute Respiratory Syndrome

SS: Suspended Solids

UV-Vis: Ultraviolet – Visible

VOCs: Variants of Concern

WBE: Wastewater-Based Epidemiology

WHO: World Health Organization

WWTP: Wastewater Treatment Plant

TLCC: Time Lagged Cross-Correlation

WTLCC: Windowed Time Lagged Cross-Correlation

TABLE OF CONTENTS

CHAPTER 1 – INTRODUCTION AND AIMS OF THE STUDY

1.1 Coronaviruses and SARS-CoV-2

On December 2019 emerged a novel coronavirus, later termed Severe Acute Respiratory Syndrome Corona Virus 2 (SARS-CoV-2), which is the causative agent of coronavirus disease 2019 (COVID-19). The SARS-CoV-2 outbreak was reported in China, and since then it has rapidly spread globally with more than 770 million confirmed cases and almost seven (7) million deaths by the 6th of September 2023 (https://covid19.who.int/). COVID-19 was declared a pandemic by the World Health Organization (WHO) on the 11th of March 2020.

Coronaviruses are an extensive family of enveloped viruses, meaning that they are surrounded by a lipid bilayer membrane. This envelope plays a crucial role in the virus's ability to infect host cells and evade the immune system. It is also worth noting, that enveloped viruses have greater susceptibility to degradation by solvents and detergents found in wastewater compared to nonenveloped ones (Anderson-Coughlin et al., 2021). The viral envelope contains viral spike proteins[1], among other proteins, that are vital for viral binding and entering host cells. One of those is the spike (S) glycoprotein that forms peplomers (or spikes) on the virion[2] surface, giving the virus its "corona" or crown-like morphology under the electron microscope (Ortiz-Prado et al., 2020).

SARS-CoV-2 primarily targets multiciliated cells[3] in the upper respiratory tract, but was also reported to infect cells outside the upper respiratory tract (Puelles et al., 2020). It can expand to the lower respiratory tract, infecting alveoli and leading to reduced gas exchange, inflammation and pulmonary disfunctions, which are typical of COVID-19 disease. It is noteworthy, that SARS CoV-2 can infect both animals and humans and is the most recent example of viral jumps, since it primarily infected animals, then evolved, and caused disease to humans too.

[1] Spike proteins form a large structure known as a spike or peplomer, projecting from the surface of an enveloped virus (*Wikipedia*, 2023, https://en.wikipedia.org/wiki/Spike_protein).

[2] A complete virus particle whose main function is to deliver its DNA or RNA genome into the host cell so that the genome can be expressed by the host cell (Hans R. Gelderblom, *Medical Microbiology*, 4th edition, Chapter 41 - Structure and Classification of Viruses https://www.ncbi.nlm.nih.gov/books/NBK8174/#:~:text=A%20complete%20virus%20particle%20is,inside%20a%20symmetric%20protein%20capsid).

[3] Multiciliated cells are cells that propel fluid through motile cilia and serve diverse functions such as feeding and locomotion in marine organisms, as well as mucus clearance, cerebrospinal fluid circulation, and egg transportation in mammals (Boutin & Kodjabachian, 2019).

Individuals who are infected shed the virus through the upper respiratory tract, with emission of infectious virus leading to secondary transmission and thus its further spread.

1.2 Wastewater-based Epidemiology (WBE)

Viruses can enter waste streams through multiple, human origin routes, including stool, urine, skin, saliva, and blood. Municipal wastewater, therefore, harbors a great variety of pathogenic viruses like poliovirus and other enteric viruses such as norovirus, hepatitis A and hepatitis E viruses (Prasek et al., 2023; Adriaenssens et al., 2018; McCall et al., 2020). Given the fact that viruses cannot reproduce independently outside a host and can endure in the environment for extended durations, wastewater-based epidemiology (WBE) offers a means to capture an almost immediate representation of the prevalence of viral diseases within a community. Fluctuations in viral concentrations over time in wastewater can serve as an indicator of the virus's presence or absence, as well as any associated outbreaks in the population and their impact on public health. Above all, routine monitoring of viruses provides valuable insights into the transmission of clinically important diseases, may prevent widespread of outbreaks, and reduces deaths associated with these pathogens (McCall et al., 2020).

While the COVID-19 pandemic persists, clinical diagnostic testing for COVID-19 on individual level does not provide a holistic indicator of health risk within community by itself (Cao & Francis, 2021). Individuals infected with SARS-CoV-2 can excrete the virus and/or viral RNA via feces, urine, saliva, and sputum (Prasek et al., 2023), and although all these sources contribute to the detection of the virus in wastewater samples, feces dominate population-level SARS-CoV-2 RNA loading in wastewater. SARS-CoV-2 can be detected in human feces for 3–4 weeks after infection, regardless of the individual showing any symptoms or not; pre-symptomatic, asymptomatic, symptomatic as well as recovered from COVID-19 individuals were found to shed the virus via feces (Cevik et al., 2021; Park et al., 2021; Bertels et al., 2022). The viral RNA can remain detectable in wastewater for several days to weeks, depending on conditions, thus, it was assumed that tracking the spatiotemporal fluctuations in RNA concentrations by means of WBE would provide a pooled, more accurate testing of all COVID-19 cases.

Knowledge of SARS-CoV-2 levels in wastewater may provide insight not only into general health trends, but it can also be integrated into models to estimate COVID-19 disease prevalence in a given population, by accounting the shedding rate, or the average amount of virus shed by an infected individual per day (Prasek et al., 2023). Estimations of the number of

infected individuals corresponding to a wastewater sample can be generated in such way. WBE for SARS-CoV-2 can also provide valuable information on the circulation of variants of concern or of interest, as classified by the WHO (https://www.who.int/activities/tracking-SARS-CoV-2-variants).

However, WBE does not stand alone in SARS-CoV-2 surveillance. Several studies have indicated differing levels of correspondence between the presence of SARS-CoV-2 RNA in wastewater and the outcomes of individual testing conducted concurrently and at the same location (Ai et al., 2021; Li et al., 2023). WBE plays an important complementary role in monitoring infection rates and is proposed as an early warning of sudden outbreaks (Morvan et al., 2022).

Wastewater viral load is used by public health agencies to spot changes in testing behavior over time or between communities (De Graaf et al., 2022), to compare the trends in reported cases and in decision-making for mitigation strategies, because examining the WBE over a long-term, allows for identification of factors strongly correlated to outbreaks. Consistent with the interim guidance provided by the World Health Organization, (WHO 2022), the European Commission has advised all European Union member states to adopt SARS-CoV-2 wastewater-based surveillance, starting from March 2021 (Commission Recommendation (EU) 2021/472, 2021). In Greece, the monitoring of SARS-CoV-2 RNA through wastewater began in February 2021.

1.3 The importance of sample characteristics

1.3.1 Physicochemical and wastewater treatment plant (WWTP) characteristics

A parameter of major concern in the study of a virus in wastewater is the implication of several factors on the recovery of viral RNA and therefore, viral detection. Generally, viruses are susceptible to inactivation when they end up in the environment. Environmental factors such as temperature, pH, UV light, inorganic anions and cations and organic matter among others, may have virucidal effects, or may inhibit viral recovery (Gundy at al., 2009; Auffret et al., 2019; Joiner et al., 2020; Amoah et al., 2022). It is worth noting however, that each wastewater sample is unique in terms of composition and therefore, inhibition of viral recovery cannot be described by a single protocol.

Several studies have been carried out in this context and quite a few parameters have been used to interpret and/or normalize the final RNA concentration. These include physicochemical wastewater characteristics like conductivity, pH, Chemical and Biochemical Oxygen Demand

(COD and BOD respectively), Suspended Solids (SS), ammonia, orthophosphate, and chloride concentration. WWTP characteristics, like influent wastewater flow rate and the size of the population it serves have also been used extensively as normalization factors (Koureas et al., 2021; Amoah et al., 2022; Wilde et al., 2022).

It is worth noting that ammonia is an established chemical indicator of human urine content in wastewater that originates from the hydrolysis of urea. Unsurprisingly, increasing ammonia concentration is associated with increasing viral RNA concentration, while pH values in the range 7.1-7.4, are associated with the highest SARS-CoV-2 concentration (Amoah et al., 2022).

SARS-CoV-2 particles have a very small size and are extremely surface active, due to their hydrophobic envelope. This makes viral particles adhere greater to solids with possible impact on viral recovery (Anderson-Coughlin et al., 2021). Hence, the penetration or adsorption of the

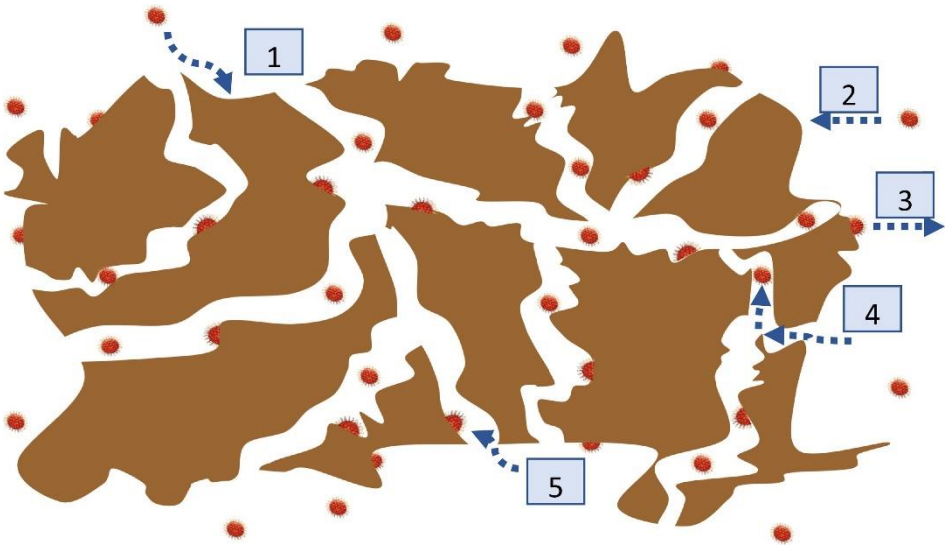

Figure 1: Schematic representation of possible interaction mechanisms of virus particles/fragments with a porous solid particle suspended in sewage. 1: mass transfer (convection and diffusion) from the surrounding bulk liquid, 2: adsorption, 3: desorption, 4: pore diffusion and 5: surface diffusion (Petala et al., 2021).

virus onto suspended solids like feces, sand, clay, etc., (**Figure 1**) could lead to underestimation of the viral load (Petala et al., 2021).

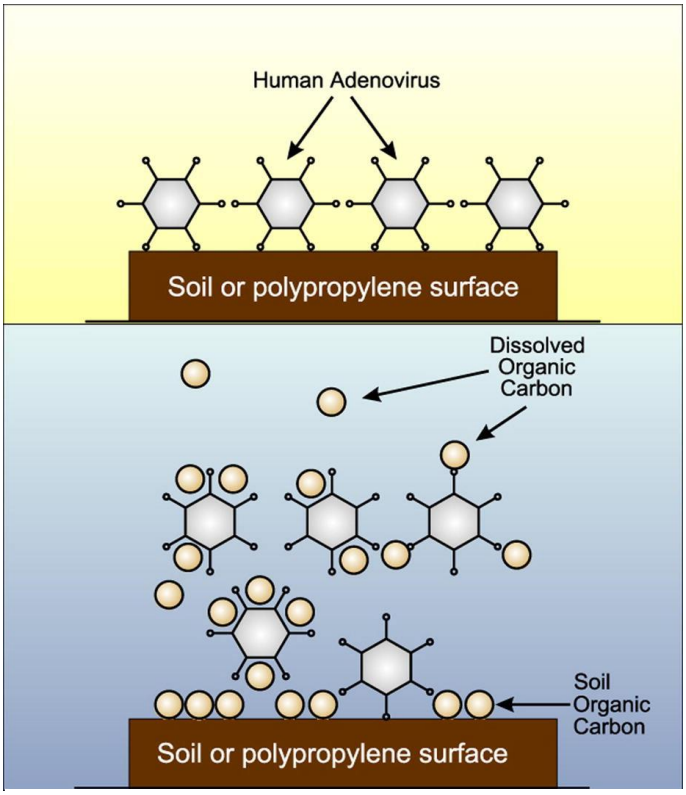

Figure 2: Schematic representation of the interaction of viruses with dissolved organic matter and solid surfaces (Wong et al., 2013).

Interestingly, it has been reported that dissolved organic matter plays a significant role in viral recovery too, as it competes with viruses for adsorption sites. Bonded organic matter on the other hand, occupies sorption sites but also provides new hydrophobic binding sites. These processes can be visualized in **Figure 2**. Consequently, the adsorption of viruses is a complex process, which depends significantly on factors like the form of organic matter and the type of virus (Zhuang and Jin, 2003; Wong et al., 2013; Petala et al., 2021). Thus, COD, BOD and SS concentrations can be indirect measures of organic loading in wastewater, and they potentially affect viral RNA recovery efficiency.

Another parameter of concern when it comes to viral load normalization is the influent flow rate of the WWTP. Influent rate is a measure of the volume of wastewater that passes through the treatment, indirectly indicating the water consumption within community and thus, the size of the population served. However, due to the potential fluctuation of the size population among several periods or even during a day, because of several factors, such as tourism, festivals, etc., there is a need to collect as representative wastewater samples as possible. That is why, collection of instantaneous samples has been abandoned for the sake of 24-hour composite samples by automatic samplers. Furthermore, depending on the type of the WWTP, increased influent rates could result from stormwater, seawater entering the sewer shed or even pool water from in-city hotels during high touristic seasons. Including that factor allows for the normalization of concentrations, in case of this kind of dilution events (Wilde et al., 2022).

1.3.2 Pandemic milestones - Seasonal characteristics

Studies encompassing the pandemic period usually include samples collected during the implementation and gradual abolition of several restriction measures (e.g., lockdowns, mandatory face coverings, online lessons, etc.) as well as the start of vaccinations and the emergence of different variants. These changes on pandemic management strategies might affect both the number of human cases and the wastewater viral load and hence, qualitative observation would be of a great epidemiological importance.

The emergence of different variants as well as the start of vaccinations, are major factors that affect viral shedding patterns too (Bivins & Bibby, 2021). Variants of Concern (VOCs), as designated by the World Health Organization (WHO), included Alpha, Beta, Gamma, Delta and Omicron variants, which may display significant differences in evasion from immunity, viral loads, shedding and incubation periods. In addition, population immunity because of vaccinations may have reduced viral load leading to changes on viral shedding patterns (Puhach et al., 2022).

As for the seasonal characteristics of the wastewater samples, the influence of rainfalls, usually during winter season, as well as the influence of the pool water from in-city hotels entering the sewer shed during high touristic seasons, are of a great importance in WBE, because of the dilution effects they may provoke. Specifically, several epidemiological studies have referred to rainfall events as a bias factor for data interpretation (Hillary et al., 2021; Bertels et al., 2022; Langeveld et al., 2023; López-Peñalver et al., 2023; Maal-Bared et al., 2023; Saingam et al., 2023), however, very few of them have actually examined their effect on viral detection. Saingam et al., 2023 observed that rain precipitation impacted SARS-CoV-2 levels and reduced WBE sensitivity.

1.4 Viral RNA extraction and quantification - Methods and Principles

1.4.1 Virus concentration

The complex nature of the wastewater sample, which affects the detection of the virus, and the low viral RNA loads in wastewater, as a result of high dilution effects, make the detection of SARS-CoV-2 difficult, compared to clinical testing. Therefore, effective viral concentration and isolation methods are essential for its sensitive detection (Zheng et al., 2022).

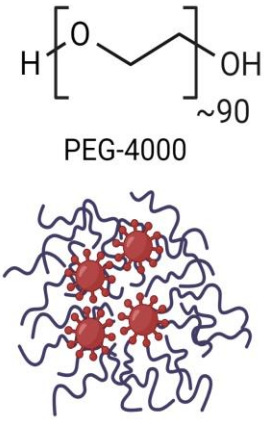

Figure 3: Schematic representation of PEG - 4000 precipitation (GenEpi-BioTrain)

Precipitation, ultracentrifugation, direct capture/lysis and centrifugal ultrafiltration are among the most common viral concentration methods.

The precipitation method usually utilizes high molecular weight polyethylene glycol – 6000 (PEG), which in combination with NaCl, is used for virus precipitation (**Figure 3**). PEG precipitation is carried out in low temperature and high salt environment and acts by altering the solubility of the viral particles causing precipitation (Sapula et al., 2021; Alexander et al., 2020). Although PEG precipitation is generally a cheap method, it is hard to implement, because of the long duration of the protocol (16 hours for precipitation) and the poor reproducibility.

Ultracentrifugation utilizes an ultracentrifuge to reach high centrifugal speeds and efficiently separate particulate from liquid matter (Zheng et al., 2022). Particulate matter can be recovered either in the form of a pellet, formed after ultracentrifugation, or retained and recovered by using a filter during ultracentrifugation (**Figure 4**). This method has a simple and easy to establish protocol, however, filters might clog, making the flow times vary. The concentration of organic material cannot be avoided too.

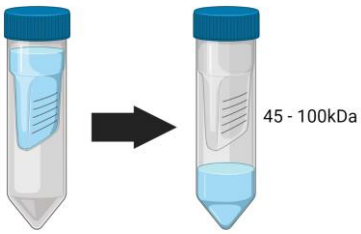

Figure 4: Ultracentrifugation filter device (GenEpi-BioTrain Programme, January 2024, ECDC)

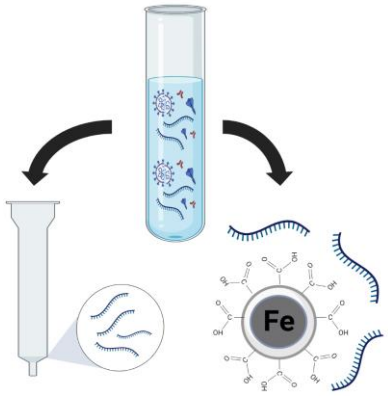

Figure 5: Direct capture/lysis of nucleic acids by silica- based columns and magnetic beads (GenEpi-BioTrain Programme, January 2024, ECDC).

Direct capture/lysis method achieves direct capture and lysis of RNA/DNA molecules. It usually utilizes silica-based columns and/or magnetic beads for nucleic acid extraction directly from the initial sample (Shi et al., 2015; **Figure 5**). Nucleic acids are retained, either onto the silica membrane, or on the surface of the metallic beads, due to electrostatic interactions; usually covalent bonding. The mechanism of silica-based extraction is further explained in paragraph 1.4.2. **Figure 6** is an overview of magnetic bead-based DNA extraction. Although direct capture of nucleic acids is favorable and time saving, the chemical properties of the sample may affect the recovery. The co-precipitation of inhibitors is hard to avoid too.

One of the most broadly used methods for viral concentration is centrifugal ultrafiltration. A pre-defined volume of sample is placed into an ultrafiltration device and the filtration process is carried out by centrifugation. Centrifugal ultrafiltration is mainly based on molecular size exclusion. Virus particles are retained on the membrane surface within its pores. Different pore sizes are selected according to the size of the particle of interest. Sample characteristics such as the pH, ionic strength, the presence of solvent or detergents, the isoelectric point of virions, etc.

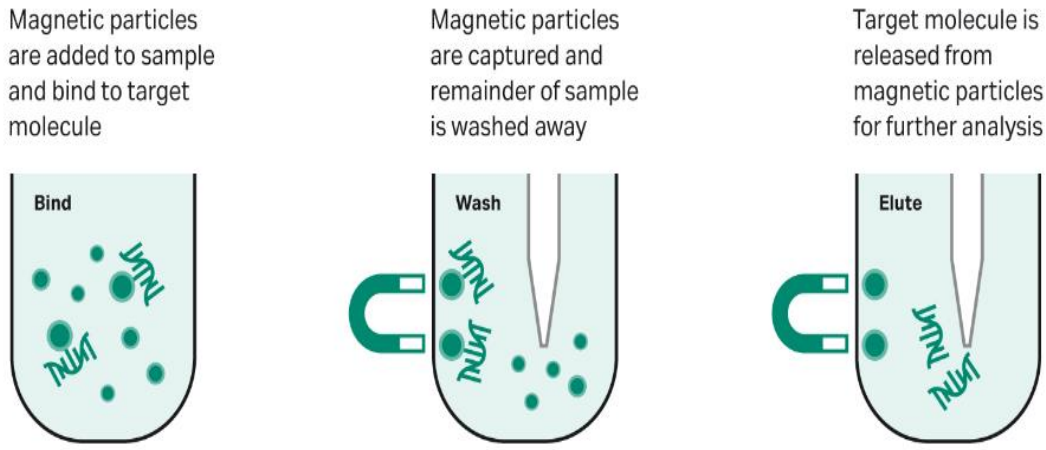

Figure 6: Magnetic bead-based DNA extraction procedure (A guide to choosing and using magnetic beads, Andrew Gane, Cytiva, May 29, 20190 https://www.cytivalifesciences.com/en/us/news-center/magnetic-beads-a-simple-guide-10001#:~:text=A%20magnetic%20force%20is%20applied,cell%20isolation%2C%20and%20protein%20purification).

do not have any influence on this physical separation technique (Burnouf-Radosevich et al., 1994; Asper et al., 2015; Alam et al., 2021).

Various centrifugal ultrafiltration devices like Centricon® (MILLIPORE, Merck) of different cut-off sizes[4] (10, 30 and 100 kDa), have been applied to concentrate SARS-CoV-2 (Medema et al., 2020; Rusiñol et al., 2020; Forés et al., 2021), performing the highest recoveries (Medema et al., 2020). The membranes in these devices are made of regenerated cellulose, which is naturally hydrophilic and exhibits the lowest non-specific protein binding of any ultrafiltration membrane (Ultracel membranes Datasheet, Millipore, Merck) (**Figure 7**). Usually, there is the necessity of a pre-centrifugation step to remove larger particles and avoid clogging of the membrane.

Figure 7: Centricon® (MILLIPORE, Merck) ultrafiltration device

1.4.2 RNA extraction and purification principles

RNA extraction generally consists of four steps: (1) cell lysis and homogenization, (2) quenching of biochemical processes, (3) nucleic acid partitioning or silica-based membrane binding, (4) RNA retrieval and purification (Cai et al., 2015).

During the first step, complete release of nucleic acids by effective cell lysis and homogenization occurs. TRIzol[5] or detergents that disrupt cells to release cellular contents are some of the chemical treatment methods used. In addition to chemical methods, enzymatic means may be employed as well.

In most cases, cell lysis/homogenization and quenching of biochemical processes are performed in the same step. Previously fragmented biomolecules that are released and subjected to an environment where enzymatic activities occur may threaten RNA integrity during the cell lysis

[4] Molecular weight cut-off (MWCO) is a method of characterization used in filtration to describe pore size distribution and retention capabilities of membranes. It is defined as the lowest molecular weight (in Daltons) at which greater than 90% of a solute with a known molecular weight is retained by the membrane (*Definition Of Molecular Weight Cut Off*, Synder Filtration, https://synderfiltration.com/learning-center/articles/membranes/molecular-weight-cut-off/#:~:text=Molecular%20weight%20cut-off%20(MWCO,is%20retained%20by%20the%20membrane.).

[5] Solution of phenol and guanidine isothiocyanate

step. Therefore, there is a need of solvents that solubilize cell contents. These should be either denaturing (e.g., phenolchloroform) or contain chaotropic agents such as guanidinium thiocyanate or urea.

Usually, nucleic acid extraction involves the partitioning of DNA from RNA. This method depends on pH (Brawerman, Mendecki, & Lee, 1972; Perry et al., 1972). At an alkaline pH, both DNA and RNA are retained in the aqueous phase. As pH decreases, DNA transitions increasingly from the aqueous phase to the organic phase and interphase. Therefore, an appropriate solvent of pH 8 is used for the extraction of DNA, while a pH at 4.8 is used to isolate RNA.

Many commercial preparations employ spin columns with silica-based (amorphous silicon dioxide) membranes for RNA extraction. Silica-based columns are largely used in RNA extraction, as they allow for fast extractions and high-quality nucleic acid yields. This method is based on the binding of RNA onto the silica membrane, washing impurities out of the membrane and finally un-binding the RNA from the membrane into a final eluent (**Figure 8**).

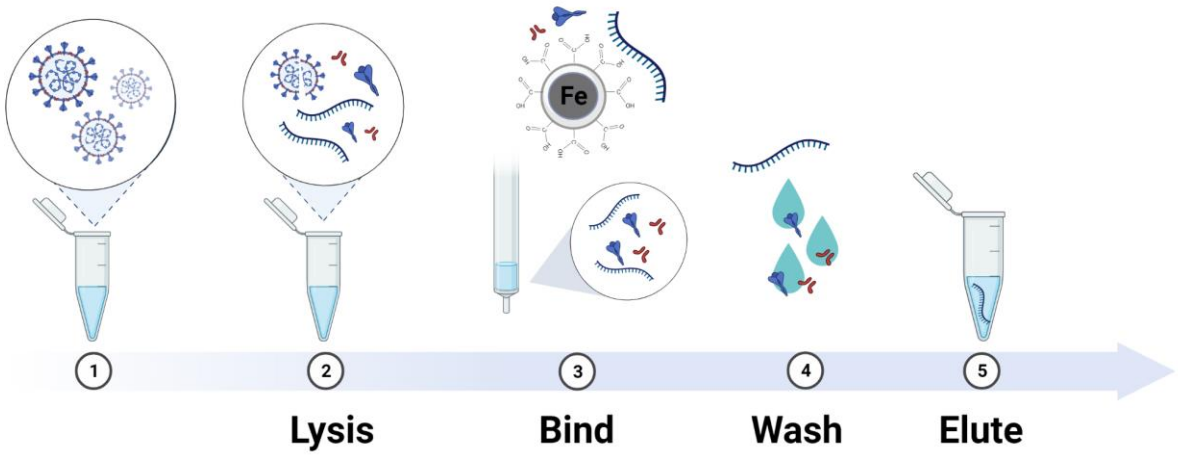

Figure 8: Brief schematic representation of RNA extraction procedure (GenEpi-BioTrain Programme, January 2024, ECDC)

The binding of RNA onto the membrane is implemented by (i) lowering the pH using a so-called binding buffer, so that the oxygen containing groups of the silica get in their conjugate acid form and attract the negatively charged RNA, (ii) introducing chaotropic salts, to disengage water molecules that surround RNA and, (iii) introducing isopropanol, to make RNA molecules less polar by lowering the dielectric constant. The extraction procedure proceeds with washing steps, during which the membrane gets cleaned of impurities and salts, usually using ethanol containing buffers. Each buffer addition in the spin column is followed by micro-centrifugation.

The elution of RNA is carried out with the addition of RNase-free water, which increases the pH and unbinds the nucleic acid from the membrane.

The frequent complexity of initial samples, as well as, the sensitivity of the following Polymerase Chain Reaction (PCR) analysis, often require a clean-up procedure of the RNA extract. Contaminants such as polyphenolic compounds, humic/fulvic acids, tannins, melanin, etc. act as inhibitors for downstream enzymatic reactions like PCR. PCR inhibitors exert their effects by interacting directly with DNA or the PCR enzymes. Their direct binding to DNA can prevent amplification, while their direct interaction with DNA polymerase can block the enzymes' activity. The removal of inhibitors or the reduction of their effects has been extensively studied and several methods have been proposed (Schrader et al., 2012). Commercial, ready to use kits are broadly used for that purpose too, and usually utilize spin columns for micro-centrifugal ultrafiltration.

1.4.3 Reverse Transcription Real-Time PCR (RT-PCR) principles

Polymerase Chain Reaction has been used for detecting a wide variety of templates across a range of scientific fields, like virology. A pair of synthetic oligonucleotides (primers) is used to hybridize with each strand of a double-stranded DNA target and defines the region that will be amplified. The hybridized primer acts as a substrate for a DNA polymerase, which commonly is Taq polymerase. Taq polymerase is derived from the bacterium Thermus aquaticus and is known for its heat stability. DNA polymerase adds deoxynucleotides sequentially and creates a complementary strand. In brief, the steps of the process are as follows: (1) denaturation - separation of the double-stranded DNA at temperatures >90°C, (2) primer annealing at 50–75°C to promote primer binding to the template, and (3) extension of the complementary DNA strand at 72–78°C (**Figure 9**). The rate of temperature change (ramp rate), the duration of the incubation at each temperature and the number of times each set of temperatures (or cycle) is repeated, are programmed and controlled by a thermal cycler (Mackay et al., 2002).

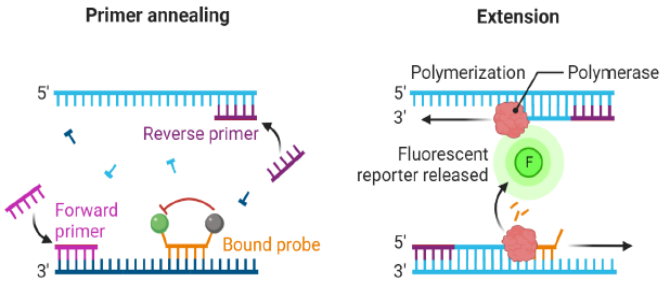

Figure 9: Fluorescent probe-based RT-PCR (GenEpi-BioTrain Programme, January 2024, ECDC)

In cases where RNA is the initial template, a reverse transcription step is needed prior to PCR-based amplification. During this step, RNA is reverse transcribed into its DNA complement by the use of a reverse transcriptase, resulting in the formation of cDNA. Newly synthesized cDNA becomes the template for the following DNA amplification.

Some of the traditional methods for amplified DNA detection include gel electrophoresis, southern blot and PCR-ELISA. However, all these methods are carried out upon reaction completion and are either time-consuming or require special handling due to harmful chemicals and/or multiple steps of processing, risking amplicons' integrity. In contrast to these conventional assays, the detection of amplicon can be visualized as the amplification progresses, by real-time PCR, an approach that has provided insights into the kinetics of the reaction. The labeling of primers, probes[6] or even the amplicon with fluorogenic molecules has made the monitoring of the amplicon, during its accumulation in real-time, possible.

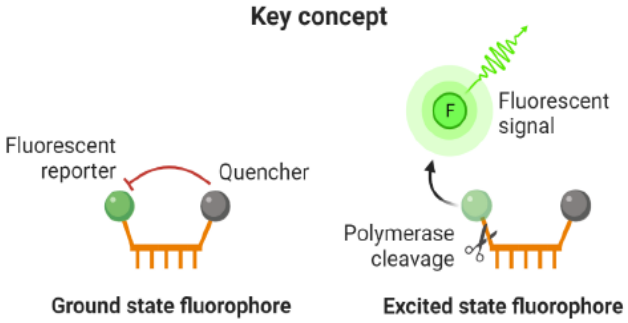

Figure 10: Key concept of fluorescence mechanism (GenEpi-BioTrain Programme, January 2024, ECDC)

Therefore, the detection of amplicon is accomplished by fluorescence (**Figure 9 and Figure 10**). This physical phenomenon is the outcome of either fluorescent dyes (commonly SYBR Green I) or hydrolysis probes (commonly TaqMan) (Bustin & Mueller, 2005). Fluorescent dyes intercalate with the newly synthesized double-stranded DNA, emitting fluorescence. At the end of each thermal cycle, the signal is measured, and the quantity of double-stranded DNA is determined. However, fluorescent dyes allow for detection of non-specific PCR products, such as primer dimers[7], in contrast to the fluorescent-labeled probes, which detect the amount of specific double-stranded DNA sequences. Probes with a fluorescent

[6] Probes are short, single-stranded DNA sequences and their primary function is to detect specifically the target DNA sequence within the amplified region. The hybridization of the probe to its complementary sequence is the cornerstone of the most popular real-time PCR chemistries (Gyllensten et al., 1988).

[7] Two primer molecules that have attached (hybridized) to each other because of strings of complementary bases in the primers. *Wikipedia*, 2023, https://en.wikipedia.org/wiki/Primer_dimer#:~:text=A%20primer%20dimer%20(PD)%20is,complementary%20bases%20in%20the%20primers.

reporter dye at the one end and a quencher dye at the other end, bind to sequences of interest during the annealing step. During extension, DNA polymerase displaces and cleaves the reporter dye. The separation of the reporter dye from the quencher dye emits fluorescent signal at the end of each PCR cycle (**Figure 9 and Figure 10**) (Mackay et al., 2002; Bustin & Mueller, 2005).

Fluorescent chemistries require both a specific input of energy for excitation and a system that allows for a particular emitted wavelength detection. The three common ways by which excitation energy can be supplied are (i) by lamp, (ii) by light-emitting diode (LED) or (iii) laser (Valasek and Repa, 2005). To record data, the energy emitted is monitored by the fluorescence detection system. Fluorescence detectors can be charge-coupled device cameras, photomultiplier tubes, or other types of photodetectors. Filters or channels of narrow wavelength are implemented to allow only the desired wavelength to reach the photodetector and be measured. Contemporary instruments usually have the ability of multiplex analysis, that is, running multiple assays in a single reaction tube, by measuring multiple discrete wavelengths at once (Navarro et al., 2015).

The quantitative analysis of the detected fluorescence is performed during the assay by the respective software, which displays the recorded fluorescence intensity versus cycle number, as a DNA amplification curve (Valasek and Repa, 2005). The ideal amplification curve is a typical sigmoidal growth curve (**Figure 11**). At early stages, amplification cannot be detected because of the background noise. The point at which the fluorescence becomes clearly detectable is called the threshold cycle (Ct). The Ct value is inversely proportional to the amount of the target sequence in the original sample and is vital for its subsequent quantification (Mackay et al., 2002).

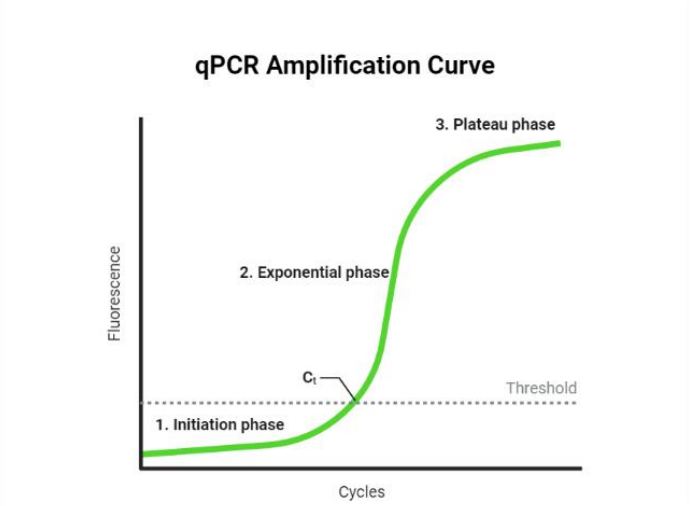

Figure 11: Typical qPCR amplification curve, (BioRender, https://www.biorender.com/template/qpcr-amplification-curve)

After the Ct point of the assay, there is enough amplicon present and the amplification rate enters a log-linear phase. Under optimal conditions, the amount of amplicon increases approximately one log10 for every three cycles. The reaction slows and enters a transition phase when the primers and the enzyme become limiting and the PCR products become inhibitory to the amplicon. Eventually, the reaction and consequently the amplification curve reaches a plateau phase, during which there is little or no increase in product yield (Mackay et al., 2002).

1.4.4 RT-PCR product quantification

The amount of amplified template produced by RT-PCR can be determined in two ways: as relative and as absolute quantification.

Relative quantification compares the expression level of a target gene in samples with different treatments. An internal reference gene, or housekeeping gene, is used to create a dilution series. As a housekeeping gene can be used any gene with known concentration and amplicon length. It is also assumed to have constant expression across different samples. During the RT-PCR assay the target gene Ct value is compared directly to the reference genes' Ct. Therefore, by relative quantification the targets' abundance is expressed in relation to a reference gene, instead of providing an absolute measure of targets' concentration (Bustin, 2000).

On the contrary, absolute quantification determines the precise transcript copy number, by comparing the Ct value of the sample of interest with a standard curve (Livak and Schmittgen, 2001). To create a standard curve, samples of different, known concentrations need to be prepared and subjected to RT-PCR analysis. The standard curve is constructed by plotting the exact RNA concentrations against their Ct values (**Figure 12**).

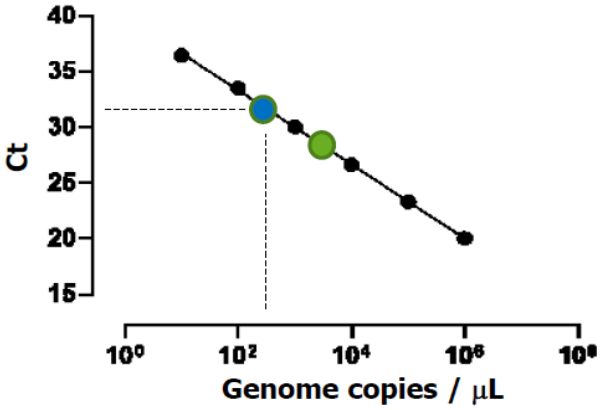

Figure 12: Typical standard qPCR curve for nucleic acid absolute quantification (GenEpi-BioTrain Programme, January 2024, ECDC)

In general, relative quantification is simpler to develop and provides sufficient information. When monitoring the progress of an infection, however, the results can be expressed in units that are common to both scientists and clinicians by absolute quantification. Absolute

quantification may also be necessary when the demonstration of changes in virus levels is difficult due to the lack of sequential specimens (Mackay et al., 2002).

1.4.5 Population size normalization – Human fecal control

The SARS-CoV-2 viral load in wastewater should be in a way related to the population served by the WWTP. However, census data and the capacity of the WWTP are static measures of the population size. In cases where WWTPs receive influent from adjacent towns or have mobile populations due to tourism, commuting or part-time residents (Maal-Bared et al. 2023), dynamic population estimates are of interest. Dynamic population in WBE for viruses is used to provide information on these community changes and to verify whether the fluctuations in viral loads are a result of changes in viral shedding rate, increasing infections or variations in the size of the population (Been et al., 2014).

The estimation of dynamic population is conducted by using wastewater characteristics or biomarkers, as normalization factors, as they account, directly or indirectly, for human fecal contribution in the wastewater. They can be endogenous or exogenous physical, chemical or biological biomarkers. Examples of broadly used factors for population normalization include the wastewater flow rate, ammonium nitrogen and several human fecal indicator organisms (bacteria and viruses that shed exclusively via human feces), such as the Pepper Mild Mottle Virus (PMMoV) and crAssphage. The measured pathogen viral nucleic acid concentrations are normalized by the biomarker of choice concentrations to account for differences in wastewater fecal strength and viral nucleic acid recovery (Arts et al., 2023). Although the normalization of wastewater has been long studied for WBE of SARS-CoV-2, there is no consensus on a single normalization strategy (Rainey et al., 2023).

PMMoV is a plant (pepper) RNA virus that it was found to be one of the most abundant virus types in human feces (Zhang et al., 2005). Its particles are persistent through standard food processing, involving high temperatures and low water activities, hence, food through ingestion is a potential source of PMMoV in human feces. Interestingly, PMMoV has not been detected in fecal samples of most animals. Samples from some animals (e.g. cows, geese, seagulls and chickens) were sometimes positive for PMMoV, but in significantly lower concentrations than those in human feces (Kitajima et al., 2018).

Cross-assembly phage (crAssphage) is a human DNA virus that has recently been proposed as a biomarker for human fecal contamination, since it is totally associated with the human gut

microbiome (Sabar et al., 2022). Koonin and Yutin, 2020, found CrAssphage to be the most abundant human-associated virus found in approximately 50% of human gut viromes, which makes it a suitable candidate for normalization in WBE studies.

Finally, as stated in paragraph 1.3.1, ammonia is an established chemical indicator of human urine content in wastewater, which originates from the hydrolysis of urea. It is also a reliable marker for population normalization, because it mostly originates from humans and not industrial discharges. Ammonia concentration in combination with WWTP flow rate are factors that have been extensively used for the normalization of SARS-CoV-2 WBE.

1.5 Determination of ion concentration

1.5.1 Ultraviolet-Visible Spectrophotometry Principle

UV-VIS spectroscopy is an analytical method for the measurement of the absorption of electromagnetic radiation (EMR) in the wavelength range of UV (100-400 nm) and VIS (400-800) by an atom or molecule, to finally determine the quantity of the substance of interest (or analyte). The method is based on the principles of light absorbance and emission, as a result of electronic transitions.

In most cases, an analyte of interest participates in a chemical reaction, resulting in the formation of a product, called a chromogen[8] (or chromophore), which absorbs light at a specific wavelength, due to its specific functional group. The chromogen exhibits peak absorbance at a wavelength or wavelength range, according to which the measuring wavelength is selected. The quantity of analyte is proportional to the quantity of chromogen produced in the reaction, and hence the analyte concentration in the sample is proportional to the amount of light absorbed by the chromogen (Akash & Rehman, 2020; Bachmann & Miller, 2020).

1.5.2 Components of UV-Vis Spectrophotometer

The components of a spectrophotometer include: i) a light source, ii) a monochromator, consisting of a) an entrance slit, b) a dispersive element and c) an exit slit, iii) a sample device/cuvette and iv) a detector (**Figure 13**).

[8] A chromogen is any structural feature that is present in the molecule and responsible to absorb EMR and hence impart color to the compound (Akash & Rehman, 2020).

Briefly, the light source provides polychromatic light over a wide range of spectrum. Different types of lamps are used for UV and Vis measurements; however, many contemporary instruments utilize a xenon flash lamp, which can cover both the UV and Vis spectra.

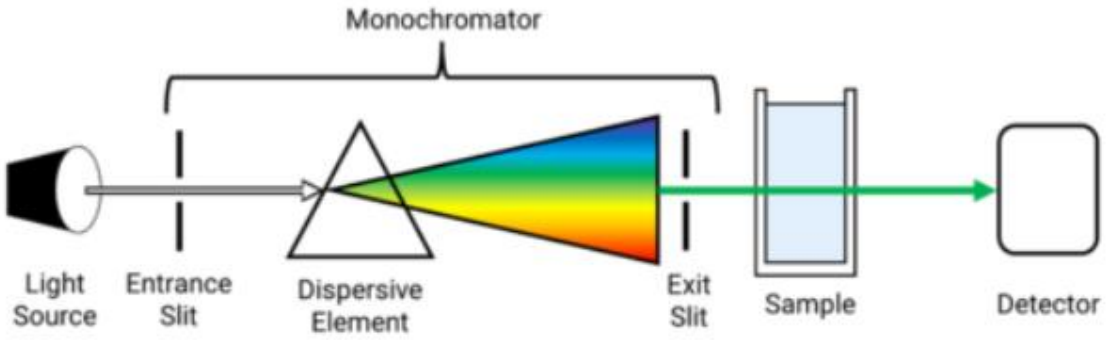

Figure 13: A basic block diagram of the elements in a single beam UV-Visible spectrometer (*Instrumentation of a UV-Visible Spectrophotometer*, Jasco, https://jascoinc.com/learning-center/theory/spectroscopy/uv-vis-spectroscopy/instrumentation/)

The monochromator is the device that receives polychromatic light (white light) and disperses the radiation into monochromatic light. More specifically, the incoming polychromatic beam is defined sharply by the entrance slit and is imparted on the dispersing element, which is usually a prism made up of quartz, fused silica or glass. The dispersing element separates the polychromatic light into visible light spectrum. Then, the exit slit allows the minimal wavelength to pass and reach the sample, which is placed into a cuvette.

Cuvettes vary in respect to shape, size, path length and transmission characteristics of required wavelength and can be made of plastic, glass or optical grade quartz. At the same time, they should not absorb the wavelength range of interest. Finally, the amount of light that passes through the sample reaches the detector, which converts light signals into electrical signals. The most commonly used type of detector is photomultiplier tubes. It contains a cathode with numerous dynodes, which emit numerous electrons for each electron hitting them, and an anode. The produced electrons are accelerated, producing even more electrons, which are collected at the anode. The resulting current is amplified and recorded (Akash & Rehman, 2020).

1.5.3 Beer-Lambert Law

A spectrophotometric measurement is the ratio of I (intensity of transmitted radiation, i.e. intensity of light reaching the photodetector) to I_0 (intensity of incident radiation, i.e., intensity of light before it hits the sample) and is called transmittance (T):

$$\mathbf{T = I/I_0}$$

The transmittance is more commonly converted into absorbance (A):

$$\mathbf{A = \log_{10}(1/T) = -\log_{10}T}$$

Beer-Lambert law describes the linear relationship between absorbance and concentration:

$$\mathbf{A = \varepsilon * b * C}$$

where A is absorbance, ε is molar absorption coefficient[9] [L/(mol*cm)] of the chromogen, b is the path length (cm) of light through the cuvette, and C is concentration (mol/L) of the analyte in the sample.

In visible spectrophotometry the absorption or the transmission of a sample can be determined by the observed color, due to color complementarity. For instance, if a solution absorbs red light (~700 nm), it appears green, because green is the complementary color of red. Practically, VIS spectrophotometers use a monochromator to narrow down a specific range of wavelengths and exclude other wavelengths, so that one particular beam of light passes through the sample solution. The regions of visible spectrum and their complementary colors can be seen in **Table 1**.

[9] Molar absorption coefficient is a physical property of the chromogen and is a measure of how strongly a chemical species absorbs at a given wavelength.

Table 1: Various regions of visible spectrum and their corresponding colours (Akash & Rehman, 2020)

Region	Complementary color	Wavelength (nm)
Violet	Yellow-green	400–435
Blue	Yellow	435–480
Green-blue	Orange	480–490
Blue-green	Red	490–500
Green	Purple	500–560
Yellow-green	Violet	560–580
Yellow	Blue	580–595
Orange	Green-blue	595–650
Red	Blue-green	650–800

1.6 Aims of the study

For this study we received wastewater samples during a broad time frame (Feb 2021 – Oct 2023), which included key societal and pandemic milestones and interventions. Specifically, the study encompasses the period, during which, strict intervention measures (e.g., lockdowns, mandatory face coverings, online lessons, etc.) and their gradual removal were implemented, as well as the start of vaccinations and the emergence of different variants.

During the early stages of the pandemic, Greece had been undergoing restriction measures depending on the amount and severity of human cases in each region. Regions were categorized as of high, medium and low danger levels and surveillance measures of less strictness were implemented respectively, often in an on-off manner, depending on the fluctuations of recorded human cases.

The objectives of the current study were to:

(1) detect and quantify SARS-CoV-2 genetic material in two WWTPs of Crete (Heraklion and Chania), Greece,

(2) determine the potential link between COVID-19 cases and SARS-CoV-2 RNA concentrations in wastewater and the potential use of WBE as a prognostic tool,

(3) better understand the correlation between the physico-chemical characteristics of the wastewater and viral recovery and quantification and

(4) evaluate the impact of in-house and community restrictions during the pandemic, on wastewater viral load, hence human cases, considering the effect of mass vaccinations and variants on viral shedding patterns.

The knowledge gained during this pandemic and the use of WBE is valuable for future management of emerging and challenging public health threats.

CHAPTER 2 – MATERIALS AND METHODS

2.1 Study population – WWTP characteristics

Our data corresponds to the two major WWTPs of Crete, associated to the two biggest cities on the island of Crete, Greece; Chania and Heraklion. These plants serve a population of approximately 97,000 and 200,000 people respectively. Both WWTPs receive wastewater from three hospitals; one general hospital in the case of the town of Chania and one general and one University hospital in the case of the city of Heraklion. Both plants also receive stormwater sewers. Moreover, since the island is one of the major tourist destinations of the country, the two plants receive major sewers from city hotels during the touristic season, that is March to October of each year.

2.2 Sample collection

Samples had been collected and transferred at the Regional Laboratory of Public Health of Crete, which participates at the consortium for the surveillance of SARS-CoV-2 in wastewater at a national level. The rest of the members of the consortium include the Central Laboratory of Public Health, the Regional Laboratory of Public Health of Thessaly, the University of Patra, the Aristotle University of Thessaloniki, the University of Ioannina and the National and Kapodistrian University of Athens. The whole consortium is governed by the National Public Health Organization. The National consortium for WBE was introduced in 2021.

For the purposes of the current study, we focused on the period from February of 2021 until October 2023; the whole surveillance study is still ongoing on a national basis.

Wastewater samples have been collected three times a week (every Tuesday, Thursday, and Friday) from each of the two WWTPs, which gave us a total of six (6) samples on a weekly basis. Approximately 2-6 L composite samples were collected via autosamplers over a 24-hour period (from morning of one day to morning of the next), one liter of which was stored in isothermal boxes with ice packs to preserve temperature at or below 4^{o}C and sent immediately for analysis. A total of 781 samples were analyzed for the needs of the current study, 392 from which were from the WWTP of Chania and 389 from the WWTP of Heraklion.

The autosampler (Hach AS950) at the WWTP of the city of Chania was programmed to collect 80 ml aliquots every 60 minutes, while the autosampler (Endress + Hauser) at the WWTP of the city of Heraklion was programmed to collect 500 ml aliquots every two hours.

Upon receipt, all samples were subsampled for both physico-chemical analyses and molecular testing. All samples were collected prior to the primary treatment trade of the WWTP.

Each sample was accompanied by a document that included data on the location, date, time, and flow rate on the sampling day, the amount of any precipitation events and the results of some physico-chemical testing that was carried out onsite (more details given in paragraph 2.3.6).

2.3 Sample processing

2.3.1 User protection

At first, samples were agitated mechanically to homogenization. Approximately 250 ml of each sample was transferred into 250 ml plastic bottles with internal cap and placed in a water bath at 60°C for 90 minutes for pasteurization. Another 250 ml bottle of each sample was stored without any treatment at -80°C for future analysis.

Heat pasteurization of wastewater samples for viral deactivation is recommended for biosafety reasons, however the extent to which it can damage short RNA fragments is yet unknown, according to the guidelines of Centers for Disease Control and Prevention (CDC, 10 March 2023, https://www.cdc.gov/nwss/testing.html) for Wastewater Surveillance. CDC states, that heat-treating wastewater is reported to improve SARS-CoV-2 measurement, however more data are needed for the confirmation of this effect.

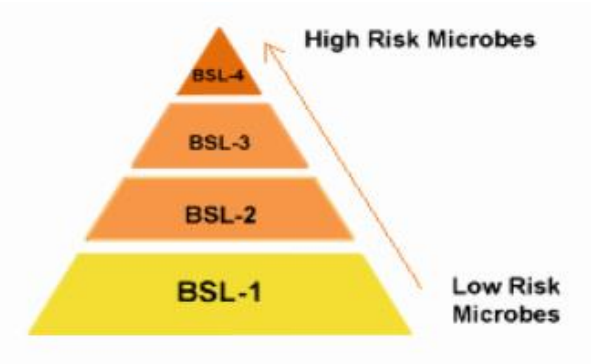

Figure 14: Biosafety Levels built-up (https://www.cdc.gov/training/quicklearns/biosafe

All processes were carried out in a Biosafety Level 3 (BSL3) facility, with unidirectional airflow and BSL-3 precautions[10]. Laboratory personnel wore personal protective equipment (lab coats, gloves, eye protection and face shields). Each BSL builds on the controls of the level before it, as can be seen in **Figure 14.**

[10] All BSL-3 precautions and safety controls can be found in the address https://www.cdc.gov/training/quicklearns/biosafety/, Recognizing the Biosafety Levels, CDC.

Laboratory waste form wastewater samples was autoclaved and managed according to BLS2 biosafety guidelines.

2.3.2 Virus concentration - ultrafiltration

Samples were processed upon receiving at the laboratory. Sample processing was performed according to the protocol of Medema et al. (2020) with slight modifications.

At first, samples were centrifuged at 3500 g (KUBOTA 5800, **Figure 15**) for 15 minutes for particulate matter precipitation. Following centrifugation, 65 ml of the supernatant liquid was introduced into an ultrafiltration device with 10kD cellulose filters (Centricon Plus 70 10K NMWL, MILLIPORE, UFC701008, Merck, **Figure 16**), with the addition of 50 µl ($1x10^5$ copies) Bovine Coronavirus (BCoV) RNA (strain S379 Riems matrix recovery control; GT-molecular; USA) for viral RNA recovery testing, and centrifuged at 3500 g for 40 minutes, or until a ~350µl concentrate was achieved.

Figure 15: KUBOTA 5800 Centrifuge

Figure 16: Centricon Plus 70 10K ultrafiltration device

Following ultrafiltration, concentrated wastewater retained in the cellulose filters was retrieved by centrifugation at 3000 g for 15 minutes, by inverting the filters upside down on an inverted cone. A concentrate of about 250-450 µl was collected, leaving the precipitate behind, and placed in a 1.5 ml sterile collection tube; its exact volume was measured and noted to be used for the normalization at a later stage.

2.3.3 SARS-CoV-2 RNA extraction

Before the extraction process, a further centrifugation of the total concentrate at 4000 g (ThermoScientific, Heraeus, Pico 17 Centrifuge, **Figure 17**) for two (2) minutes was performed to discard as much of the precipitate as possible. 200µl of the supernatant was used for RNA extraction using the AllPrep PowerViral DNA/RNA kit (Qiagen, Hilden, Germany) according to the users' manual, with the addition of 8µl carrier RNA to optimize the final extracted RNA concentration. The extraction procedure is described and explained based on the AllPrep PowerViral DNA/RNA kit Handbook.

Figure 17: ThermoScientific, Heraeus, Pico 17 Centrifuge

The components of the AllPrep PowerViral DNA/RNA kit are shown in **Table 2**.

Table 2: Kit components

AllPrep PowerViral DNA/RNA Kit	(50)
Catalog no.	28000-50
Number of preps	50
PowerBead Tubes, Glass 0.1 mm	50
MB Spin Columns	50
Solution PM1	55 ml
Solution IRS	15 ml
Solution PM3	36 ml
Solution PM4	3 x 24 ml
Solution PM5	30 ml
RNase-Free Water	10 ml
Collection Tubes (2.2 ml)	2 x 25
Collection Tubes (2 ml)	4 x 50
Quick Start Protocol	1

Before the extraction process, the solution PM1, which contains guanidinium thiocyanate, needed to be warmed at 55oC for 10 min for precipitates to dissolve, and was used while still warm. Given that this extraction kit aims to isolate DNA and RNA, a mixture of PM1 and β-mercaptoethanol needed to be prepared to achieve RNA isolation, as β-mercaptoethanol aids in ribonuclease (RNase) deactivation. The final β-ME concentration should be 10 µl/ml. The RNA extraction procedure was carried out as follows:

1. 200 µl of the viral concentrate were placed into a 2 ml collection tube and 600 µl of the PM1/β-ME mixture were added. A further addition of 8 µl of Carrier RNA was implemented to optimize RNA recovery. The mixture was agitated by vortexing for 30s and incubated for 5 min at room temperature.
2. 150 µl of Solution IRS were then added, the solution was vortexed briefly to mix and was incubated at 4°C for 5 min.
3. After incubation, the mixture was centrifuged at 13,000 x g for 1 min. Avoiding the pellet, 700 µl of the supernatant were transferred to a clean 2.2 ml Collection Tube.
4. 600 µl each of Solution PM3 and Solution PM4 were added to the 2.2 ml collection tube and the mix was vortexed briefly. Solution PM3 contains guanidine hydrochloride and a surfactant agent (t-Octylphenoxypolyethoxyethanol) and leads to the capture of the total nucleic acid content in lysates on the MB Spin Column filter membrane. Solution PM4 contains ethanol.
5. 625 µl of the mix were transferred into an MB Spin Column and centrifuged at 13,000 x g for 1 min. The flow through was discarded. This step was repeated two more times, until all the supernatant had been loaded onto the MB Spin Column.
6. Solution PM5, which contains isopropanol, was mechanically shaken to mix and 600 µl were added to the MB Spin Column for washing. The spin column was then subjected to centrifugation at 13,000 x g for 1 min. The flow through was discarded.
7. 600 µl of Solution PM4 were added to the spin column for further washing by centrifugation at 13,000 x g for 1 min. The flow-through was discarded and the spin column was subjected to further centrifugation until dry at 13,000 x g for 2 min.
8. The MB Spin Column was placed in a clean 2 ml Collection Tube and 100 µl of RNase-Free Water were added to the center of the MB Spin Column membrane. The membrane with the RNase-free water was incubated for at least 1 min.
9. The RNA extract was obtained after centrifugation at 13,000 x g for 1 min and the MB Spin Column was discarded.

Figure 18 schematically represents the extraction procedure. The use of PowerBead Tubes was omitted since sample bead beating was not performed.

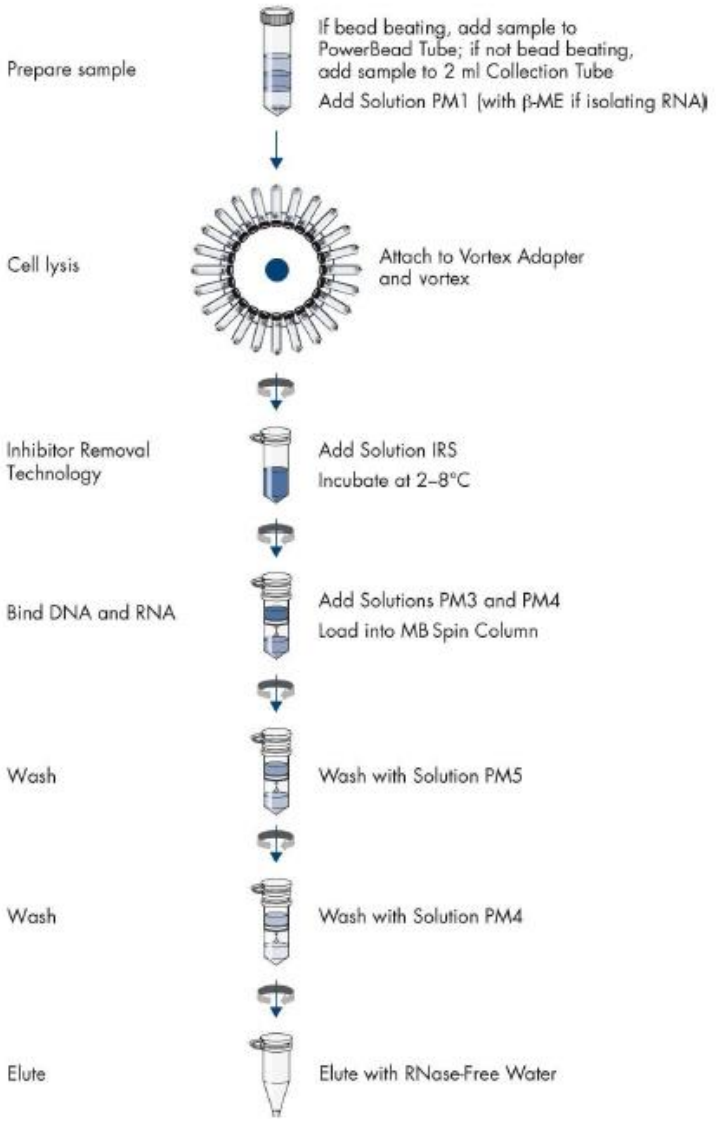

Figure 18: AllPrep PowerViral DNA/RNA kit procedure

2.3.4 Inhibitor Removal

The eluted RNA (100μl) was processed with the use of the OneStep PCR Inhibitor kit (Zymo Research, California) to remove as many of the remaining inhibitors as possible. The columns that the kit utilizes contain a matrix that has been specifically designed for efficient removal of polyphenolic compounds, humic/fulvic acids, tannins, melanin, etc. The protocol (https://files.zymoresearch.com/protocols/_d6030_onestep_pcr_inhibitor_removal_kit.pdf) is described below:

1. The column with the matrix was inserted into a collection tube, provided with the kit.
2. 600 μl of the Prep-Solution were added to the column and the column was subjected to centrifugation at 8,000 x g for 3 minutes.
3. The prepared column was transferred to a sterilized 1.5 ml microcentrifuge tube and the RNA extract (100 μl) was added to the column.
4. The final RNA eluate was obtained after centrifugation at 16,000 x g for 3 minutes.

All RNA extracts were kept at -80oC upon PCR analysis.

2.3.5 qPCR processes and RNA quantification

Rdrp SARS-CoV-2 gene (Protisvalor, France) was used in unknown samples to test the effect of inhibitors, while BCoV was used to determine the viral recovery. The actual concentrations of Rdrp SARS-CoV-2 and of BCoV were determined by digital Real-time PCR (QIAcuity One, Qiagen, **Figure 19**).

For BCoV quantification we spiked each wastewater sample prior to processing, with 50μl of aliquoted virus, which contained 10^5 RNA copies. The RT-Digital PCR protocol and quantities were prepared according to the manufacturers' instructions and the cycling program was carried out as follows: one cycle at 50 °C for 30 min, followed by one cycle at 95 °C for 2 min and then 45 cycles of 10 s at 95 °C and 30 s at 55°C.

Figure 19: QIAcuity One digital RT-PCR, Qiagen

The molecular detection of the virus was performed with the Water-Sars-Cov-2 Real-time PCR kit (IDEXX, USA) that targets both N1 and N2 genes and the quantification of the amplified RNA was performed through a standard curve, developed by 10-fold serial dilutions, with the

EURM-019 standard. The assay limit of detection was set at approximately one (1) RNA copy per reaction. Real time RT-qPCR assay was performed in triplicates on a Mic - qPCR cycler (Bio Molecular Systems, Australia, **Figure 20**).

Briefly, each reaction contained 10 μL SARS-CoV-2 Mix, 10 μL of RNA MMix and 5 μL purified RNA sample in a total volume of 25 μL. The cycler was programmed as follows: one reverse transcription cycle for 15 min at 50 °C, followed by denaturation cycle with 1 min duration at 95 °C and 45 amplification cycles, each consisting of 15 sec at 95 °C and 30 sec at 60 °C.

Figure 20: Mic - qPCR cycler (Bio Molecular Systems, Australia)

6-Carboxyfluorescein (6-FAM) was used as a reporter dye at the 5' label. 6-FAM is a fluorescent dye with an absorption wavelength of 495 nm and an emission wavelength of 517 nm (**Figure 21**). Black Hole Quencher – 1 (BHQ-1) was used at the 3' label.

As positive control was used the N1 SARS-CoV-2 target provided with the PCR kit (IDEXX, USA) and as negative control was used RNAse free water. Controls were included in each run. Reactions were considered positive if the cycle threshold was below 40 cycles.

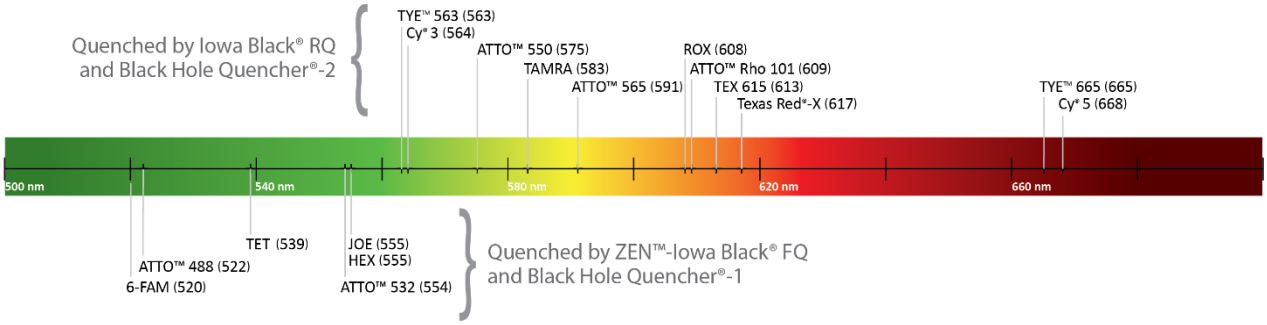

Figure 21: Emission wavelengths of reporter dyes and the appropriate quenchers (IDT, Integrated DNA Technologies, https://www.idtdna.com/pages/education/decoded/article/qpcr-probes-selecting-the-best-reporter-dye-and-quencher)

2.3.6 Physico-chemical water quality parameters

Both participating WWTPs provided data on influent flows in m^3 per day, temperature (°C), biochemical oxygen demand (BOD, mg/L), chemical oxygen demand (COD, mg/L), pH, total Nitrogen, and total suspended solids (TSS, mg/L) for the day of sampling. Influent flow and temperature data were measured in real-time using automated controllers.

Figure 22: SevenCompact pH meter S220 (Mettler-Toledo, US)

Upon arrival of the samples at the laboratory, pH, conductivity, ammonium nitrogen, ortho-phosphate, and chloride ions concentration were determined. pH was determined by the use of SevenCompact pH meter S220 (Mettler-Toledo, US) (**Figure 22**). The pH meter was calibrated by the use of three calibration buffers at pH 4,7 and 10 supplied by Merck Millipore and quality control was performed once a month, by measuring a Certified Reference Material pH buffer at pH 7.41, supplied by Merck Millipore.

Figure 23: Cond 7110 Conductivity Benchtop Meter with a TetraCon 325 electrode (WTW, Xylem Analytics, Germany)

Conductivity was determined using a Cond 7110 Conductivity Benchtop Meter with a TetraCon 325 electrode (WTW, Xylem Analytics, Germany) (**Figure 23**). The instrument was calibrated according to manufacturers' instructions, by the use of a conductivity potassium chloride buffer at 1,41 mS/cm, supplied by Merck Millipore. Quality control was performed once a month by the use of the same buffer.

Ions were quantified by spectrophotometric analysis (Spectroquant prove 300, Merck) following the corresponding test kit protocol for each ion, commercially prepared by Merck (Darmstadt, Germany). All protocols are in accordance with the "Standard Methods for the Examination of Water and Wastewater", published by the American Public Health Association (APHA) (Lipps et al., 2023) and all instruments are officially certified for proper operation.

The Spectroquant prove 300 instrument (**Figure 24**) comes with electronically stored calibration functions for all test kits. The calibration curves were tested for their performance by certified materials, as explained below. Measurement values can be immediately read off from the display, expressed in the desired form. Methods corresponding to the test kits which belong to Spectroquant analysis system are automatically selected by the instrument when the respective bar code is inserted into the spectrophotometer. Cells of different path lengths are also automatically identified, and the correct measuring range is selected.

Figure 24: Spectroquant prove 300 spectrophotometer (Merck)

It is worth noting that due to the complexity and turbidity of the wastewater samples, they were all subjected to filtration by Whatman Polyvinylidene Difluoride (PVDF) syringe filters of 45 μm pore diameter prior to spectrophotometric analysis.

A sample-blank measurement of each wastewater sample took place prior to analysis, to eliminate background signal due to the turbidity and/or color of the filtered wastewater sample.

A reagent-blank sample for each described below method was prepared and measured, every twenty (20) measurements performed, according to the procedure steps, but using distilled (DI) water instead of wastewater sample, to determine contamination in the DI system or reagents.

A zero-test using just DI water was performed as programmed by the instrument, each time ten (10) samples were analyzed, to assess the purity and the absence of turbidity in the DI system, as well as the good quality of the measuring cuvette.

Ammonium Nitrogen ($NH4^+$ -N) quantification - Ammonium test kit (Cat. No. 1006830001, Merck)

The method is analogous to APHA 4500-NH3 F. The measuring range of the kit is 2.0-150 ± 0.51 mg/l $NH4^+$ -N. The calibration curve of the method, as listed in the test kit Certificate of Analysis (CoA), can be found in **Appendix 6.1**. The evaluation of the calibration curve as well as the precision of the method was performed once a month by the use of a Certified Reference

Material standard solution supplied by Merck Millipore (Ammonium CRM Standard solution 50 mg/l NH_4-N in H_2O). The standard solutions' concentration was chosen so that its concentration was within the expected range of the samples.

Method Principle:

Ammonium Nitrogen ($NH4^+$ -N) occurs partially in the form of ammonium ions and partly as ammonia. A pH-dependent equilibrium exists between the two forms. In strongly alkaline solution ammonium nitrogen is present almost exclusively as ammonia, which reacts with hypochlorite ions to form monochloramine, which in turn reacts with 2-chlorphenol or Thymol to form indophenol blue. This is then determined photometrically at 690 nm. Because of the inherent yellow coloration of the reagent blank, the measured solution is greenish-yellow towards green.

Kit Components:

1. Reagent NH4-1
2. Reagent NH4-2 (contains sodium nitroprusside, troclosene sodium, dihydrate)

Test kit protocol:

1. 5 ml of Reagent NH4-1 were pipetted into a test tube.
2. 0.2 ml of pretreated sample were added into the test tube and the mixture was mechanically agitated
3. 1 microspoon of Reagent NH4-2 was added into the test tube and the mixture was vigorously agitated until the reagent was completely dissolved.
4. The solution was left to stand for 15 min (reaction time) and then placed into a 10 mm cell for photometric measurement.

Chloride quantification – Chloride test kit (Cat. No. 1148970001, Merck)

The method is analogous to APHA 4500-Cl- E. The measuring range of the kit is 2.5-250 ± 0.14 mg/l Cl^-. The calibration curves of the method, as listed in the test kit Certificate of Analysis (CoA), can be found in **Appendix 6.2**. The evaluation of the calibration curve as well as the precision of the method was performed once a month by the use of a Certified Reference Material standard solution supplied by Merck Millipore (Chloride CRM Standard solution 250 mg/l Cl^- in H_2O). The standard solution was diluted using volumetric flasks to 100 mg/l final concentration, to lay within the expected range of the samples.

Method principle:

Chloride ions react with mercury (II) thiocyanate to form the mercury (II) chloride. The thiocyanate released during the process, reacts with iron (III) ions to form red iron (III) thiocyanate which is determined photometrically at 445 nm.

Kit Components:

1. Reagent Cl-1
2. Reagent Cl-2 (contains Methanol, Mercury (II) thiocyanate)

Test kit protocol:

1. 1 ml of pre-treated sample was pipetted into a test tube.
2. 2.5 ml of Reagent Cl-1 were added to the sample and the solution was agitated to mix.
3. 0.5 ml of Reagent Cl-2 were added to the solution and the mixture was agitated.
4. The sample was left to stand for exactly 1 min (reaction time) and then placed into a 10 mm cell for photometric measurement.

In some cases, a 1:2 dilution of the sample with Milli-Q water was needed, due to the high chloride concentration of samples.

Orthophosphate quantification – Phosphate test kit (Cat. No. 1148420001, Merck)

The method is analogous to APHA 4500-P C. The measuring range of the kit is 1.5-92 ± 0.06 mg/l PO_4^{3-}. The calibration curves of the method, as listed in the test kit Certificate of Analysis (CoA), can be found in **Appendix 6.3**. The evaluation of the calibration curve as well as the precision of the method was performed once a month by the use of a Certified Reference Material standard solution supplied by Merck Millipore (Phosphate CRM Standard solution 1000 mg/l PO_4 in H_2O). The standard solution was diluted using volumetric flasks to 20 mg/l final concentration, to lay within the expected range of the samples.

Method principle:

Orthophosphate ions in sulfuric solution react with ammonium vanadate and ammonium heptamolybdate to form orange-yellow molybdovanadophosphoric acid that is determined photometrically at 410 nm.

Kit Components:

1. Reagent PO_4-1 (contains sulfuric acid)

Test kit protocol:

1. 5 ml of pre-treated sample were pipetted into a test tube.
2. 1.2 ml of Reagent PO_4-1 were added to the sample and mixed.
3. The sample was placed into a 10 mm cell for photometric measurement.

2.4 Determination of inhibition and recovery efficiency

The efficiency of the methods used in recovering SARS-CoV-2 from wastewater was determined by calculating the inhibition and viral recovery.

The effect of inhibitors was tested with the addition of known concentration (1µl) of the Rdrp Sars-cov-2 gene (Protisvalor, France) in unknown samples. Un-spiked wastewater samples were also analyzed to help in accurate estimation of inhibition. All spiking was done in triplicate. The equation given below was used to assess the inhibition of the process:

$$\%\ \text{Inhibition} = 100 - \left(\frac{(\text{with spike} - \text{no spike})}{\text{water spike}}\right) \text{x } 100$$

Viral recovery was determined by calculating the percentage of BCoV regained, as follows:

$$\text{viral recovery } \% = \frac{[\text{BCoV measured}]}{[\text{BCoV expected}]} \text{ x } 100$$

The final concentration of the virus was calculated according to the following equation:

$$\text{C recovery adjusted} = \text{C x } \frac{100\ \%}{\text{BCR } \%}$$

2.5 Viral load normalization

The results were given in gene copies/L:

$$= \frac{1000}{65\ \text{ml}} \text{ x } \frac{\text{RNA copies}}{65\ \text{ml}} \text{ x dilution factor}$$

where:

$$\frac{\text{RNA copies}}{65\text{ ml}} = \frac{\text{RNA copies}}{\mu\text{l}} \text{ x } 100 \text{ x } \frac{\text{total volume of concetrate}}{\text{extracted volume of conentrate}}$$

gene copies/100,000 population based on the population officially served from each WWTP:

$$= \frac{\frac{\text{RNA copies}}{\text{L}} \text{ x } 1000 \text{ x flow rate x } 10^5}{\text{population served by each WWTP}}$$

and in gene copies/100,000 dynamic population based on the concentration of ammonium nitrogen.

$$= \frac{\frac{\text{RNA copies}}{\text{L}} \text{x } 1000 \text{ x flow rate x } 10^5}{\text{dynamic population based on ammonium nitrogen}}$$

The dynamic population was estimated considering the typical NH_4^+-N excretion per individual per day, as follows:

$$\text{Dynamic population} = \frac{\text{Ammonium Nitrogen Concentration } \left(\frac{\text{mg}}{\text{l}}\right) \text{x flow rate}}{7}$$

2.6 COVID-19 cases and wastewater viral load cross-correlations

2.6.1 Data Smoothing

To perform the calculations on the RNA gene copy data against the COVID-19 cases, as well as, the physico-chemical factors of the wastewater samples, a 5-day moving average was used. This average reduced the noise introduced by day-to-day variability and highlighted the overall trends which might have been obscured by the daily fluctuations.

The 5-day moving average smoothing was implemented both for the viral load in wastewater and the human cases, to cover the lack of daily data on viral load, in contrast to the human cases; we only received three (3) samples per city per week, whereas human cases were recorded on a daily basis.

2.6.2 Cross-correlation

Spearman correlation was applied to reveal any potential correlation between viral gene copies in wastewater and human cases. The choice of Spearman correlation was made since it is a non-parametric one to describe if two variables X and Y are related by any monotonic function.

The Spearman correlation coefficient value varies between -1 and +1. We conclude positive correlation if the correlation coefficient is positive and strong correlation the closer it gets to 1.

More specifically, the value of the Spearman correlation coefficient indicated the direction of the association between the variables. If the value was positive, an increase in X led to an increase in Y as well. If the sign was negative, an increase in X led to a decrease in Y.

Along with the abovementioned correlation, a p-value was also calculated, to indicate the probability of recording the observed correlation if no actual correlation existed.

2.6.3 Time lagged cross-correlation

We calculated the time lagged cross-correlation (TLCC) by calculating the Spearman correlation, while we shifted the Y variable forward and backward by a preset of a maximum temporal shift (lag).

For each lag, a p-value was also reported; in cases where the p-value was > 0.05, the estimated correlation was disregarded.

The purpose of this analysis was to evaluate the time gap between the fluctuations of the viral load in wastewater and the respective fluctuations in human cases and denote which factor preceded, for the whole study period.

CHAPTER 3 – RESULTS AND DISCUSSION

3.1 Standard and amplification curves

We have collected and tested a total of 771 samples until today and the surveillance is still in progress. The molecular analysis of the samples was performed once or twice per week by real-time PCR.

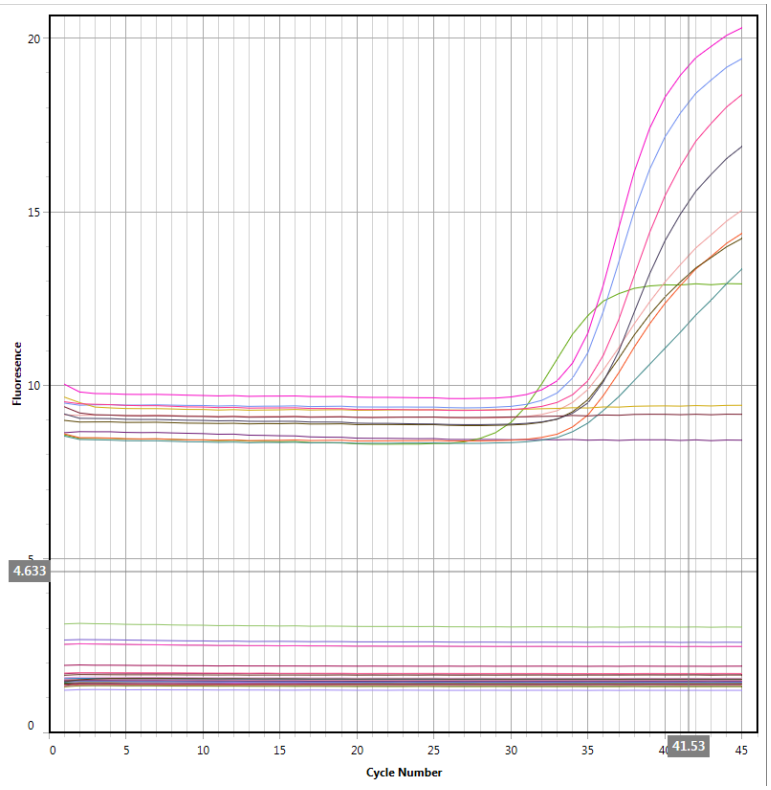

Figure 25: Amplification curves of wastewater viral RNA extracts (x axis – cycle number, y axis - fluorescence)

The molecular detection of the virus was performed with the Water-Sars-Cov-2 Real-time PCR kit (IDEXX, USA) that targets both N1 and N2 genes. A representative example of the obtained amplification curves is presented in **Figure 25**, as acquired via the Mic-PCR cycler software. The sigmoidal green curve with a Ct value ~ 28 cycles is the assays' positive control.

The quantification of the amplified RNA was performed through a standard curve, developed by 10-fold serial dilutions, with the EURM-019 standard (**Figure 27**). The assay limit of detection was set at approximately one (1) RNA copy per reaction. The coefficient of determination was R^2 = 0.9986, indicating strong liner relationship between Ct values and standard concentrations (serial dilutions). The amplification plot of the standard curve is presented in **Figure 26**.

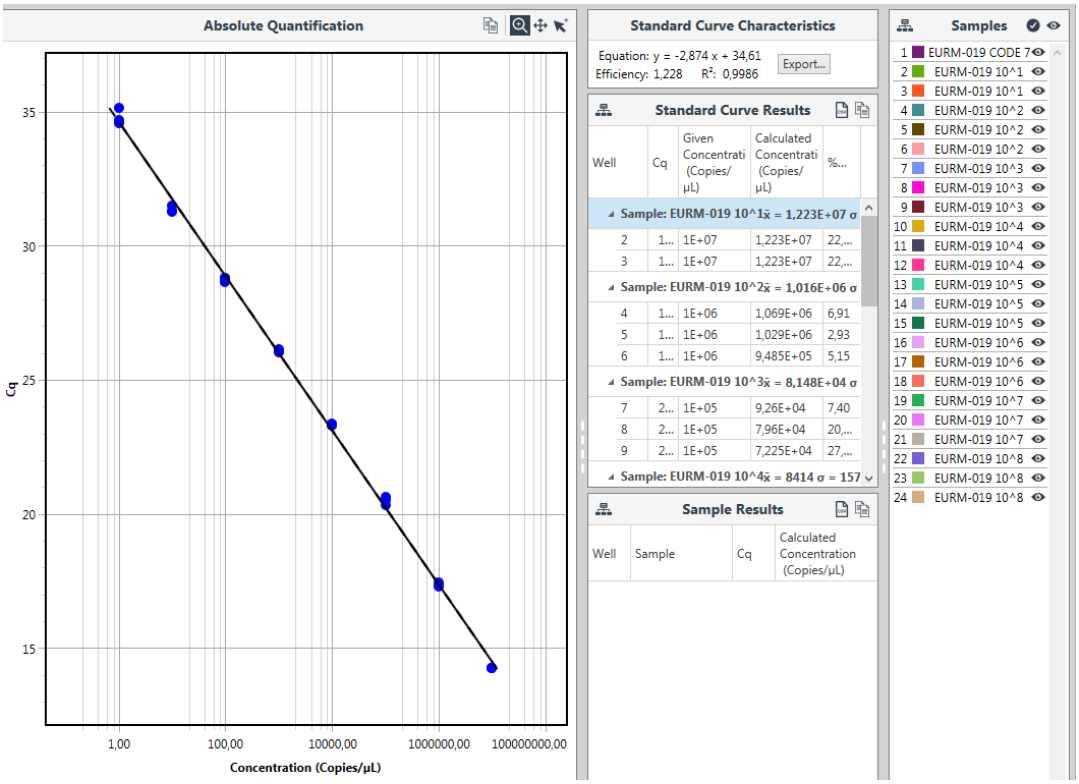

Figure 27: Standard curve constructed with the EURM-019 standard by serial dilutions and in triplicates (x axis – Concentration (copies/µl), y axis – Ct number)

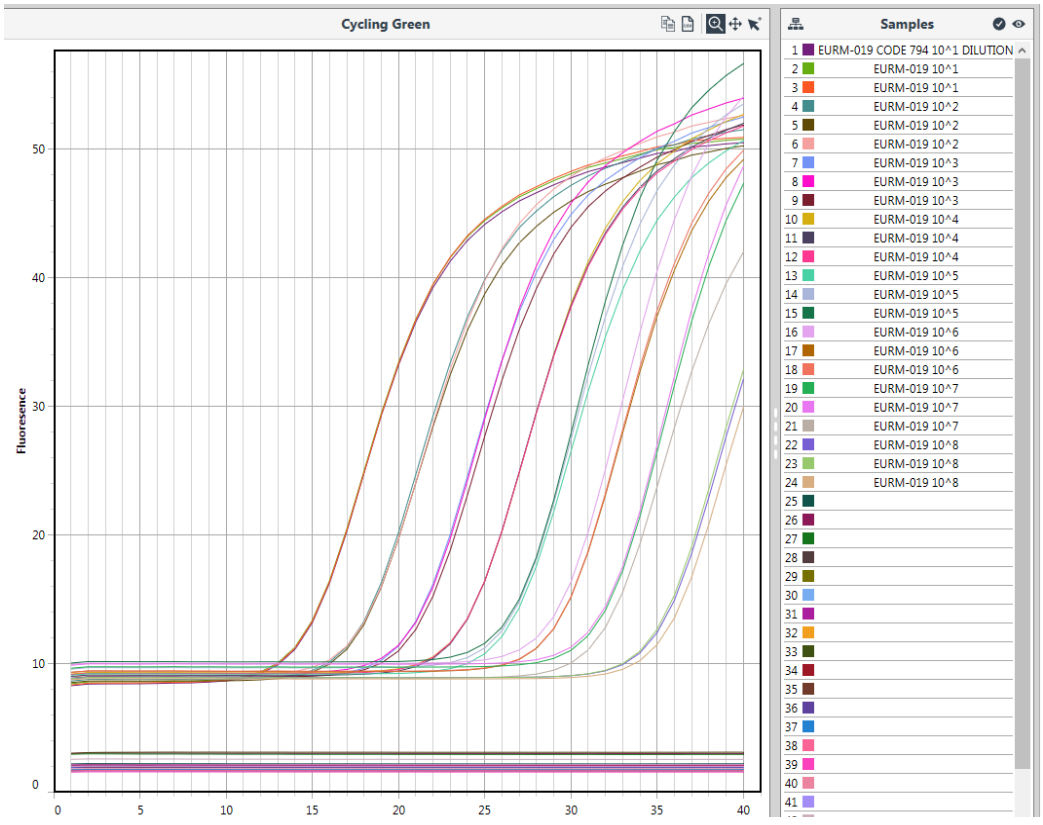

Figure 26: Standard amplification curves (x axis – cycle number, y axis - fluorescence)

3.2 Raw data input and processing

Viral concentrations as obtained by the RT-PCR, were registered on a daily basis in an extensive database for SARS-CoV-2 surveillance, constructed in our laboratory, alongside with the physicochemical characteristics of each sample, for both cities (**Appendices 6.4 and 6.5**). The expression of viral concentration was normalized in this database as well, by using the respective equations described in paragraphs 2.4 and 2.5.

3.3 COVID-19 surveillance data

Data for the local COVID-19 cases for both cities (Chania and Heraklion) were provided from the Hellenic National Public Health Organization.

Data concerning restriction measures that were implemented during the period under investigation were obtained from the Hellenic Institute for Occupational Health and Safety (https://www.elinyae.gr/en). All restriction measures were recorded in an extensive database (**Appendix 6.6**) for further processing.

Since we did not test for variant distribution in wastewater samples, we relied on the data retrieved from human cases. For the period of interest, data were collected from the web site https://covariants.org/per-country. **Figure 28** represents the variant distribution in Greece from August 2020 to January 2024.

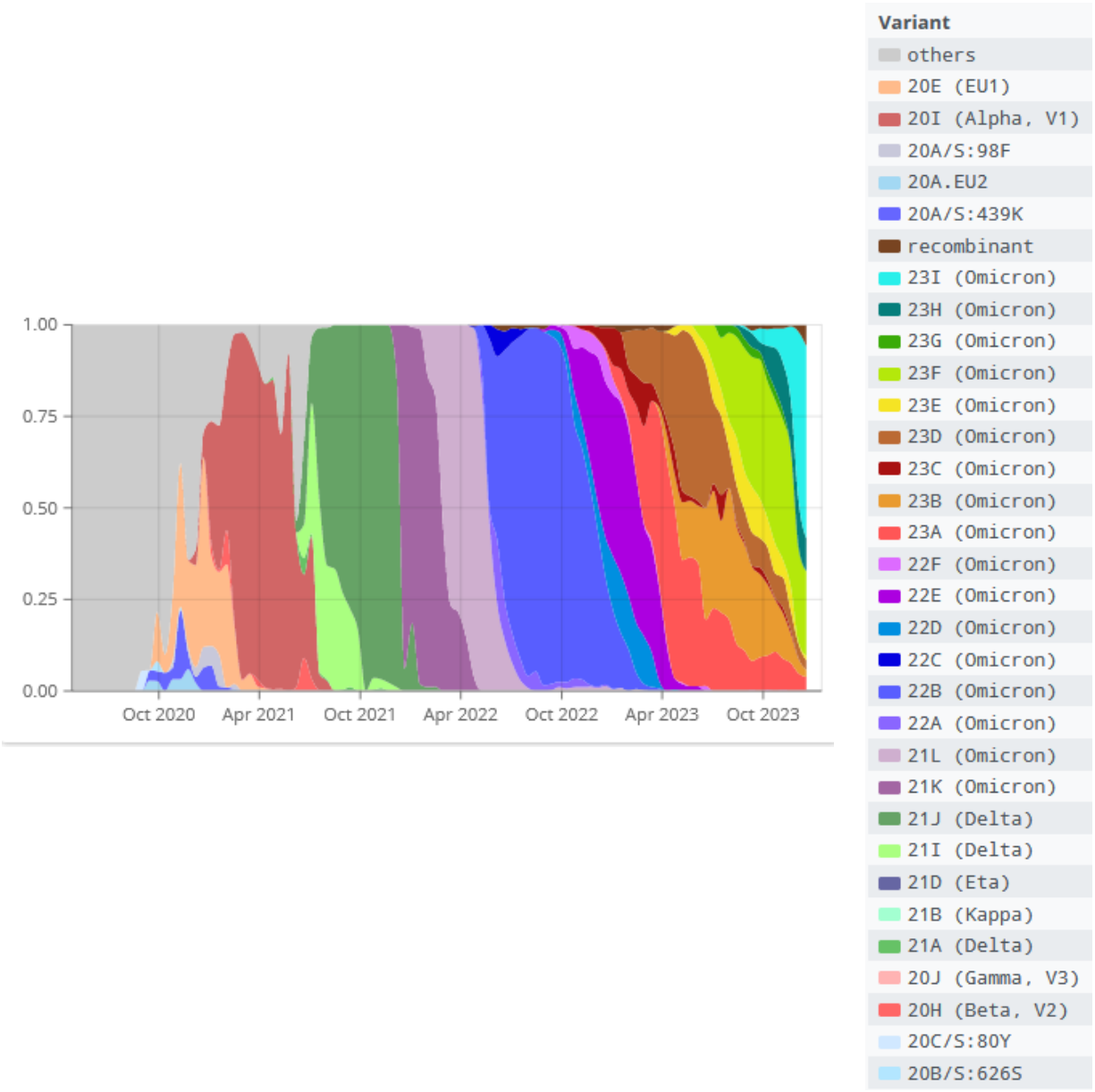

Figure 28: SARS-CoV-2 variants distribution in Greece, from August 2020 to January 2024, https://covariants.org/per-country

3.4 SARS-CoV-2 viral load in wastewater during the study period

The sampling period of our study includes the months from February 2021 to October 2023 and was divided into six sub-periods, based on crucial milestones during the pandemic. This was to examine the possible influence of these milestones and societal behavioral changes on viral load.

The days before the start of sample collection (25 February 2021), Greece was undergoing in-house restriction measures from 9 pm to 5 am, and in person operation for all educational

structures was implemented. The first sub-period included the days from 24/02/2021 (start of sampling) to 28/04/2021, which is a day before the start of random testing of airline passengers coming from abroad. All sub-periods are shown in **Table 3** accordingly.

Notable differences were observed among the sub-periods regarding the viral load values, between the two cities, and among the different expressions of viral load, before and after normalization.

The maximum mean value among the sub-periods, in gc/L (667822 gc/L), for the city of Heraklion was recorded during the first sub-period (24/02/2021-28/04/2021), when the Delta variant was dominant, and home restrictions were implemented. This might explain the high viral load values. Viral load values for served and dynamic population were acquired after normalization and maximum mean values were observed during the same period.

The minimum mean viral load value in gc/L (64543 gc/L) for the city of Heraklion was recorded during the second sub-period (29/4/2021 (random testing of airline passengers) - 27/6/2021), which is a reasonable result of the strict restrictions implemented during the past two months, and the clinical testing and restriction of infected individuals coming from abroad. Minimum mean values expressed in gc/served and gc/dynamic population were observed during the same sub-period as well.

As regards the city of Chania, the maximum mean value in gc/L was observed during the first sub-period too (487220 gc/L), although with a slight difference to the maximum mean value (456956 gc/L) recorded during the fifth sub-period (26/11/2021 when the first Omicron case was recorded - 31/5/2022). However, in this case, the normalized maximum mean values, referring to served and dynamic population, were observed during the fifth sub-period. This difference is attributed to the normalization factors – population and ammonium nitrogen (dynamic population) and the excess rainfall events during that period. It seems that rainwater entering the sewer shed diluted the wastewater, lowering the ammonium nitrogen concentrations, hence resulting in higher gc/dynamic population values.

Interestingly, the minimum mean viral load value in gc/L (46014 gc/L) for the city of Chania was recorded during the fourth sub-period (13/9/2021 opening of schools - 25/11/2021).

Table 3: Viral load values corresponding to sampling sub-periods for Heraklion and Chania

City	Intervals	gc/L			gc/served population			gc/10^6 dynamic population		
	Measures + variants	**min**	**max**	**mean**	**min**	**max**	**mean**	**min**	**max**	**mean**
Heraklion	24/02/2021- 28/04/2021 (in-house restrictions)	23434	5863452	667822	3.8E+11	9.5E+13	1.1E+13	3.6E+11	8.7E+13	1.0E+13
	29/4/2021 (random testing of airline passengers) - 27/6/2021	9921	225535	64543	1.6E+11	3.7E+12	1.0E+12	1.7E+11	4.3E+12	1.1E+12
	28/6/2021 (end of in-house restrictions) - 12/9/2021	19922	602875	125087	3.3E+11	1.0E+13	2.1E+12	3.3E+11	1.0E+13	2.2E+12
	13/9/2021 (schools open) - 25/11/2021	6300	277736	80533	1.3E+11	5.2E+12	1.4E+12	9.4E+10	4.6E+12	1.2E+12
	26/11/2021(first omicron case) - 31/5/2022	63155	2109544	575500	1.2E+12	3.8E+13	1.1E+13	8.6E+11	3.5E+13	1.0E+13
	1/6/2022 (end of mask use) – 6/10/2023 (today)	14940	1418772	328793	2.4E+11	2.6E+13	5.8E+12	2.4E+11	2.0E+13	4.8E+12
Chania	24/02/2021- 28/04/2021 (in-house restrictions)	8009	2480440	487220	1.3E+11	4.6E+13	9.3E+12	1.8E+11	4.3E+13	9.7E+12
	29/4/2021 (random testing of airline passengers) - 27/6/2021	617	296660	80441	1.1E+10	5.1E+12	1.4E+12	1.1E+10	6.8E+12	1.4E+12
	28/6/2021 (end of in-house restrictions) - 12/9/2021	9860	440712	99221	1.8E+11	8.8E+12	1.9E+12	1.7E+11	8.4E+12	1.7E+12
	13/9/2021 (schools open) - 25/11/2021	10571	115185	46014	2.0E+11	2.0E+12	7.9E+11	1.8E+11	3.0E+12	8.1E+11
	26/11/2021(first omicron case) - 31/5/2022	38588	1737192	456956	6.2E+11	3.6E+13	9.5E+12	6.5E+11	5.5E+13	1.2E+13
	1/6/2022 (end of mask use) – 6/10/2023 (today)	17806	1103120	262431	3.2E+11	2.1E+13	4.7E+12	3.1E+11	1.8E+13	4.5E+12

3.5 SARS-CoV-2 viral load and cases fluctuations during the pandemic

From the time our sampling started (February 2021) to the end of June 2021, Greece was undergone restriction measures depending on the amount and severity of human cases in each region. Regions were categorized as of high, medium, and low danger levels and surveillance measures of less strictness were implemented respectively. Restrictions included obligatory in-house stay hours, market activity, primary and secondary education operation (in-person or distance learning) and differentiated for each danger level (**Appendix 6.6**). A brief timeline of

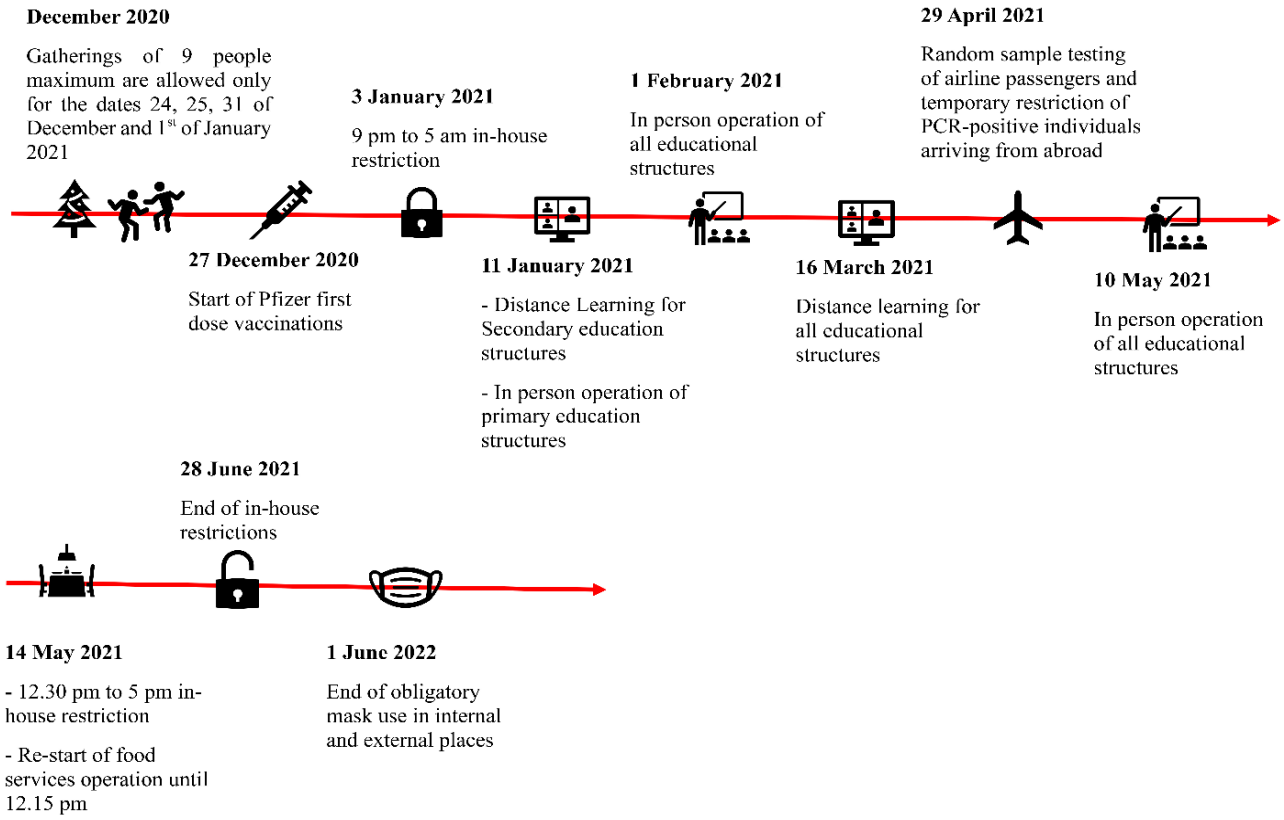

Figure 29: Pandemic time-point restrictions diagram – representative of both cities

the pandemic milestones and changes is presented in **Figure 29**. Both cities, Chania and Heraklion, are described by this timeline, as differences in surveillance levels and timing were minor.

In our study, wastewater viral load trends seem to be relatable to changes in restriction measures within community (**Figure 30**), to the emergence of different variants, as well as the trending of COVID-19 confirmed cases (**Figure 31**). **Figure 31** is constructed by using the dataset of the WWTP of Chania, however, is representative of both the WWTPs.

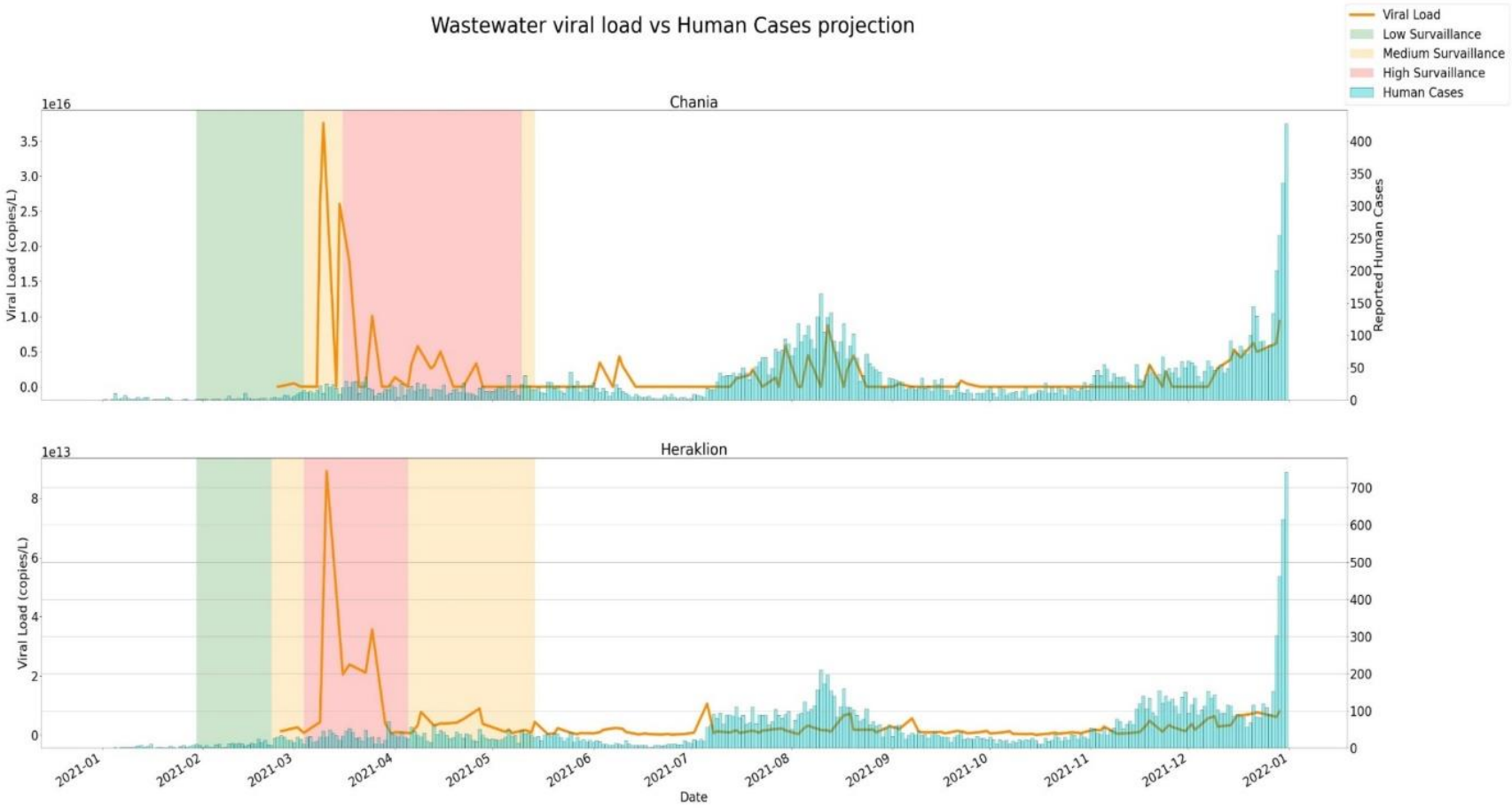

Figure 30: Wastewater viral load versus human cases and restriction measures projection for the cities of Chania and Heraklion

The days before the start of sample collection (25 February 2021), Greece was undergoing in-house restriction measures from 9 pm to 5 am, and in person operation for all educational structures was implemented. The wastewater viral load was trending rapidly upwards during March 2021, possibly due to the increased infections in educational structures. By the middle of March 2021, the operation of all educational structures was suspended by distance learning and viral load presented a decrease (**Figure 29**, **Figure 30** and **Figure 31**).

As observed in **Figure 30,** March 2021 was a high surveillance month for both cities, implying strong intervention measures within community activities. For the city of Heraklion though, the interventions were implemented a little earlier than those in Chania, capturing the sharp increase in viral load while in quarantine. For both cities, the viral load significantly decreased during the forthcoming weeks. However, in the case of Chania, higher loads were observed for a longer time, possibly because of the late high level surveillance intervention.

The Delta variant emerged in early April 2021, leading to gradual viral load increase until May, when Easter Holidays ended (**Figure 31)**. It is worth noting that during that time, the number of human cases recorded was significantly lower than expected, considering the high levels of wastewater viral load. This could be attributed to the incapability of correct clinical testing at that time, and/or the inaccurate data on COVID-19 confirmed cases (asymptomatic or symptomatic but not tested individuals). In addition, these differences could be a result of the insufficient immunity against SARS-CoV-2, because the vaccinations by then had just started, with a very small population percentage being vaccinated with the first dose, including mostly health care professionals. Moreover, we should always keep in mind that even asymptomatic or human cases in the late phase of the disease may continue shedding the virus in their feces.

Vaccination rate is an important factor for SARS-CoV-2 transmission, shedding and subsequently viral RNA occurrence in wastewater (Puhach et al., 2022). The study of Bivins and Bibby, 2021, showed that a university mass vaccination of students leaded to minimal or undetected on some days, wastewater viral RNA load, after the second vaccine dose, concluding that mass vaccination reduced viral shedding in wastewater. Moreover, Yaniv et al., 2021, described that SARS-CoV-2 RNA detected in wastewater showed a steady decrease when over 50% of the population was vaccinated. However, they observed that the antibodies produced by the vaccine were less effective in neutralizing the Delta variant, indicating differences of vaccine effectiveness regarding the prevalent variant.

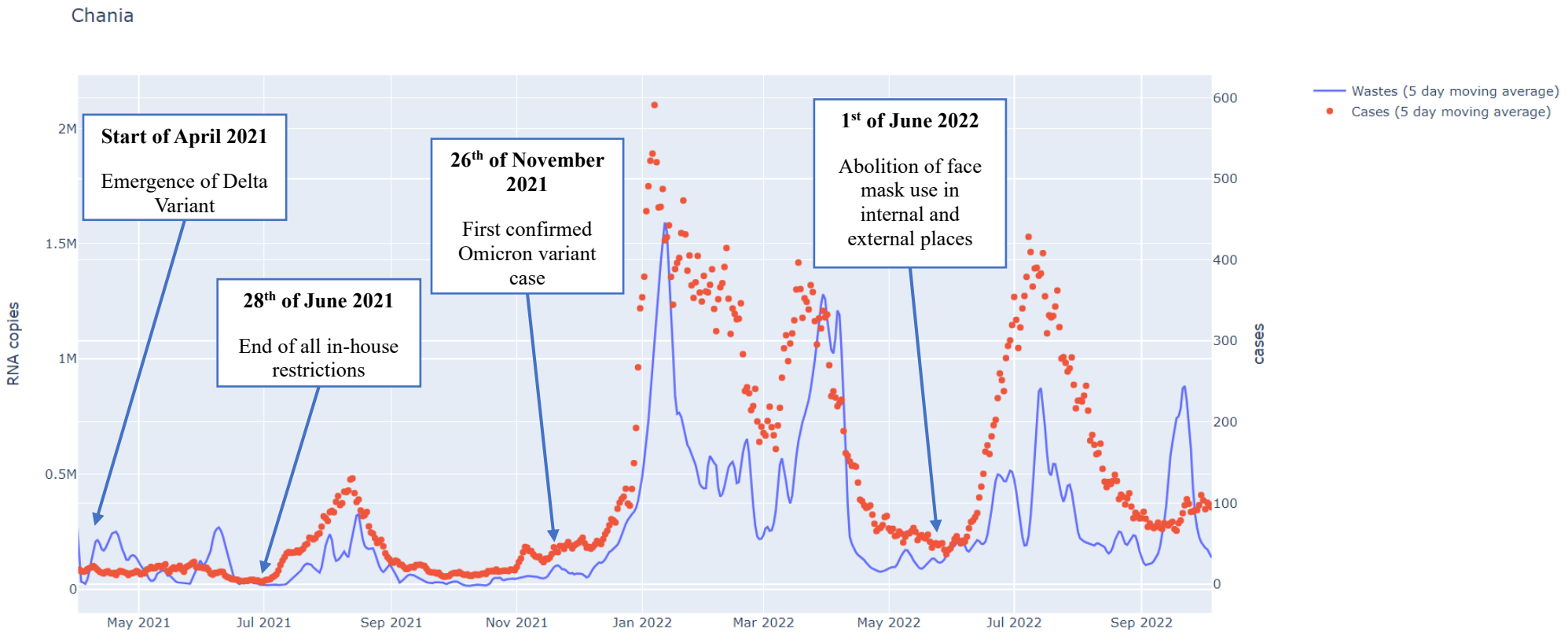

Figure 31: Wastewater viral load versus human cases from April of 2021 to October of 2022 for the city of Chania

On April 29th, random testing of airline passengers from abroad was implemented and a slight decrease in viral load was observed. On the 10th of May 2021, in person operation of all schools was re-established and on the 14th of May 2021, in-house restriction was applied between 12.30 pm and 5 pm, with the addition of the re-start of all food services. Wastewater viral load showed a gradual increase in the upcoming days, until the first week of June, when a gradual decrease began. Wastewater viral load and human cases trends were relatively stable until the first week of July, when a slow increase started. This can be attributed to the fact that until the end of June (June 28th 2021) all in-house restrictions had ended (**Figure 29** and **Figure 31**). Possibly both the end of pandemic restrictions and the peak of touristic activity on the island of Crete, resulted in increased wastewater viral load levels and human cases. Trends were heading upwards at that time and until the 10th of August.

Pandemic restriction measures and specifically lockdowns, have been broadly found to affect COVID-19 confirmed cases and wastewater viral load (Hillary et al., 2021; Martin et al., 2020). Indicatively, the results of the study conducted by Martin et al., 2020 showed a significant reduction of RNA concentration in wastewater during the lockdown measures implemented in the country.

By the end of August 2021 wastewater viral load and human cases had decreased significantly.

Human cases and wastewater viral load showed slight and comparable fluctuations during the forthcoming weeks, from the end of September 2021 to the beginning of November 2021, when the fluctuations became more noticeable. The first confirmed case of the Omicron variant in Greece was recorded on the 26th of November 2021 (**Figure 31**). From that time on, the wastewater viral load increased rapidly, noting the highest values ever recorded by the end of January 2022, which is in agreement with the incidences recorded during that time too. Omicron variant has shown faster viral replication and clearance than the wild-type SARS-CoV-2 and the delta variant, despite exhibiting milder symptoms. It is worth highlighting that this rapid viral load increase was also observed during and after Christmas holidays. From the end of January 2022 to the end of February 2022, the viral load decreased. By the middle of March 2022, the viral load increased and reached a peak during Easter holidays (18 to 25 April 2022) but decreased significantly from then until the end of May (**Figure 31**).

The abolition of obligatory mask use in internal and external places took place on June the 1st of 2022. From then on, a rapid and sudden increase both in viral load and in COVID-19 cases was observed, which peaked by the start of July 2022. Viral load in agreement with human

cases, noted high levels during the summer season of 2022 and dropped gradually from the start of August to the first week of September 2022. By the end of September, a peak in viral load was observed, which could be attributed to the opening of schools on the 12th of September (**Figure 31**). It is noteworthy that human incidences at that point, did not show a similar trend, although they noted slight increasing trends too, possibly as a result of insufficient clinical testing of infected individuals, or mild symptomatology or reduced recording of positive tests.

The trend of viral load during the following months until today, was in accordance to changes in community activities and habits (Christmas, Easter, and Summer Holidays), following the pattern described above. However, the correspondence between the COVID- 19 cases and the viral load was less accurate from October 2022 until today, with the latter displaying more noticeable peaks (**Figure 32**). This may be attributed to mainly two facts; the vaccine- or infection-driven immunity of individuals that lead to asymptomatic or of mild symptoms and thus, not recorded infections, and the reduced frequency of clinical testing within the community after the second year of the pandemic. The values noted both for human cases and viral load moved in notably lower levels than before, due to the same facts (**Figure 32**).

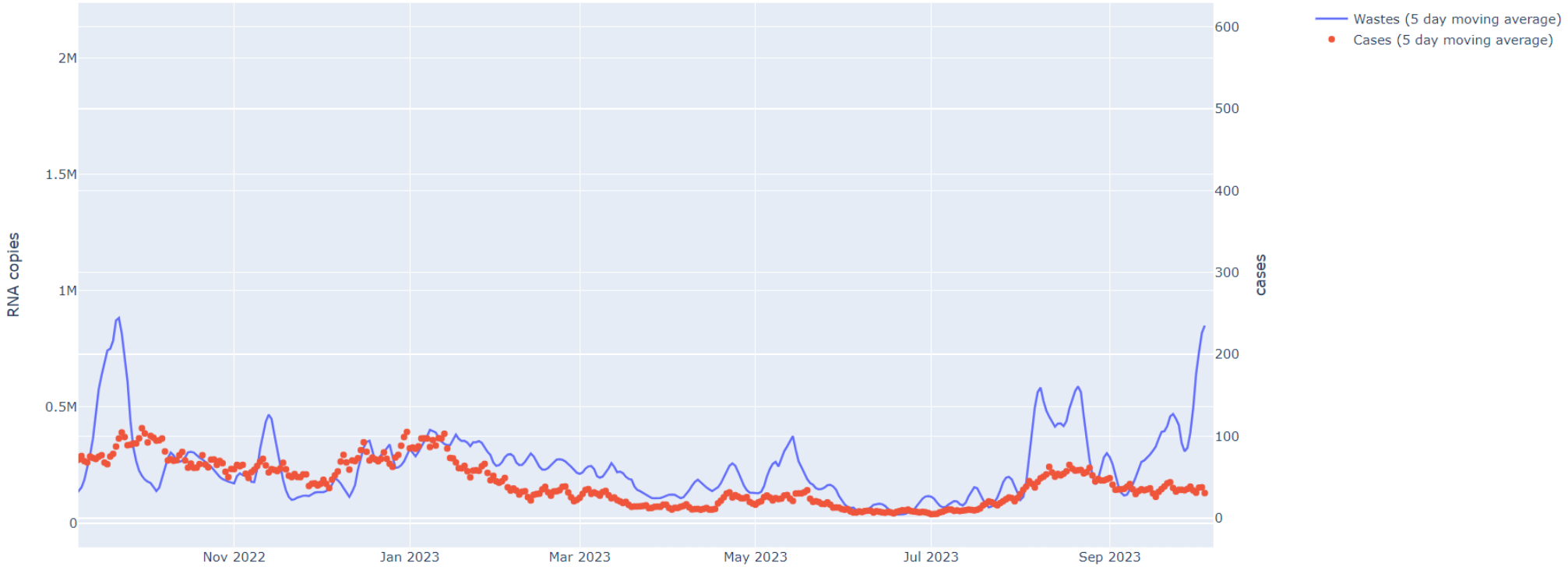

Figure 32: Wastewater viral load versus human cases from September of 2022 to October of 2023 for the city of Chania

3.6 Influence of rain events on viral load

The influence of rainfalls and the subsequent dilution of wastewater samples on SARS-CoV-2 RNA detection has been referred to several epidemiological studies, as a bias factor for data interpretation (Hillary et al., 2021; Bertels et al., 2022; Langeveld et al., 2023; López-Peñalver et al., 2023; Maal-Bared et al., 2023; Saingam et al., 2023). However, few studies to date have examined the actual effect of rainfall on virus detection.

In the study of Nguyen Quoc et al. (2022) the rain precipitation was demonstrated to lead to decreasing trends of SARS-CoV-2 RNA concentrations in wastewaters, despite the increasing COVID-19 cases. Saingam et al. (2023) observed that rain precipitation impacted SARS-CoV-2 levels and reduced WBE sensitivity.

To evaluate the influence of rain events and the consecutive dilution of the wastewater on viral load, we collected rainfall data (millimeters of rain) from the National Observatory of Athens database – Meteo (https://meteosearch.meteo.gr/data/index.cfm). We recorded the millimeters of rain noted during the day of sampling and on the day before the sampling day, to consider all dilution events that could affect the wastewater samples. Rainfalls and wastewater viral load data on respective dates were compared, after processing, using the OriginPro software (**Figure** to **Figure 40**). We should note at this point, that the graphs presenting the rainfall incidences, though constructed with trending lines, should not be interpreted as of describing rain fluctuations. Rain events are generally better described as single points, because they represent single events, but in our case, where a big dataset was used, trending lines were used for better visualization.

Figure and **Figure 34** include the whole dataset of the sampling period (02/2021-10/2023) for the city of Chania (**Figure**) and Heraklion (**Figure 34**), respectively. To investigate the effect of rainfall events on viral load, in case they occurred either during the sampling day or on the day before, or even both, we split the rainfall periods into dry (spring and summer) and wet (autumn and winter) and focused on rainfalls during the day and the previous day of sampling for each of these periods for each city in separate.

Figure and Figure 36, respectively for Chania and Heraklion, are representative of rainfalls that occurred during dry periods. We firstly focused on the city of Chania (**Figure **) to study the effect of rainwater on viral load during summer (1/8/2021-

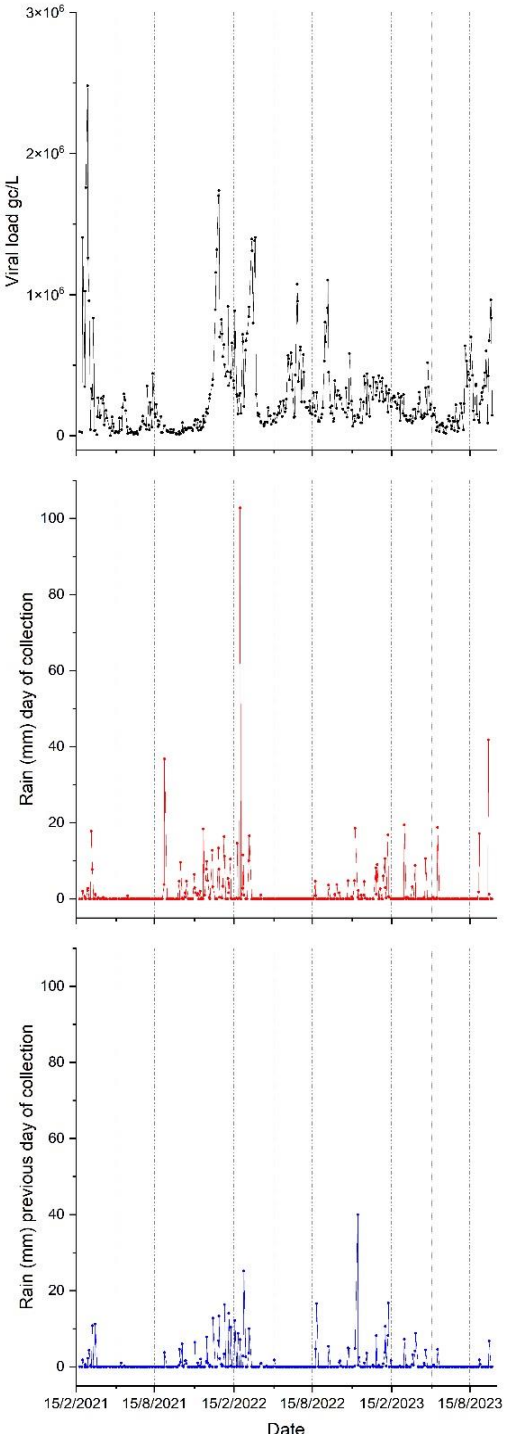

Figure 33: Viral load fluctuations and rainfall incidences on the sampling day and on the day before, for the whole sampling period and the WWTP of Chania 2021-2023

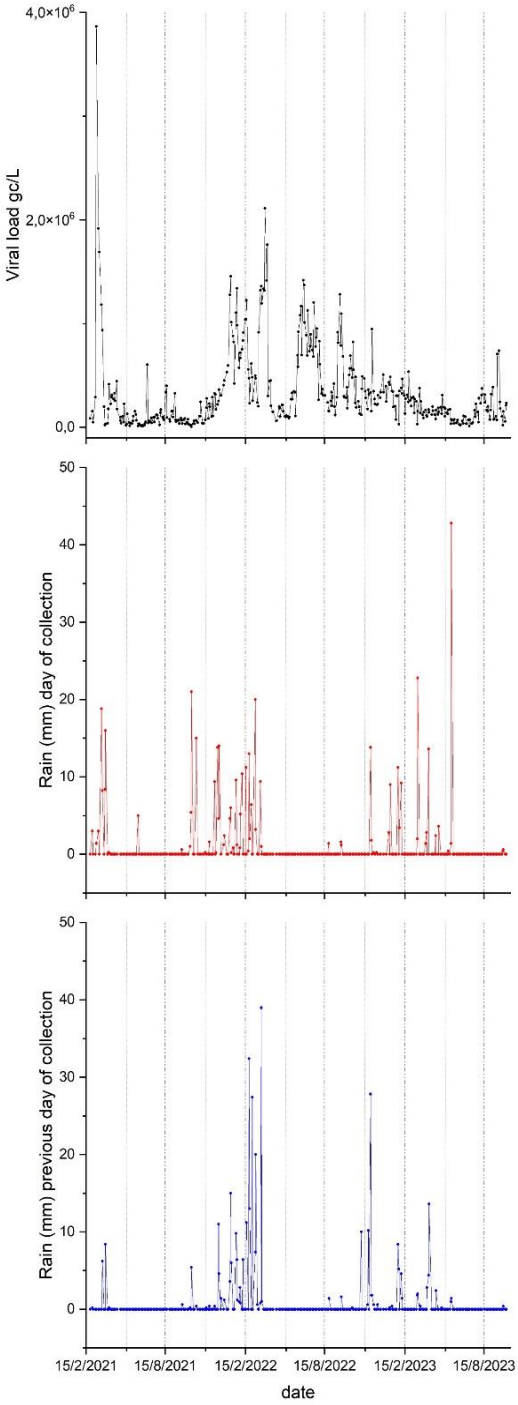

Figure 34: Viral load fluctuations and rainfall incidences on the sampling day and on the day before, for the whole sampling period and the WWTP of Heraklion 2021-2023

26/9/2021), when we expected to observe higher viral loads because of increased hosted

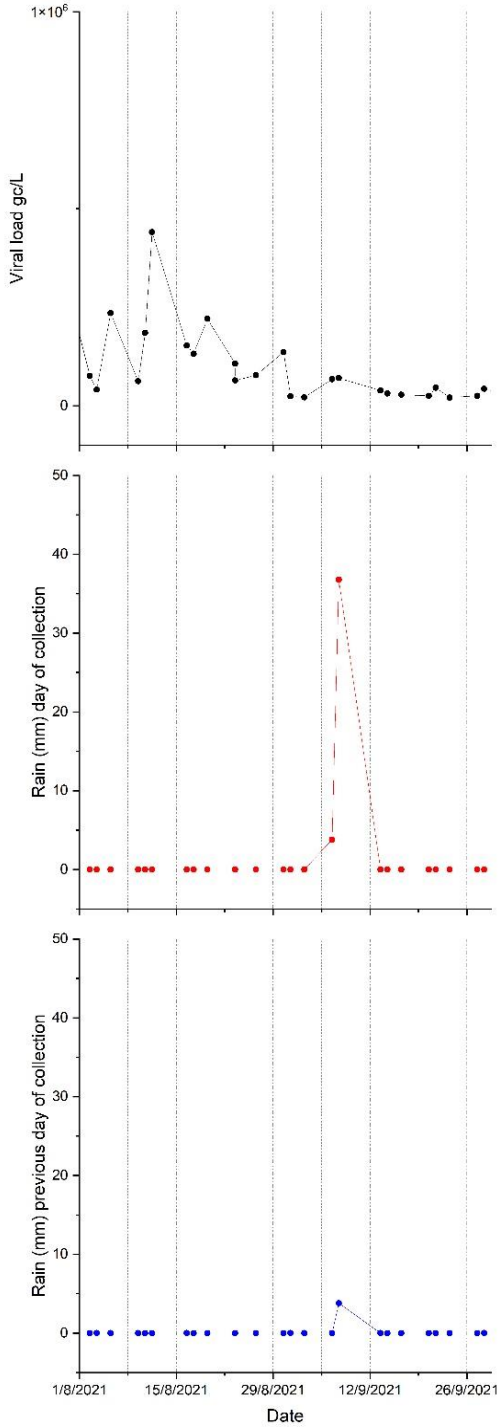

Figure 35: Viral load fluctuations and rainfall incidences on the sampling day and on the day before, for a dry period and the WWTP of Chania in 2021

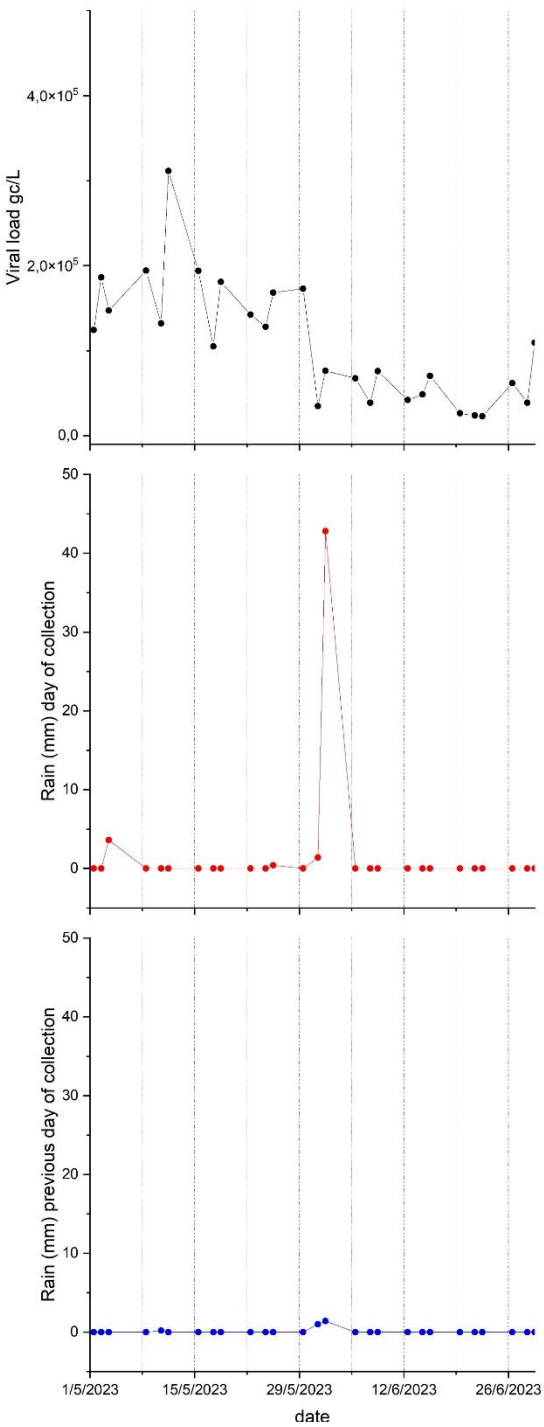

Figure 36: Viral load fluctuations and rainfall incidences on the sampling day and on the day before, for a dry period and the WWTP of Heraklion in 2023

population (tourists) and the lack of dilution events. Viral load during that period was

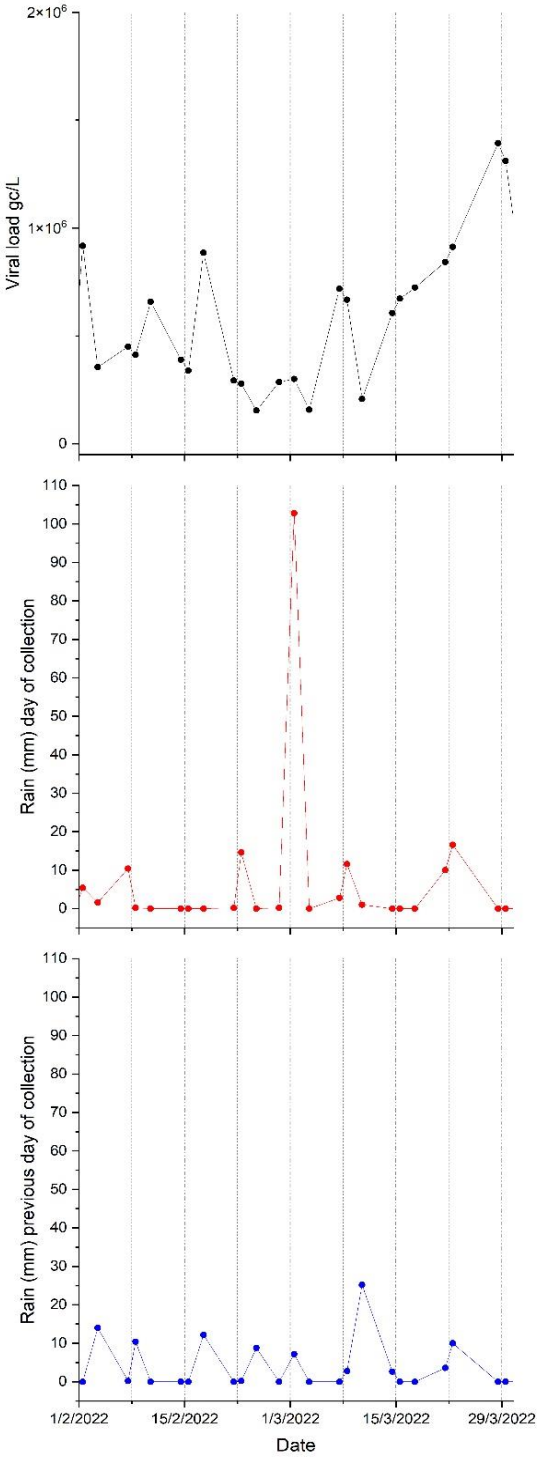

Figure 37: Viral load fluctuations and rainfall incidences on the sampling day and on the day before, for a wet period and the WWTP of Chania in 2022

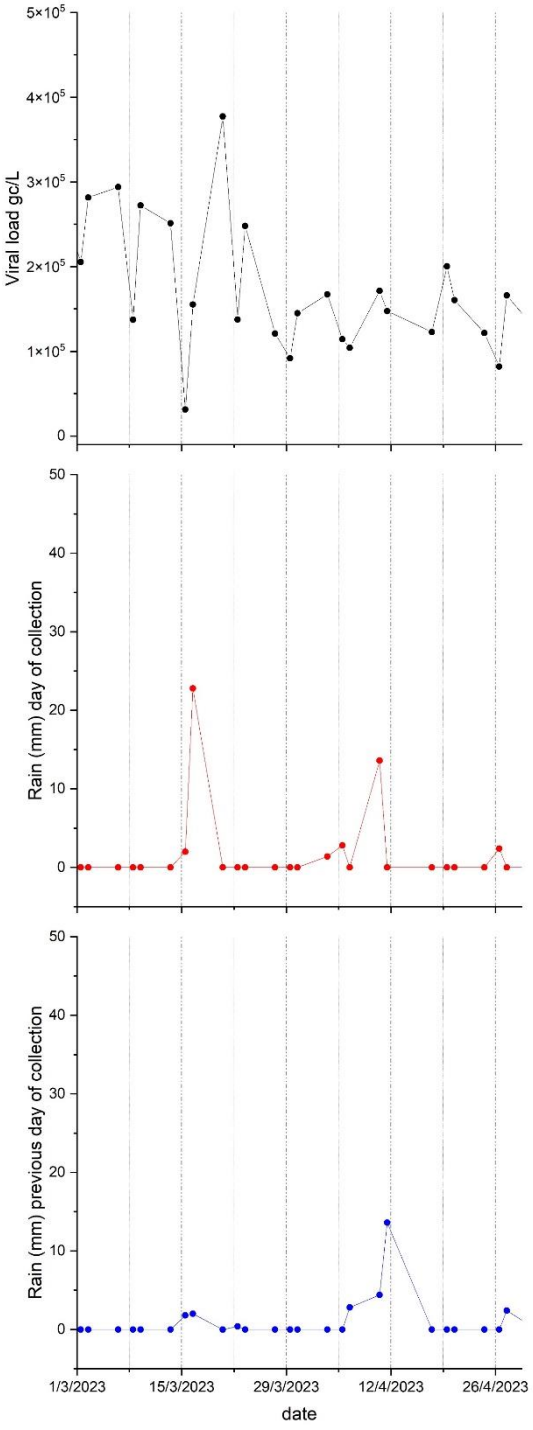

Figure 38: Viral load fluctuations and rainfall incidences on the sampling day and on the day before, for a wet period and the WWTP of Heraklion in 2023

relatively high, indeed, until a sharp decrease took place that coincided with two samples collected during rainfall events; the first rainfall occurred at the day of sampling of

the first sample, while the previous day was not rainy, and the second sample was collected during a much heavier rainy day accompanied by a light rain on the day before.

As regards the city of Heraklion (**Figure 36**) for a different but still dry period (May and June 2023), a heavy rainfall event during the sampling day together with a much lighter rainfall on the day before, caused a sharp decline in viral load.

Figure and Figure 38 are representative of wet periods, during which several rainfalls have been occurring, for the city of Chania and Heraklion respectively. The time frame of these two graphs are periods without touristic activity, in addition to the increase of rainfall events, and hence, dilution of samples.

In the case of Chania (**Figure **), the increase of rainfalls is obvious enough, as February and March are usually of the rainiest months in Greece. Viral load trend fluctuates more intensively and, in most cases, is in agreement with the rainfall data. However, the impact of light rainfall events is not easily distinguishable during that period. A heavy rainfall event on the first days of March 2022 though, had a more noticeable effect on viral load trends.

Accordingly, for Heraklion (**Figure 38**), we can observe intense fluctuations of viral load. However, not many rainfalls were recorded during that time (March and April 2023). A noticeable, but lighter than the aforementioned rainfall recorded in Chania occurred by the middle of March 2023, which also surprisingly, resulted in a sharper viral load decrease.

Figure is representative of a dry period, during which rainfall incidents were recorded both on the sampling day and the day before sampling, for the city of Chania. Wastewater samples' viral load value showed a small but rapid decrease when a rainfall occurred during the days of sampling. When a strong rainfall event occurred the day before, the respective viral load value was not that much affected. However, for the same dry period, when a rainfall event took place both on the day of sampling and on the day before, the respective wastewater viral load decreased rapidly.

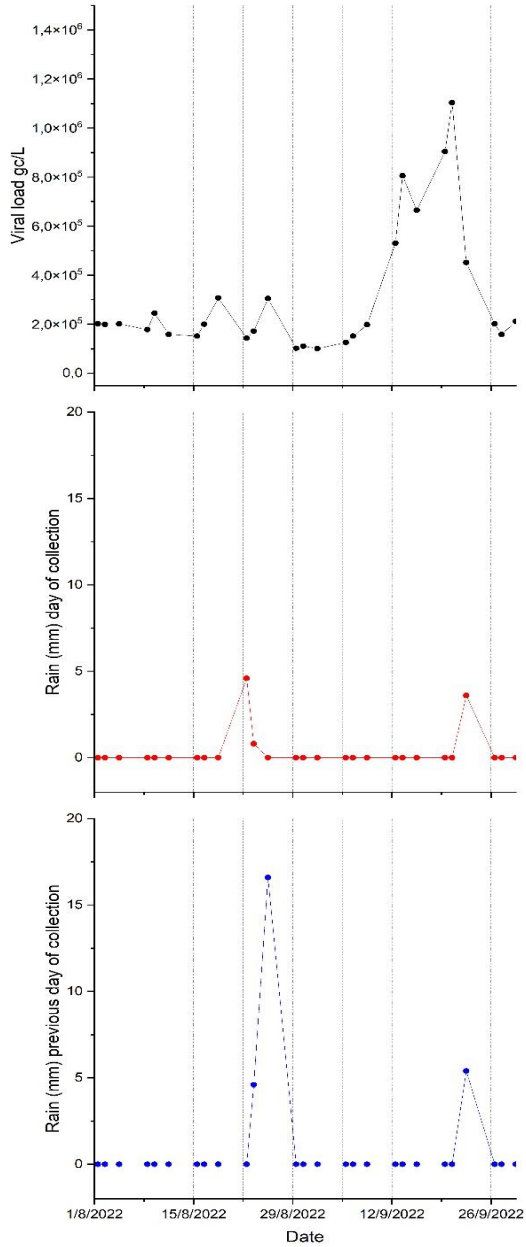

Figure 39: Viral load fluctuations and rainfall incidences on the sampling day and on the day before, for a dry period and the WWTP of Chania in 2022

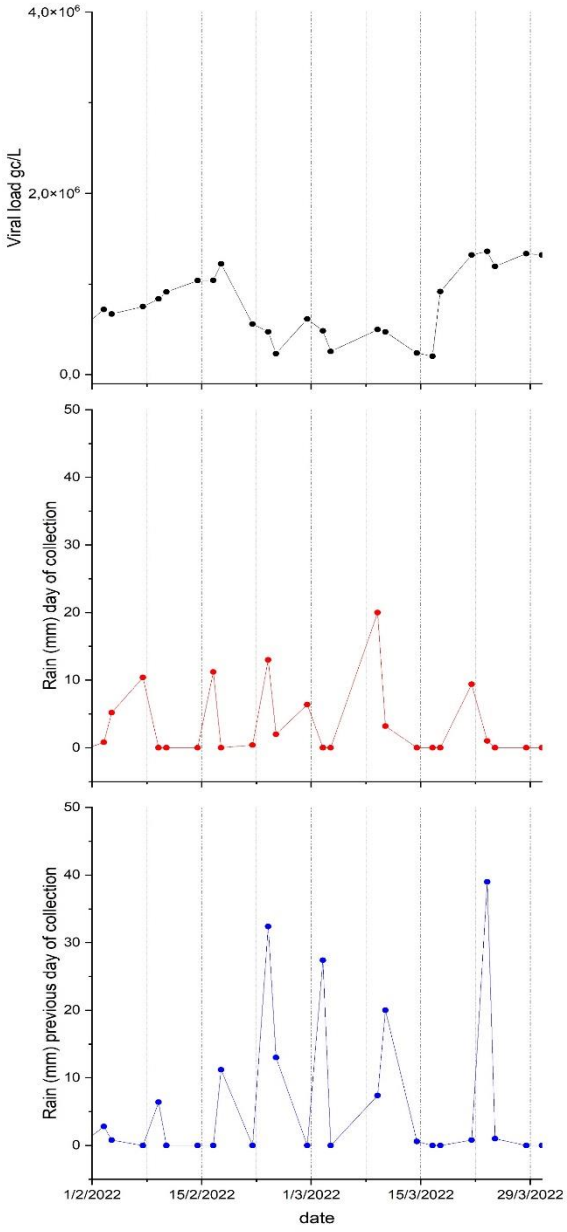

Figure 40: Viral load fluctuations and rainfall incidences on the sampling day and on the day before, for a wet period and the WWTP of Heraklion in 2022

Figure 40 is representative of a wet period (February and March 2022), during which many rainfall events were recorded both during the sampling day and the day before, for the city of Heraklion. Viral load values were fluctuating in generally low levels during that time and they dropped even more by the fourth week of February 2022, when heavy rainfalls were recorded on both the days of interest. Low viral loads were observed until the third week of March 2022.

3.7 Physico-chemical characteristics of wastewater samples and SARS-CoV-2 concentrations of the WWTPs

Physico-chemical characteristics of the untreated wastewater of the two WWTPs varied considerably depending on seasonality and between the cities. For instance, the average influent flow rate ranged from an average value of 17792 m^3/Day for the WWTP of Chania (**Table 4**), to an average of 33020 m^3/Day for the WWTP of Heraklion (**Table 5**). This is attributed to the fact that Chania WTTP serves approximately 97,000 people, whilst the Heraklion WWTP serves approximately 200,000 people. It is worth noting that during winter season, the influent rate of both cities is higher, due to the entering of rainwater in the sewer shed (**Table 6**). We considered as winter season the months from November to April each year and as summer season the months from May to October. The decision was taken considering the opening of hotels and the start and ending of rain events in our region.

The WWTP of Chania receives seawater during windy days because the sea waves can enter the drain system. This causes, apart from a higher influent flow rate in the WWTP, an increase in chloride ions concentration, which explains why the maximum concentration of chloride ions is significantly higher for the WWTP of Chania (870 mg/L) comparatively to Heraklion (330 mg/l), while the respective average value for Chania WWTP is 124 mg/L; lower compared to Heraklion (204 mg/l) (**Table 4**). Hence, in accordance with the flow rate, average chloride concentration differs significantly between the two WWTPs.

It is worth noting that high chloride ions concentrations have been found to promote reduced viral RNA concentrations, when sodium hypochlorite is used as a disinfection agent, according to Zhang et al. (2020) and Hemalatha et al. (2021).

The wastewater pH and conductivity values of the two WTTPs were not significantly divergent. For both parameters however, the Heraklion WWTP showed a slight but considerable higher average value.

As regards to the effects of pH on wastewater viral load, Amoah et al. (2022) made an interesting observation, that pH values in the range 7.1-7.4, are associated with the highest SARS-CoV-2 concentration. The study performed by Bardi and Oliaee (2021) indicated that pH values lower than 5.4, together with a volatile fatty acid concentration above 2000 mg/L leaded to total absence of SARS-CoV-2 genes.

High conductivity values have been related to road de-icing, according to Langeveld et al. (2023) or very low flow rates, usually during dry summer periods. However, in our case, road de-icing is extremely rare. Thus, high conductivity values are a possible result of seawater entrance into the sewer shed, causing increased concentrations of several ions, such as chloride ions, as stated before.

The COD, BOD and SS average values were considerably higher for the city of Chania, indicating more complex and polluted wastewater. This may be attributed to the fact that the WWTP of Chania receives industrial wastewater too.

COD, BOD and SS concentrations, as indirect measures of organic loading in wastewater, can potentially affect viral RNA recovery efficiency, because of the viral particle affinity to organic solids as extensively studied by Petala et al. (2021) and other research groups (Zhuang and Jin, 2003; Wong et al., 2013).

The ammonium nitrogen and phosphorus average concentrations were significantly higher for the WWTP of Heraklion, and this could be attributed to the larger population served by this WWTP. Moreover, ammonium nitrogen concentration ranged among the seasons, in accordance with the influent rate fluctuations, because of the existence or absence of rainfall dilution events (**Table 7**).

The concentration of different ions of interest can be underestimated because of dilution, as a result of heavy rain events. In our case, this was particularly important for ammonium nitrogen determination, because this parameter was used for normalization. In addition to the interpretation of ion concentrations, it is worth noting that ammonium nitrogen concentrations reached a peak during the summer months, because both of the lack of rainfalls and the massive tourist population arrival on Crete.

Table 4: Wastewater characteristics of the WTTP of Chania

	Influent flow (m3/Day)	pH	Chloride (mg/L)	Conductivity (ms/cm)	COD (mg/L)	BOD (mg/L)	Phosphate (mg/L)	Ammonium Nitrogen (mg/L)	Suspended Solids (mg/L)
Minimum	13820	6.89	42	0.495	282	160	3	10	152
Maximum	32982	7.99	870	4.460	1530	660	28	58	936
Mean	17792	7.42	124	1.012	679	429	16	39	401
Median	17423	7.4	108	0.963	685	430	16	41	376

Table 5: Wastewater characteristics of the WTTP of Heraklion

	Influent flow (m3/Day)	pH	Chloride (mg/L)	Conductivity (ms/cm)	COD (mg/L)	BOD (mg/L)	Phosphate (mg/L)	Ammonium Nitrogen (mg/L)	Suspended Solids (mg/L)
Minimum	21022	6.60	76	0.454	178	110	4	14	60
Maximum	39000	8.31	330	5.250	2369	520	28	74	1260
Mean	33020	7.70	202	1.320	578	280	17	46	227
Median	32950	7.71	198	1.234	561	266	17	46	210

Table 6: Influent flow rate (m3/Day) of the WWTPs of Heraklion and Chania during winter and summer seasons

	Heraklion				Chania			
	winter season 2021-2022	**summer season 2022**	**winter season 2022-2023**	**summer season 2023**	**winter season 2021-2022**	**summer season 2022**	**winter season 2022-2023**	**summer season 2023**
Minimum	31000	30900	29189	21022	14362	15174	13960	16332
Maximum	39000	37512	35570	31754	32982	20488	24334	20696
Mean	36098	34003	32836	30742	19642	17562	16769	17335

Table 7: Ammonium Nitrogen concentrations (mg/l) of the WWTPs of Heraklion and Chania during winter and summer seasons

	Heraklion				Chania			
	winter season 2021-2022	**summer season 2022**	**winter season 2022-2023**	**summer season 2023**	**winter season 2021-2022**	**summer season 2022**	**winter season 2022-2023**	**summer season 2023**
Minimum	22.8	41.4	13.8	30.0	9.9	31.5	22.8	36.2
Maximum	69.9	73.2	73.5	65.0	44.7	57.6	52.8	55.5
Mean	42.2	52.7	44.5	49.0	31.6	42.9	38.6	43.7

3.8 Time-lagged Cross-Correlation between COVID-19 cases and viral load

The correlation of COVID-19 cases and viral load in wastewater has been graphically observed in paragraph 3.8. In this study, we aimed to describe this correlation by statistical means too.

It is broadly noted that individuals infected with SARS-CoV-2 can excrete virus and/or viral RNA through multiple bodily secretions (Prasek et al., 2023), of which faeces dominate population-level SARS-CoV-2 RNA loading in wastewater. SARS-CoV-2 can be detected in infected individuals' faeces, regardless of the presence of any symptoms; even pre-symptomatic and asymptomatic individuals were found to shed the virus via faeces (Cevik et al., 2021; Park et al., 2021; Bertels et al., 2022). Delays between the presentation of symptoms, testing and the reporting of test results were also commonly observed in different countries (Li et al., 2023). Moreover, it is worth highlighting that there is a substantial period that elapses between the viral infection and the emergence of any symptoms, known as the viral incubation time. Given the above, clinical testing provides, not in real-time and possibly underestimated insights into the viral occurrence within community, while WBE studies might provide information on the onset of outbreaks and/or give a more realistic perspective of viral circulation within community.

In this context, we correlated COVID-19 cases and wastewater viral load, aiming to note the possible time-gap between their fluctuations on corresponding periods and thus, evaluate the early warning capacity of our study. To do so, we calculated the time lagged cross-correlation (TLCC) by shifting the recorded COVID-19 cases data by an offset and calculating the Spearman cross-correlation between SARS-COV-2 RNA load and COVID-19 cases for every shift. A maximum offset of $\pm$ 30 days was used. For each lag, a p-value was also reported; in cases where the p-value was > 0.05, then the estimated correlation was disregarded.

Figure 41 represents a TLCC graph constructed by using the data of the city of Heraklion for the whole study period. The blue line represents the Spearman correlation coefficient and the purple line, the p value. The red dotted line is set at zero point indicating the center, while the green dotted line represents the peak synchrony point, meaning the point at which the best correlation between SARS-COV-2 RNA load and COVID-19 cases is achieved.

At peak synchrony the value of the Spearman correlation coefficient is ~0.82 and the p-value is ~8.9×10^{-226}, indicating strong correlation between the variables. Peak synchrony is achieved

at the offset of -3 days, implying that the wastewater viral load was preceding by three (3) days the COVID-19 cases in Heraklion during the study period.

A corresponding graph for the city of Chania is presented in **Figure 42**. In this case, the value of the Spearman correlation coefficient is ~0.70 at peak synchrony and the p-value is ~1.3×10^{-134}, indicating strong correlation between the variables. Peak synchrony is achieved at the offset of +2 days, implying that the COVID-19 cases were preceding the wastewater viral load by 2 days in Chania during the study period.

The correlation of confirmed COVID-19 cases and wastewater viral load was significantly differentiated in the two investigated cities. For the city of Heraklion, wastewater viral load was preceding the cases by three days on average, implying that the wastewater can, indeed, at some degree predict the incidences of infection and thus, the outbreaks. On the contrary, the cross-correlation estimates are not performing likewise for the city of Chania.

This observation can be attributed to a variety of factors, including the varying wastewater characteristics between the two cities. Moreover, several studies that have been carried out in this context, have indicated differing levels of correspondence between the presence of SARS-CoV-2 RNA in wastewater and the outcomes of individual testing conducted concurrently and at the same location (Ai et al., 2021; Li et al., 2023). Specifically, Li et al. (2023) highlighted the importance and divergence of the correlation between the two variables at the pre-peak and post-peak stages of an outbreak. Researchers in this study concluded, that WBE showed better capability in capturing new cases than active cases due to the higher shedding loads from new patients. Therefore, a more focused correlation approach on outbreaks would be more accurate in evaluating the dynamics between the two variables.

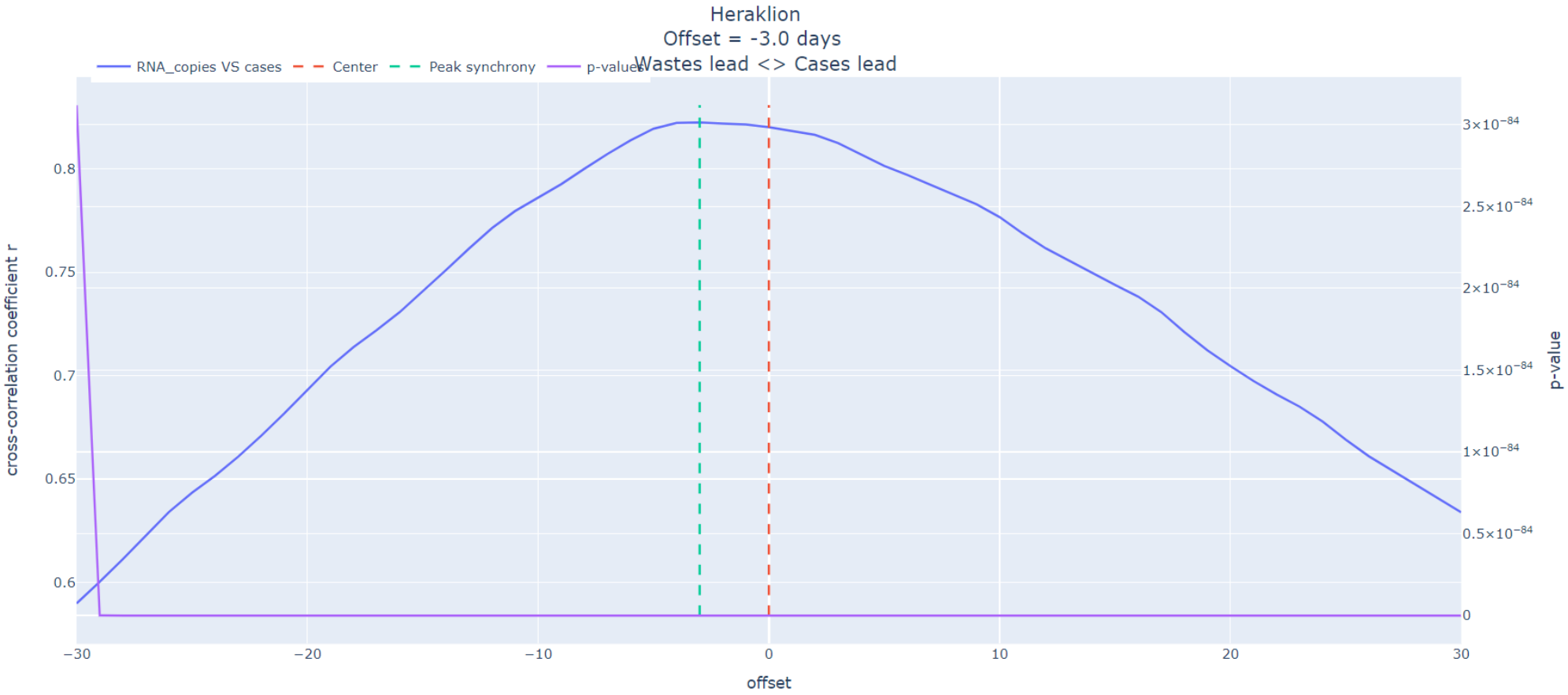

Figure 41: TLCC graph for the city of Heraklion, for the whole study period

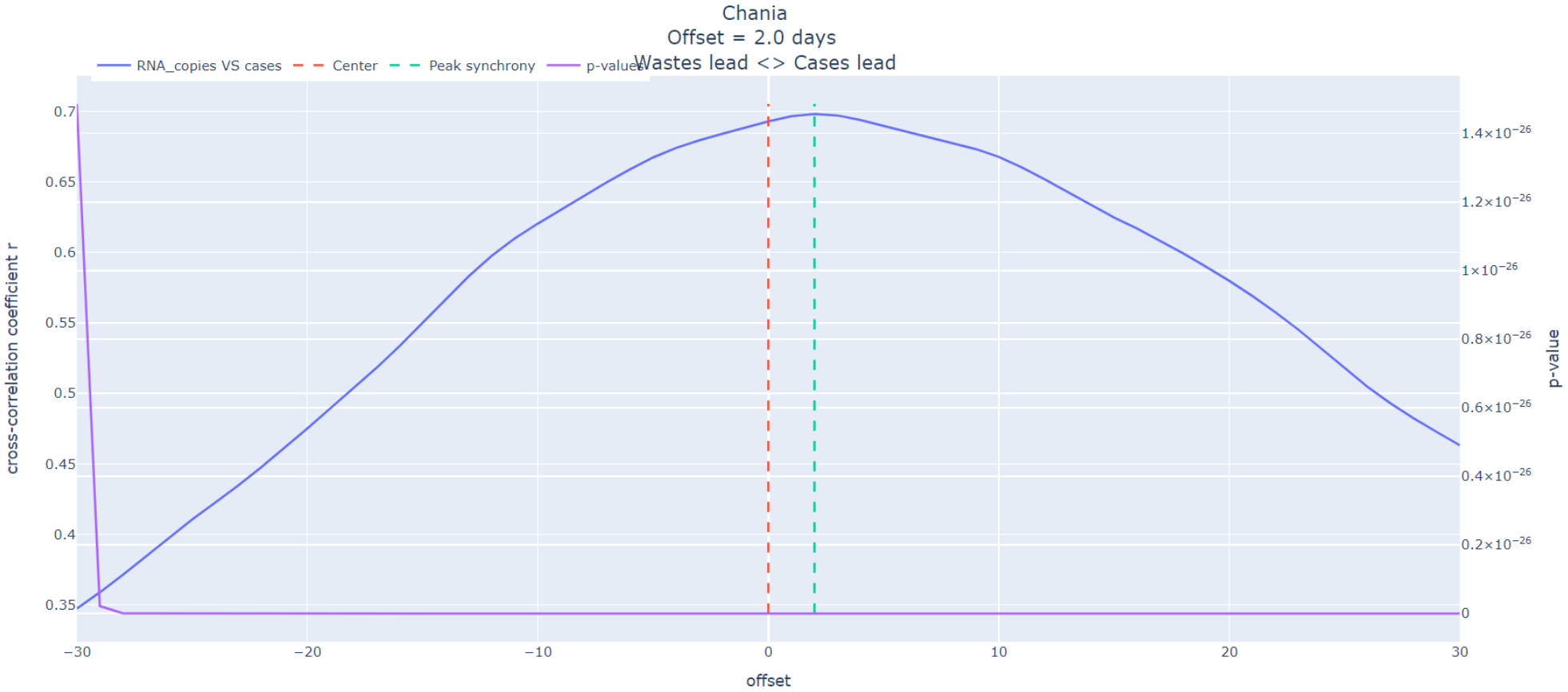

Figure 42: TLCC graph for the city of Chania, for the whole study period

3.9 Wastewater prediction on COVID-19 cases by means of machine learning

In the context of WBE for SARS-CoV-2 monitoring, several studies have examined the use of wastewater as a prognostic tool for forecasting outbreaks in human cases. The forecasting of COVID-19 cases relies on the fact that there is a considerable time gap between viral infection and the onset of symptoms (viral incubation time) and is usually achieved by implementing machine learning (ML) strategies (Cao & Francis, 2021; (Koureas et al., 2021; Lai et al., 2023; Vaughan et al., 2023; López-Peñalver et al., 2023; Hill et al., 2023). ML is valuable for analyzing large datasets because its performance is enhanced through self-improvement, by using provided data. ML also allows for the selection of specific models that can learn from data, recognize patterns, and make predictions with minimal human intervention (Vaughan et al., 2023).

In our study we used python and sikit-learn and xgboost libraries for the machine learning analysis.

Figure 43 and **Figure 44** demonstrate the trained models for the city of Chania and Heraklion respectively. We trained the models (red dots) by providing them with respective-date data on wastewater viral load and human cases, for a pre-defined time period (blue line). We then subtracted only the data on human cases for the remaining study period, to test the accordance and accuracy the model develops to the real values. The predicted cases are depicted with green dots.

Interestingly, the model seems to be able to predict the pattern of the COVID-19 cases that followed, but provides a different estimation regarding the number of recorded incidences. However, it should be noted, that the period for which the prediction was made (May to October 2023) might not be the optimal, because of the reduced clinical testing resulting from community behavioral changes. Additionally, physico-chemical wastewater characteristics should be taken under consideration when ML strategies are implemented as well, because they directly affect the recovery of viral RNA from wastewater.

The complexity of the relationship between sewage measurements and disease spread is broadly admitted. Koureas et al., 2021 in their study, developed 14 different machine learning models from different training datasets, but could not identify a single one as the overall best performing in terms of correlation, accuracy and generalizability. That

fact can be interpreted considering a wide variety of factors, like technical characteristics of the WWTP, chemical composition and physicochemical properties of the wastewater samples, environmental parameters, analytical issues, sampling procedures, changes in surveillance practices, alteration in the virus's properties because of the emergence of different variants, as well as vaccinations. It is also noteworthy, that Koureas et al. (2021) observed that the strength association between actual and predicted cases varied over time, and specifically between the periods for the first and second epidemic wave. The ratio of sewage RNA measurements to reported cases decreased in comparison to the first wave, which could be attributed to the different variant being prevalent in each wave, different climatological parameters, different testing rate and behaviors related to seeking healthcare.

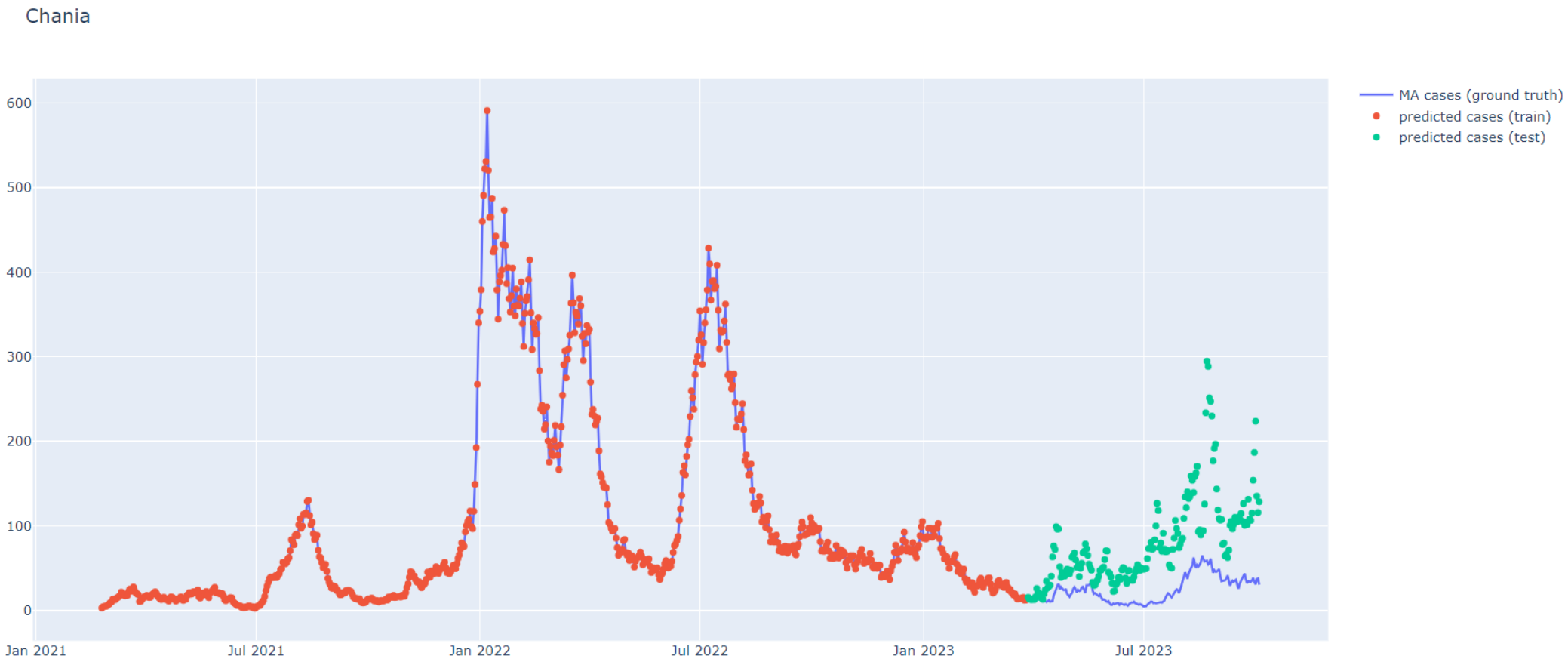

Figure 43: Predictions on cases for the city of Chania by machine learning

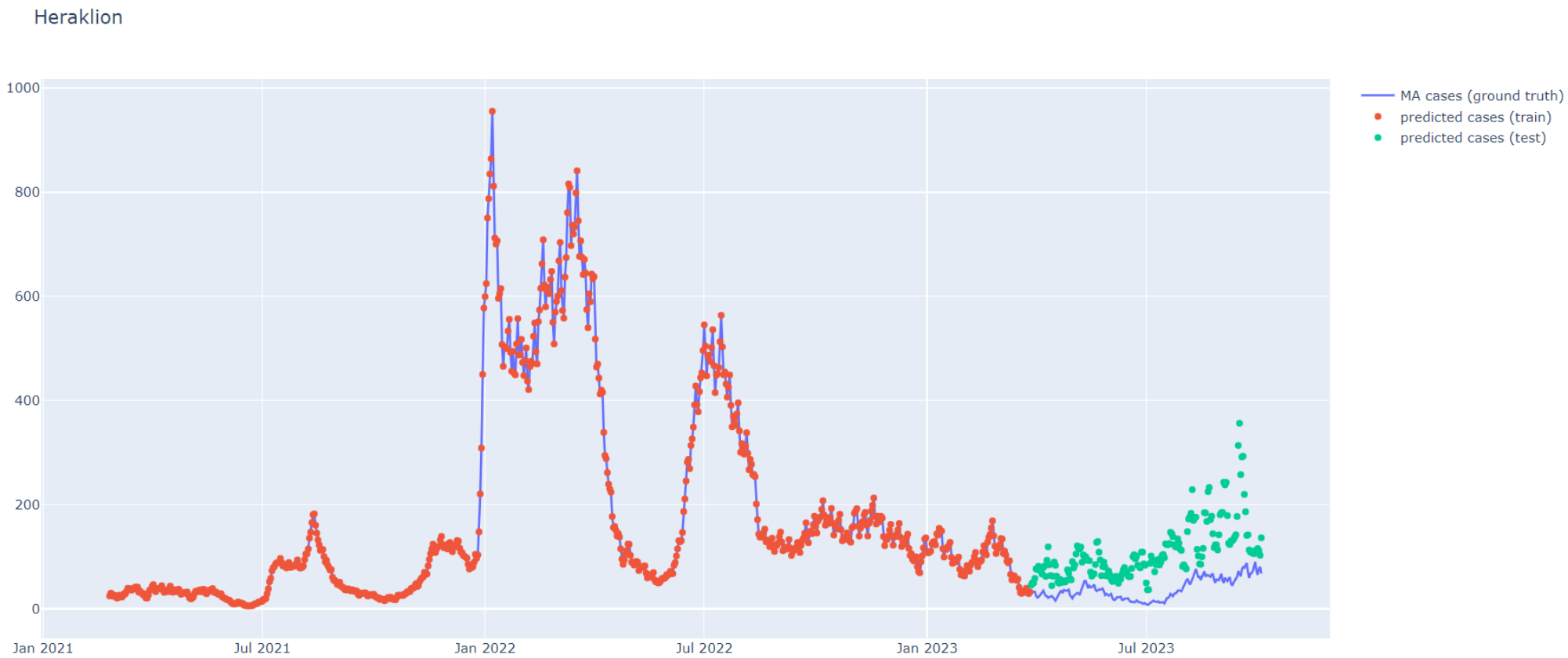

Figure 44: Predictions on cases for the city of Heraklion by machine learning

CHAPTER 4 – CONCLUSIONS

4.1 Conclusions

In conclusion, utilizing wastewater as a tool for WBE presents a valuable approach for monitoring viral RNA, especially in the context of SARS-CoV-2 surveillance. However, the complexity of the wastewater matrix, which can be influenced by various factors, highlights the challenge of implementing a uniform model across different regions and countries. Physicochemical parameters such as total and/or suspended solids, pH, conductivity, etc., can significantly impact the recovery of viral RNA. Moreover, the presence of numerous inhibitors necessitates careful calculation for inhibition and recovery.

The use of wastewater as an early warning tool for SARS-CoV-2 is complicated by the variability of the time gap to the occurrence of human cases, which is affected by the emergence of various virus variants as well. However, a statistically significant but not a linear correlation was observed between wastewater viral load and human cases. To enhance the reliability and comparability of results, standardizing protocols becomes vital, either by adopting common protocols or by implementing ring trials. Finally, the importance of population dynamics in different analytical approaches (use of different parameters for normalization) further emphasizes the need for a holistic and flexible strategy in WBE.

4.2 Limitations of the study

In the pursuit of understanding viral RNA dynamics in wastewater, methodological choices, environmental effects, and the complexities associated with viral shedding and immunity must all be considered in order to provide a balanced interpretation of our findings. The limitations of our study are listed below:

- The use of supernatant liquid instead of the solid particulate matter of each sample, may have introduced variability in the results, since a portion of viral RNA might have retained on solid particles.
- The impact of rain on viral load was acknowledged, but normalization of this effect was not achieved, introducing a potential source of bias.
- We did not test for specific variants of the virus, which limits the ability to discern the prevalence and dynamics of particular strains in the studied samples.
- The reliance on only two genes for analysis may have underestimated our results.
- Testing frequency for each WWTP was not daily, potentially missing fluctuations in viral RNA concentrations.

- The study could not encompass all human cases, like asymptomatic individuals, which might affect the comprehensiveness of the findings.
- The inability to distinguish among asymptomatic, new, active, and convalescent cases impedes a more in-depth understanding of infection dynamics.
- Thorough examination of the actual effects of various immunization regimens, including variations in vaccines, doses, and time gaps until the third dose could not be provided by this study.
- Estimating the true impact of immunity against different variants, and subsequently the variability in viral shedding in feces, remains a challenge.
- Data recorded corresponded to prefectures rather than cities, necessitating extrapolation and potentially introducing uncertainties in the spatial representation of the findings.
- The correlation between wastewater viral load and COVID-19 cases would possibly be more accurate if it was focused on the onset and/or ending of outbreaks.

4.3 Future prospects

In acknowledging the limitations inherent in our WBE study, we propose recommendations to elevate the quality and scope of future research in this scientific field. We advocate for:

- Promotion of national networks for collaborative data collection and analysis.
- Promotion of adoption of common protocols across research initiatives.
- Facilitation of interdisciplinary collaboration, recognizing the expertise of diverse scientific fields.
- Comprehensive surveillance incorporating elements of the so called exposome[11], such as the assessment of heavy metals on biofilms, microplastics, pharmaceuticals, persistent organic pollutants (POPs), antimicrobial resistance genes (ARGs), and organisms of emerging concern.

[11] The exposome is a concept used to describe environmental exposures that an individual encounters throughout life, and how these exposures impact biology and health. It encompasses both external and internal factors, including chemical, physical, biological, and social factors that may influence human health., *Wikipedia*, 9 January 2024, https://en.wikipedia.org/wiki/Exposome .

CHAPTER 5 – REFERENCES

Adriaenssens, E. M., Farkas, K., Harrison, C., Jones, D. L., Allison, H. E., & McCarthy, A. J. (2018). Viromic Analysis of Wastewater Input to a River Catchment Reveals a Diverse Assemblage of RNA Viruses. *mSystems*, *3*(3), e00025-18. https://doi.org/10.1128/mSystems.00025-18

Ai, Y., Davis, A., Jones, D., Lemeshow, S., Tu, H., He, F., Ru, P., Pan, X., Bohrerova, Z., & Lee, J. (2021). Wastewater SARS-CoV-2 monitoring as a community-level COVID-19 trend tracker and variants in Ohio, United States. *Science of The Total Environment*, *801*, 149757. https://doi.org/10.1016/j.scitotenv.2021.149757

Akash, M. S. H., & Rehman, K. (2020). Ultraviolet-Visible (UV-VIS) Spectroscopy. In M. S. H. Akash & K. Rehman, *Essentials of Pharmaceutical Analysis* (pp. 29–56). Springer Nature Singapore. https://doi.org/10.1007/978-981-15-1547-7_3

Alam, K. S., Fatema-Tuj-Johora, Mst., & Khan, G. M. A. (2021). Fundamental aspects and developments in cellulose-based membrane technologies for virus retention: A review. *Journal of Environmental Chemical Engineering*, *9*(6), 106401. https://doi.org/10.1016/j.jece.2021.106401

Alexander, M. R., Rootes, C. L., van Vuren, P. J., & Stewart, C. R. (2020). Concentration of infectious SARS-CoV-2 by polyethylene glycol precipitation. *Journal of Virological Methods*, *286*, 113977. https://doi.org/10.1016/j.jviromet.2020.113977

Amoah, I. D., Abunama, T., Awolusi, O. O., Pillay, L., Pillay, K., Kumari, S., & Bux, F. (2022). Effect of selected wastewater characteristics on estimation of SARS-CoV-2 viral load in wastewater. *Environmental Research*, *203*, 111877. https://doi.org/10.1016/j.envres.2021.111877

Anderson-Coughlin, B. L., Shearer, A. E. H., Omar, A. N., Wommack, K. E., & Kniel, K. E. (2021). Recovery of SARS-CoV-2 from Wastewater Using Centrifugal Ultrafiltration. *Methods and Protocols*, *4*(2), 32. https://doi.org/10.3390/mps4020032

Arts, P. J., Kelly, J. D., Midgley, C. M., Anglin, K., Lu, S., Abedi, G. R., Andino, R., Bakker, K. M., Banman, B., Boehm, A. B., Briggs-Hagen, M., Brouwer, A. F., Davidson, M. C., Eisenberg, M. C., Garcia-Knight, M., Knight, S., Peluso, M. J., Pineda-Ramirez, J., Diaz Sanchez, R., … Wigginton, K. R. (2023). Longitudinal and quantitative fecal shedding dynamics of SARS-CoV-2, pepper mild mottle virus, and crAssphage. *mSphere*, *8*(4), e00132-23. https://doi.org/10.1128/msphere.00132-23

Asper, M., Hanrieder, T., Quellmalz, A., & Mihranyan, A. (2015). Removal of xenotropic murine leukemia virus by nanocellulose based filter paper. *Biologicals*, *43*(6), 452–456. https://doi.org/10.1016/j.biologicals.2015.08.001

Auffret, M. D., Brassard, J., Jones, T. H., Gagnon, N., Gagné, M.-J., Muehlhauser, V., Masse, L., Topp, E., & Talbot, G. (2019). Impact of seasonal temperature transition, alkalinity and other abiotic factors on the persistence of viruses in swine and dairy manures. *Science of The Total Environment*, *659*, 640–648. https://doi.org/10.1016/j.scitotenv.2018.12.306

Bachmann, L. M., & Miller, W. G. (2020). Spectrophotometry. In *Contemporary Practice in Clinical Chemistry* (pp. 119–133). Elsevier. https://doi.org/10.1016/B978-0-12-815499-1.00007-7

Bardi, M. J., & Oliaee, M. A. (2021). Impacts of different operational temperatures and organic loads in anaerobic co-digestion of food waste and sewage sludge on the fate of SARS-CoV-2. *Process Safety and Environmental Protection*, *146*, 464–472. https://doi.org/10.1016/j.psep.2020.11.035

Been, F., Rossi, L., Ort, C., Rudaz, S., Delémont, O., & Esseiva, P. (2014). Population Normalization with Ammonium in Wastewater-Based Epidemiology: Application to Illicit Drug Monitoring. *Environmental Science & Technology*, *48*(14), 8162–8169. https://doi.org/10.1021/es5008388

Bendicho, C., & Lavilla, I. (2017). Sewage ☆. In *Reference Module in Chemistry, Molecular Sciences and Chemical Engineering* (p. B9780124095472115197). Elsevier. https://doi.org/10.1016/B978-0-12-409547-2.11519-7

Bertels, X., Demeyer, P., Van den Bogaert, S., Boogaerts, T., van Nuijs, A. L. N., Delputte, P., & Lahousse, L. (2022). Factors influencing SARS-CoV-2 RNA concentrations in wastewater up to the sampling stage: A systematic review. *Science of The Total Environment*, *820*, 153290. https://doi.org/10.1016/j.scitotenv.2022.153290

Bivins, A., & Bibby, K. (2021). Wastewater Surveillance during Mass COVID-19 Vaccination on a College Campus. *Environmental Science & Technology Letters*, *8*(9), 792–798. https://doi.org/10.1021/acs.estlett.1c00519

Boutin, C., & Kodjabachian, L. (2019). Biology of multiciliated cells. *Current Opinion in Genetics & Development*, *56*, 1–7. https://doi.org/10.1016/j.gde.2019.04.006

Brawerman, G., Mendecki, J., & Lee, S. Y. (1972). Isolation of mammalian messenger ribonucleic acid. *Biochemistry*, *11*(4), 637–641. https://doi.org/10.1021/bi00754a027

Burnouf-Radosevich, M., Appourchaux, P., Huart, J. J., & Burnouf, T. (1994). Nanofiltration, a New Specific Virus Elimination Method Applied to High-Purity Factor IX and Factor XI Concentrates. *Vox Sanguinis*, *67*(2), 132–138. https://doi.org/10.1111/j.1423-0410.1994.tb01647.x

Bustin, S. (2000). Absolute quantification of mRNA using real-time reverse transcription polymerase chain reaction assays. *Journal of Molecular Endocrinology*, *25*(2), 169–193. https://doi.org/10.1677/jme.0.0250169

Bustin, S. A., & Mueller, R. (2005). Real-time reverse transcription PCR (qRT-PCR) and its potential use in clinical diagnosis. *Clinical Science*, *109*(4), 365–379. https://doi.org/10.1042/CS20050086

Cai, W. M., Chionh, Y. H., Hia, F., Gu, C., Kellner, S., McBee, M. E., Ng, C. S., Pang, Y. L. J., Prestwich, E. G., Lim, K. S., Ramesh Babu, I., Begley, T. J., & Dedon, P. C. (2015). A Platform for Discovery and Quantification of Modified Ribonucleosides in RNA. In *Methods in Enzymology* (Vol. 560, pp. 29–71). Elsevier. https://doi.org/10.1016/bs.mie.2015.03.004

Cao, Y., & Francis, R. (2021). On forecasting the community-level COVID-19 cases from the concentration of SARS-CoV-2 in wastewater. *Science of The Total Environment*, *786*, 147451. https://doi.org/10.1016/j.scitotenv.2021.147451

Cevik, M., Tate, M., Lloyd, O., Maraolo, A. E., Schafers, J., & Ho, A. (2021). SARS-CoV-2, SARS-CoV, and MERS-CoV viral load dynamics, duration of viral shedding, and infectiousness: A systematic review and meta-analysis. *The Lancet Microbe*, *2*(1), e13–e22. https://doi.org/10.1016/S2666-5247(20)30172-5

de Graaf, M., Langeveld, J., Post, J., Carrizosa, C., Franz, E., Izquierdo-Lara, R. W., Elsinga, G., Heijnen, L., Been, F., van Beek, J., Schilperoort, R., Vriend, R., Fanoy, E., de Schepper, E. I. T., Koopmans, M. P. G., & Medema, G. (2023). Capturing the SARS-CoV-2 infection pyramid within the municipality of Rotterdam using longitudinal sewage surveillance. *Science of The Total Environment*, *883*, 163599. https://doi.org/10.1016/j.scitotenv.2023.163599

Forés, E., Bofill-Mas, S., Itarte, M., Martínez-Puchol, S., Hundesa, A., Calvo, M., Borrego, C. M., Corominas, L. L., Girones, R., & Rusiñol, M. (2021). Evaluation of two rapid ultrafiltration-based methods for SARS-CoV-2 concentration from wastewater. *Science of The Total Environment*, *768*, 144786. https://doi.org/10.1016/j.scitotenv.2020.144786

Gundy, P. M., Gerba, C. P., & Pepper, I. L. (2009). Survival of Coronaviruses in Water and Wastewater. *Food and Environmental Virology*, *1*(1), 10. https://doi.org/10.1007/s12560-008-9001-6

Gyllensten, U. B., & Erlich, H. A. (1988). Generation of single-stranded DNA by the polymerase chain reaction and its application to direct sequencing of the HLA-DQA locus. *Proceedings of the National Academy of Sciences*, *85*(20), 7652–7656. https://doi.org/10.1073/pnas.85.20.7652

Hemalatha, M., Kiran, U., Kuncha, S. K., Kopperi, H., Gokulan, C. G., Mohan, S. V., & Mishra, R. K. (2021). Surveillance of SARS-CoV-2 spread using wastewater-based epidemiology: Comprehensive study. *Science of The Total Environment*, *768*, 144704. https://doi.org/10.1016/j.scitotenv.2020.144704

Hill, D. T., Alazawi, M. A., Moran, E. J., Bennett, L. J., Bradley, I., Collins, M. B., Gobler, C. J., Green, H., Insaf, T. Z., Kmush, B., Neigel, D., Raymond, S., Wang, M., Ye, Y., & Larsen, D. A. (2023). Wastewater surveillance provides 10-days forecasting of COVID-19 hospitalizations superior to cases and test positivity: A prediction study. *Infectious Disease Modelling*, *8*(4), 1138–1150. https://doi.org/10.1016/j.idm.2023.10.004

Hillary, L. S., Farkas, K., Maher, K. H., Lucaci, A., Thorpe, J., Distaso, M. A., Gaze, W. H., Paterson, S., Burke, T., Connor, T. R., McDonald, J. E., Malham, S. K., & Jones, D. L. (2021). Monitoring SARS-CoV-2 in municipal wastewater to evaluate the success of lockdown

measures for controlling COVID-19 in the UK. *Water Research*, *200*, 117214. https://doi.org/10.1016/j.watres.2021.117214

Joiner, C. L., Oidtmann, B. C., Rimmer, G. S. E., McPherson, N. J., Dixon, P. F., & Paley, R. K. (2021). Survival of viral haemorrhagic septicaemia virus and infectious haematopoietic necrosis virus in the environment and dried on stainless steel. *Transboundary and Emerging Diseases*, *68*(4), 2295–2307. https://doi.org/10.1111/tbed.13888

Kitajima, M., Sassi, H. P., & Torrey, J. R. (2018). Pepper mild mottle virus as a water quality indicator. *Npj Clean Water*, *1*(1), 19. https://doi.org/10.1038/s41545-018-0019-5

Koonin, E. V., & Yutin, N. (2020). The crAss-like Phage Group: How Metagenomics Reshaped the Human Virome. *Trends in Microbiology*, *28*(5), 349–359. https://doi.org/10.1016/j.tim.2020.01.010

Koureas, M., Amoutzias, G. D., Vontas, A., Kyritsi, M., Pinaka, O., Papakonstantinou, A., Dadouli, K., Hatzinikou, M., Koutsolioutsou, A., Mouchtouri, V. A., Speletas, M., Tsiodras, S., & Hadjichristodoulou, C. (2021). Wastewater monitoring as a supplementary surveillance tool for capturing SARS-COV-2 community spread. A case study in two Greek municipalities. *Environmental Research*, *200*, 111749. https://doi.org/10.1016/j.envres.2021.111749

Lai, M., Cao, Y., Wulff, S. S., Robinson, T. J., McGuire, A., & Bisha, B. (2023). A time series based machine learning strategy for wastewater-based forecasting and nowcasting of COVID-19 dynamics. *Science of The Total Environment*, *897*, 165105. https://doi.org/10.1016/j.scitotenv.2023.165105

Langeveld, J., Schilperoort, R., Heijnen, L., Elsinga, G., Schapendonk, C. E. M., Fanoy, E., De Schepper, E. I. T., Koopmans, M. P. G., De Graaf, M., & Medema, G. (2023). Normalisation of SARS-CoV-2 concentrations in wastewater: The use of flow, electrical conductivity and

crAssphage. *Science of The Total Environment*, *865*, 161196. https://doi.org/10.1016/j.scitotenv.2022.161196

Li, D., & Liu, S. (2019). Detection of River Water Quality. In *Water Quality Monitoring and Management* (pp. 211–220). Elsevier. https://doi.org/10.1016/B978-0-12-811330-1.00007-7

Li, X., Kulandaivelu, J., Guo, Y., Zhang, S., Shi, J., O'Brien, J., Arora, S., Kumar, M., Sherchan, S. P., Honda, R., Jackson, G., Luby, S. P., & Jiang, G. (2022). SARS-CoV-2 shedding sources in wastewater and implications for wastewater-based epidemiology. *Journal of Hazardous Materials*, *432*, 128667. https://doi.org/10.1016/j.jhazmat.2022.128667

Li, X., Zhang, S., Sherchan, S., Orive, G., Lertxundi, U., Haramoto, E., Honda, R., Kumar, M., Arora, S., Kitajima, M., & Jiang, G. (2023). Correlation between SARS-CoV-2 RNA concentration in wastewater and COVID-19 cases in community: A systematic review and meta-analysis. *Journal of Hazardous Materials*, *441*, 129848. https://doi.org/10.1016/j.jhazmat.2022.129848

Lipps, W. C., Braun-Howland, E. B., & Baxter, T. E. (Eds.). (2023). *Standard methods for the examination of water and wastewater* (24th edition). American Public Health Association.

Livak, K. J., & Schmittgen, T. D. (2001). Analysis of Relative Gene Expression Data Using Real-Time Quantitative PCR and the 2−ΔΔCT Method. *Methods*, *25*(4), 402–408. https://doi.org/10.1006/meth.2001.1262

López-Peñalver, R. S., Cañas-Cañas, R., Casaña-Mohedo, J., Benavent-Cervera, J. V., Fernández-Garrido, J., Juárez-Vela, R., Pellín-Carcelén, A., Gea-Caballero, V., & Andreu-Fernández, V. (2023). Predictive potential of SARS-CoV-2 RNA concentration in wastewater to assess the dynamics of COVID-19 clinical outcomes and infections. *Science of The Total Environment*, *886*, 163935. https://doi.org/10.1016/j.scitotenv.2023.163935

Maal-Bared, R., Qiu, Y., Li, Q., Gao, T., Hrudey, S. E., Bhavanam, S., Ruecker, N. J., Ellehoj, E., Lee, B. E., & Pang, X. (2023). Does normalization of SARS-CoV-2 concentrations by Pepper Mild Mottle Virus improve correlations and lead time between wastewater surveillance and clinical data in Alberta (Canada): Comparing twelve SARS-CoV-2 normalization approaches. *Science of The Total Environment*, *856*, 158964. https://doi.org/10.1016/j.scitotenv.2022.158964

Mackay, I. M. (2002). Real-time PCR in virology. *Nucleic Acids Research*, *30*(6), 1292–1305. https://doi.org/10.1093/nar/30.6.1292

Martin, J., Klapsa, D., Wilton, T., Zambon, M., Bentley, E., Bujaki, E., Fritzsche, M., Mate, R., & Majumdar, M. (2020). Tracking SARS-CoV-2 in Sewage: Evidence of Changes in Virus Variant Predominance during COVID-19 Pandemic. *Viruses*, *12*(10), 1144. https://doi.org/10.3390/v12101144

McCall, C., Wu, H., Miyani, B., & Xagoraraki, I. (2020). Identification of multiple potential viral diseases in a large urban center using wastewater surveillance. *Water Research*, *184*, 116160. https://doi.org/10.1016/j.watres.2020.116160

Medema, G., Heijnen, L., Elsinga, G., Italiaander, R., & Brouwer, A. (2020). *Presence of SARS-Coronavirus-2 in sewage* [Preprint]. Occupational and Environmental Health. https://doi.org/10.1101/2020.03.29.20045880

Morvan, M., Jacomo, A. L., Souque, C., Wade, M. J., Hoffmann, T., Pouwels, K., Lilley, C., Singer, A. C., Porter, J., Evens, N. P., Walker, D. I., Bunce, J. T., Engeli, A., Grimsley, J., O'Reilly, K. M., & Danon, L. (2022). An analysis of 45 large-scale wastewater sites in England to estimate SARS-CoV-2 community prevalence. *Nature Communications*, *13*(1), 4313. https://doi.org/10.1038/s41467-022-31753-y

Navarro, E., Serrano-Heras, G., Castaño, M. J., & Solera, J. (2015). Real-time PCR detection chemistry. *Clinica Chimica Acta*, *439*, 231–250. https://doi.org/10.1016/j.cca.2014.10.017

Nguyen Quoc, B., Saingam, P., RedCorn, R., Carter, J. A., Jain, T., Candry, P., Gattuso, M., Huang, M.-L. W., Greninger, A. L., Meschke, J. S., Bryan, A., & Winkler, M. K. H. (2022). Case Study: Impact of Diurnal Variations and Stormwater Dilution on SARS-CoV-2 RNA Signal Intensity at Neighborhood Scale Wastewater Pumping Stations. *ACS ES&T Water*, *2*(11), 1964–1975. https://doi.org/10.1021/acsestwater.2c00016

Ortiz-Prado, E., Simbaña-Rivera, K., Gómez- Barreno, L., Rubio-Neira, M., Guaman, L. P., Kyriakidis, N. C., Muslin, C., Jaramillo, A. M. G., Barba-Ostria, C., Cevallos-Robalino, D., Sanches-SanMiguel, H., Unigarro, L., Zalakeviciute, R., Gadian, N., & López-Cortés, A. (2020). Clinical, molecular, and epidemiological characterization of the SARS-CoV-2 virus and the Coronavirus Disease 2019 (COVID-19), a comprehensive literature review. *Diagnostic Microbiology and Infectious Disease*, *98*(1), 115094. https://doi.org/10.1016/j.diagmicrobio.2020.115094

Park, S., Lee, C.-W., Park, D.-I., Woo, H.-Y., Cheong, H. S., Shin, H. C., Ahn, K., Kwon, M.-J., & Joo, E.-J. (2021). Detection of SARS-CoV-2 in Fecal Samples From Patients With Asymptomatic and Mild COVID-19 in Korea. *Clinical Gastroenterology and Hepatology*, *19*(7), 1387-1394.e2. https://doi.org/10.1016/j.cgh.2020.06.005

Perry, R. P., La Torre, J., Kelley, D. E., & Greenberg, J. R. (1972). On the lability of poly(A) sequences during extraction of messenger RNA from polyribosomes. *Biochimica et Biophysica Acta (BBA) - Nucleic Acids and Protein Synthesis*, *262*(2), 220–226. https://doi.org/10.1016/0005-2787(72)90236-5

Petala, M., Dafou, D., Kostoglou, M., Karapantsios, Th., Kanata, E., Chatziefstathiou, A., Sakaveli, F., Kotoulas, K., Arsenakis, M., Roilides, E., Sklaviadis, T., Metallidis, S., Papa, A.,

Stylianidis, E., Papadopoulos, A., & Papaioannou, N. (2021). A physicochemical model for rationalizing SARS-CoV-2 concentration in sewage. Case study: The city of Thessaloniki in Greece. *Science of The Total Environment*, *755*, 142855. https://doi.org/10.1016/j.scitotenv.2020.142855

Prasek, S. M., Pepper, I. L., Innes, G. K., Slinski, S., Betancourt, W. Q., Foster, A. R., Yaglom, H. D., Porter, W. T., Engelthaler, D. M., & Schmitz, B. W. (2023). Variant-specific SARS-CoV-2 shedding rates in wastewater. *Science of The Total Environment*, *857*, 159165. https://doi.org/10.1016/j.scitotenv.2022.159165

Puelles, V. G., Lütgehetmann, M., Lindenmeyer, M. T., Sperhake, J. P., Wong, M. N., Allweiss, L., Chilla, S., Heinemann, A., Wanner, N., Liu, S., Braun, F., Lu, S., Pfefferle, S., Schröder, A. S., Edler, C., Gross, O., Glatzel, M., Wichmann, D., Wiech, T., … Huber, T. B. (2020). Multiorgan and Renal Tropism of SARS-CoV-2. *New England Journal of Medicine*, *383*(6), 590–592. https://doi.org/10.1056/NEJMc2011400

Puhach, O., Meyer, B., & Eckerle, I. (2022). SARS-CoV-2 viral load and shedding kinetics. *Nature Reviews Microbiology*. https://doi.org/10.1038/s41579-022-00822-w

Rainey, A. L., Liang, S., Bisesi, J. H., Sabo-Attwood, T., & Maurelli, A. T. (2023). A multistate assessment of population normalization factors for wastewater-based epidemiology of COVID-19. *PLOS ONE*, *18*(4), e0284370. https://doi.org/10.1371/journal.pone.0284370

Rusiñol, M., Martínez-Puchol, S., Forés, E., Itarte, M., Girones, R., & Bofill-Mas, S. (2020). Concentration methods for the quantification of coronavirus and other potentially pandemic enveloped virus from wastewater. *Current Opinion in Environmental Science & Health*, *17*, 21–28. https://doi.org/10.1016/j.coesh.2020.08.002

Sabar, M. A., Honda, R., & Haramoto, E. (2022). CrAssphage as an indicator of human-fecal contamination in water environment and virus reduction in wastewater treatment. *Water Research*, *221*, 118827. https://doi.org/10.1016/j.watres.2022.118827

Saingam, P., Li, B., Nguyen Quoc, B., Jain, T., Bryan, A., & Winkler, M. K. H. (2023). Wastewater surveillance of SARS-CoV-2 at intra-city level demonstrated high resolution in tracking COVID-19 and calibration using chemical indicators. *Science of The Total Environment*, *866*, 161467. https://doi.org/10.1016/j.scitotenv.2023.161467

Sapula, S. A., Whittall, J. J., Pandopulos, A. J., Gerber, C., & Venter, H. (2021). An optimized and robust PEG precipitation method for detection of SARS-CoV-2 in wastewater. *Science of The Total Environment*, *785*, 147270. https://doi.org/10.1016/j.scitotenv.2021.147270

Schrader, C., Schielke, A., Ellerbroek, L., & Johne, R. (2012). PCR inhibitors—Occurrence, properties and removal. *Journal of Applied Microbiology*, *113*(5), 1014–1026. https://doi.org/10.1111/j.1365-2672.2012.05384.x

Shi, X., Chen, C.-H., Gao, W., Chao, S., & Meldrum, D. R. (2015). Parallel RNA extraction using magnetic beads and a droplet array. *Lab on a Chip*, *15*(4), 1059–1065. https://doi.org/10.1039/C4LC01111B

Valasek, M. A., & Repa, J. J. (2005). The power of real-time PCR. *Advances in Physiology Education*, *29*(3), 151–159. https://doi.org/10.1152/advan.00019.2005

Vaughan, L., Zhang, M., Gu, H., Rose, J. B., Naughton, C. C., Medema, G., Allan, V., Roiko, A., Blackall, L., & Zamyadi, A. (2023). An exploration of challenges associated with machine learning for time series forecasting of COVID-19 community spread using wastewater-based epidemiological data. *Science of The Total Environment*, *858*, 159748. https://doi.org/10.1016/j.scitotenv.2022.159748

Wilde, H., Perry, W. B., Jones, O., Kille, P., Weightman, A., Jones, D. L., Cross, G., & Durance, I. (2022). Accounting for Dilution of SARS-CoV-2 in Wastewater Samples Using Physico-Chemical Markers. *Water*, *14*(18), 2885. https://doi.org/10.3390/w14182885

Wong, K., Voice, T. C., & Xagoraraki, I. (2013). Effect of organic carbon on sorption of human adenovirus to soil particles and laboratory containers. *Water Research*, *47*(10), 3339–3346. https://doi.org/10.1016/j.watres.2013.03.029

Yaniv, K., Ozer, E., Lewis, Y., & Kushmaro, A. (2021). RT-qPCR assays for SARS-CoV-2 variants of concern in wastewater reveals compromised vaccination-induced immunity. *Water Research*, *207*, 117808. https://doi.org/10.1016/j.watres.2021.117808

Zhang, D., Ling, H., Huang, X., Li, J., Li, W., Yi, C., Zhang, T., Jiang, Y., He, Y., Deng, S., Zhang, X., Wang, X., Liu, Y., Li, G., & Qu, J. (2020). Potential spreading risks and disinfection challenges of medical wastewater by the presence of Severe Acute Respiratory Syndrome Coronavirus 2 (SARS-CoV-2) viral RNA in septic tanks of Fangcang Hospital. *Science of The Total Environment*, *741*, 140445. https://doi.org/10.1016/j.scitotenv.2020.140445

Zhang, T., Breitbart, M., Lee, W. H., Run, J.-Q., Wei, C. L., Soh, S. W. L., Hibberd, M. L., Liu, E. T., Rohwer, F., & Ruan, Y. (2005). RNA Viral Community in Human Feces: Prevalence of Plant Pathogenic Viruses. *PLoS Biology*, *4*(1), e3. https://doi.org/10.1371/journal.pbio.0040003

Zheng, X., Deng, Y., Xu, X., Li, S., Zhang, Y., Ding, J., On, H. Y., Lai, J. C. C., In Yau, C., Chin, A. W. H., Poon, L. L. M., Tun, H. M., & Zhang, T. (2022). Comparison of virus concentration methods and RNA extraction methods for SARS-CoV-2 wastewater surveillance. *Science of The Total Environment*, *824*, 153687. https://doi.org/10.1016/j.scitotenv.2022.153687

Zhuang, J., & Jin, Y. (2003). Virus Retention and Transport as Influenced by Different Forms of Soil Organic Matter. *Journal of Environmental Quality*, *32*(3), 816–823. https://doi.org/10.2134/jeq2003.8160

CHAPTER 6 – APPENDICES

6.1 Calibration curves and data for Ammonium test kit (Merck Millipore)

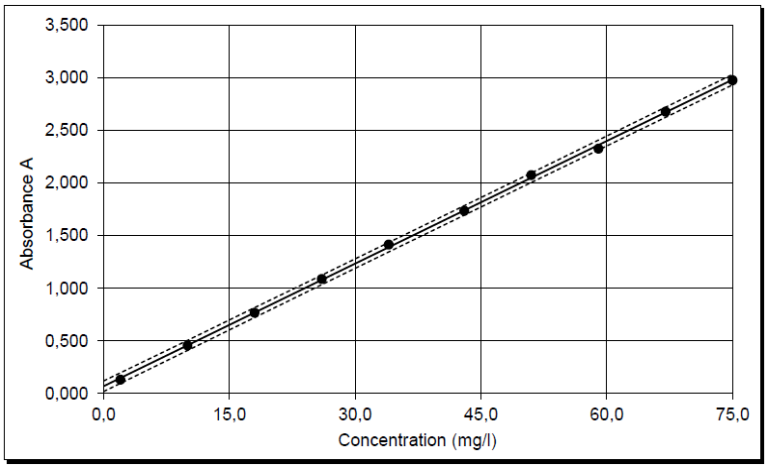

n = 10	
Conc. / Konz. (Standard / Patrón) mg/l NH_4-N	Absorbance Extinktion Extinción
2,0	0,131
10,0	0,456
18,0	0,767
26,0	1,088
34,0	1,414
43,0	1,736
51,0	2,075
59,0	2,327
67,0	2,678
75,0	2,976

Calibration Function / Kalibrierfunktion / Función de calibración ISO 8466-1 / DIN 38402 A51	Target value Sollwert Valor nominal	Lot value Chargenwert Valor del lote	
Slope / Steigung / Pendiente Tolerance +/- / Tolerancia	0,0384 ± 0,0012	0,0388	✓
Ordinate segment / Ordinatenabschnitt / Intersecto en ordenadas		0,069	
Reagent blank / Reag.blindwert / Valor en blanco del react Tolerance +/- / Tolerancia	0,060 ± 0,020 A	0,055 A	✓
Confidential interval (P=95%) Vertrauensbereich (95% Wahrscheinlichkeit) / Intervalo de confianza (95 % de probabilidad)	± 2,0 mg/l	± 1,2 mg/l	✓
Standard Deviation of the Method Verfahrensstandardabweichung / Desviación estándar del procedimiento		± 0,48 mg/l	✓
Variation Coefficient of the Method Verfahrensvariationskoeffizient / Coeficiente de variación del procedimiento	± 2,5 %	± 1,2%	✓

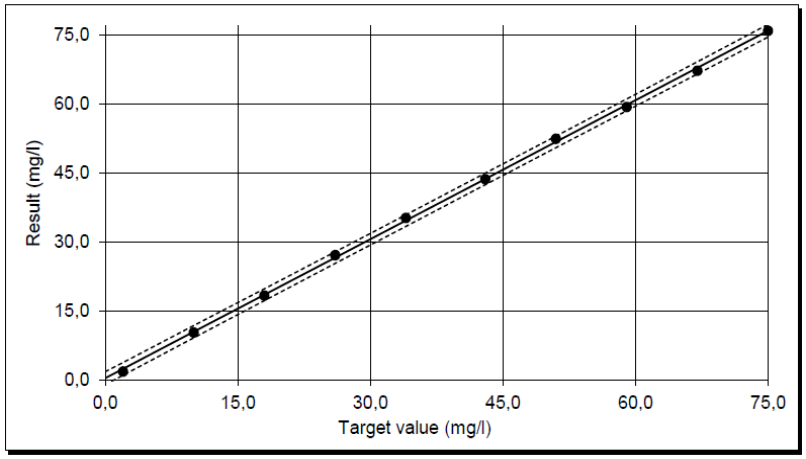

n = 10	
Target value Sollwert Valor nominal (Standard / Patrón) mg/l NH_4-N	Result Messergebnis / Resultado (Standard / Patrón) mg/l NH_4-N
2,0	1,9
10,0	10,4
18,0	18,4
26,0	27,2
34,0	35,3
43,0	43,7
51,0	52,5
59,0	59,4
67,0	67,3
75,0	76,0

Calibration Function / Kalibrierfunktion / Función de calibración ISO 8466-1 / DIN 38402 A51	Target value Sollwert Valor nominal	Lot value Chargenwert Valor del lote	
Slope / Steigung / Pendiente Tolerance +/- / Tolerancia	1,00 ± 0,03	1,01	✓
Ordinate segment / Ordinatenabschnitt / Intersecto en ordenadas		0,4	
Reagent blank / Reag.blindwert / Valor en blanco del react Tolerance +/- / Tolerancia	0,060 ± 0,020 A	0,055 A	✓
Confidential interval (P=95%) Vertrauensbereich (95% Wahrscheinlichkeit) / Intervalo de confianza (95 % de probabilidad)	± 2,0 mg/l	± 1,2 mg/l	✓
Standard Deviation of the Method Verfahrensstandardabweichung / Desviación estándar del procedimiento		± 0,51 mg/l	✓
Variation Coefficient of the Method Verfahrensvariationskoeffizient / Coeficiente de variación del procedimiento	± 2,5 %	± 1,3%	✓

6.2 Calibration curves and data for Chloride test kit (Merck Millipore)

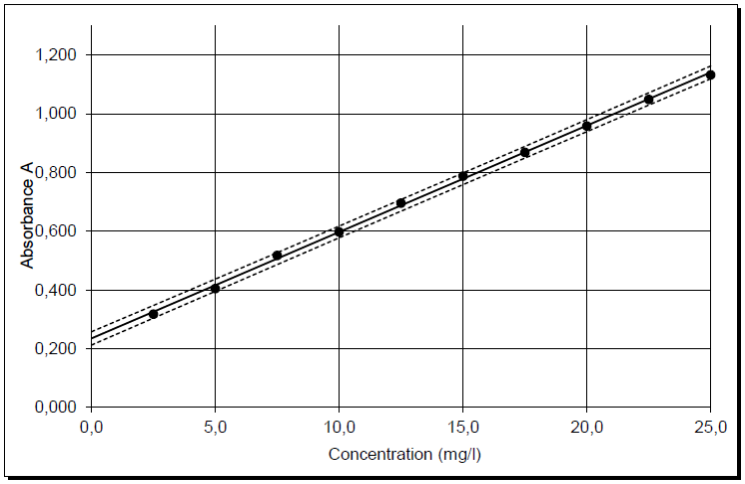

n = 10	
Conc. / Konz. (Standard / Patrón) mg/l Cl^-	Absorbance Extinktion Extinción
2,5	0,318
5,0	0,405
7,5	0,518
10,0	0,598
12,5	0,696
15,0	0,788
17,5	0,869
20,0	0,959
22,5	1,049
25,0	1,133

Calibration Function / Kalibrierfunktion / Función de calibración ISO 8466-1 / DIN 38402 A51	Target value Sollwert Valor nominal	Lot value Chargenwert Valor del lote	
Slope / Steigung / Pendiente Tolerance +/- / Tolerancia	0,0355 ± 0,0011	0,03625	✓
Ordinate segment / Ordinatenabschnitt / Intersecto en ordenadas		0,235	
Reagent blank / Reag.blindwert / Valor en blanco del react Tolerance +/- / Tolerancia	0,225 ± 0,020 A	0,239 A	✓
Confidential interval (P=95%) Vertrauensbereich (95% Wahrscheinlichkeit) / Intervalo de confianza (95 % de probabilidad)	± 0,7 mg/l	± 0,5 mg/l	✓
Standard Deviation of the Method Verfahrensstandardabweichung / Desviación estándar del procedimiento		± 0,22 mg/l	✓
Variation Coefficient of the Method Verfahrensvariationskoeffizient / Coeficiente de variación del procedimiento	± 2,5 %	± 1,6%	✓

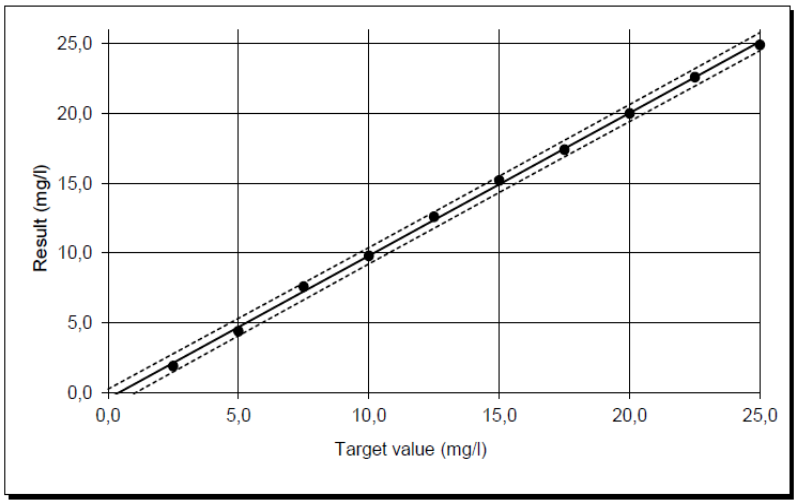

n = 10	
Target value Sollwert Valor nominal (Standard / Patrón) mg/l Cl^-	Result Messergebnis / Resultado (Standard / Patrón) mg/l Cl^-
2,5	1,9
5,0	4,4
7,5	7,6
10,0	9,8
12,5	12,6
15,0	15,2
17,5	17,4
20,0	20,0
22,5	22,6
25,0	24,9

Calibration Function / Kalibrierfunktion / Función de calibración ISO 8466-1 / DIN 38402 A51	Target value Sollwert Valor nominal	Lot value Chargenwert Valor del lote	
Slope / Steigung / Pendiente Tolerance +/- / Tolerancia	1,00 ± 0,03	1,02	✓
Ordinate segment / Ordinatenabschnitt / Intersecto en ordenadas		-0,4	
Reagent blank / Reag.blindwert / Valor en blanco del react Tolerance +/- / Tolerancia	0,225 ± 0,020 A	0,239 A	✓
Confidential interval (P=95%) Vertrauensbereich (95% Wahrscheinlichkeit) / Intervalo de confianza (95 % de probabilidad)	± 0,7 mg/l	± 0,6 mg/l	✓
Standard Deviation of the Method Verfahrensstandardabweichung / Desviación estándar del procedimiento		± 0,24 mg/l	✓
Variation Coefficient of the Method Verfahrensvariationskoeffizient / Coeficiente de variación del procedimiento	± 2,5 %	± 1,7%	✓

6.3 Calibration curves and data for Phosphate test kit (Merck Millipore)

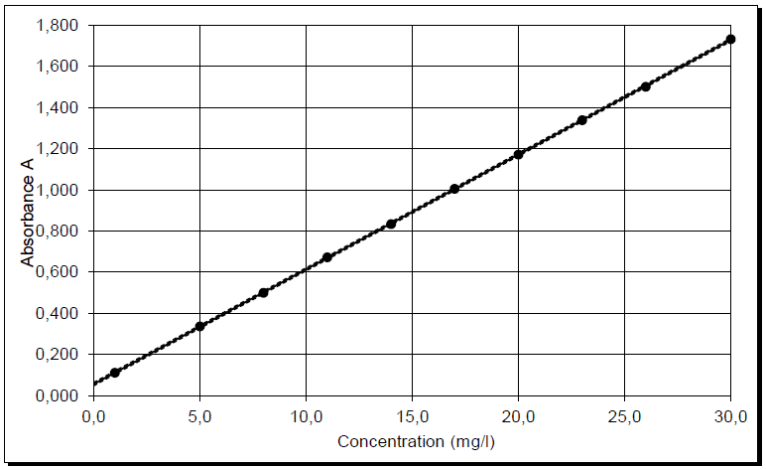

n = 10	
Conc. / Konz. (Standard / Patrón) mg/l PO_4-P	Absorbance Extinktion Extinción
1,0	0,111
5,0	0,336
8,0	0,500
11,0	0,672
14,0	0,834
17,0	1,005
20,0	1,172
23,0	1,339
26,0	1,501
30,0	1,733

Calibration Function / Kalibrierfunktion / Función de calibración ISO 8466-1 / DIN 38402 A51		Target value Sollwert Valor nominal	Lot value Chargenwert Valor del lote	
Slope / Steigung / Pendiente	Tolerance +/- / Tolerancia	0,0555 ± 0,0017	0,0558	✓
Ordinate segment / Ordinatenabschnitt / Intersecto en ordenadas			0,056	
Reagent blank / Reag.blindwert / Valor en blanco del react	Tolerance +/- / Tolerancia	0,060 ± 0,015 A	0,054 A	✓
Confidential interval (P=95%) Vertrauensbereich (95% Wahrscheinlichkeit) / Intervalo de confianza (95 % de probabilidad)		± 0,7 mg/l	± 0,1 mg/l	✓
Standard Deviation of the Method Verfahrensstandardabweichung / Desviación estándar del procedimiento			± 0,05 mg/l	✓
Variation Coefficient of the Method Verfahrensvariationskoeffizient / Coeficiente de variación del procedimiento		± 2,5 %	± 0,3%	✓

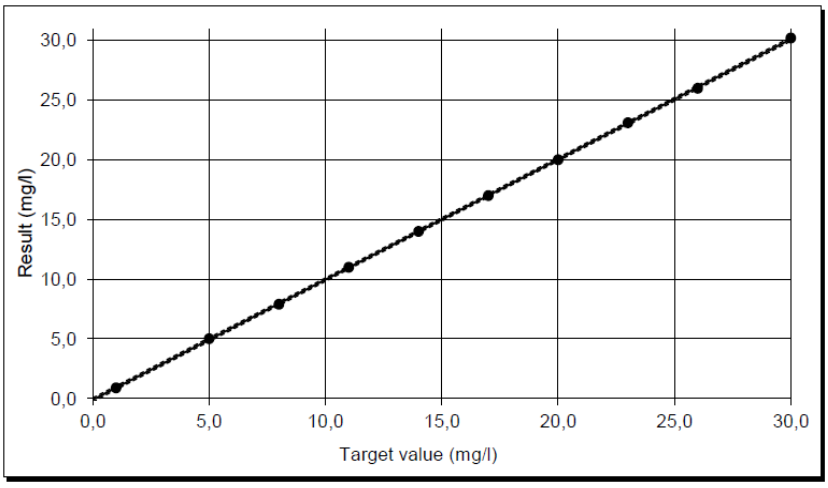

n = 10	
Target value Sollwert Valor nominal (Standard / Patrón) mg/l PO_4-P	Result Messergebnis / Resultado (Standard / Patrón) mg/l PO_4-P
1,0	0,9
5,0	5,0
8,0	7,9
11,0	11,0
14,0	14,0
17,0	17,0
20,0	20,0
23,0	23,1
26,0	26,0
30,0	30,2

Calibration Function / Kalibrierfunktion / Función de calibración ISO 8466-1 / DIN 38402 A51		Target value Sollwert Valor nominal	Lot value Chargenwert Valor del lote	
Slope / Steigung / Pendiente	Tolerance +/- / Tolerancia	1,00 ± 0,03	1,01	✓
Ordinate segment / Ordinatenabschnitt / Intersecto en ordenadas			-0,1	
Reagent blank / Reag.blindwert / Valor en blanco del react	Tolerance +/- / Tolerancia	0,060 ± 0,015 A	0,054 A	✓
Confidential interval (P=95%) Vertrauensbereich (95% Wahrscheinlichkeit) / Intervalo de confianza (95 % de probabilidad)		± 0,7 mg/l	± 0,1 mg/l	✓
Standard Deviation of the Method Verfahrensstandardabweichung / Desviación estándar del procedimiento			± 0,06 mg/l	✓
Variation Coefficient of the Method Verfahrensvariationskoeffizient / Coeficiente de variación del procedimiento		± 2,5 %	± 0,4%	✓

6.4 Indicative Sample Data for the city of Heraklion

Α/Α	ΔΕΥΑ	Ημερομηνία και περίοδος δειγματοληψίας (1)	Ημερομηνία παραλαβής	Ημερομηνία επεξεργασίας δείγματος	Εκτίμηση ικού φορτίου(RNA copies/L)	Εκτίμηση ικού φορτίου(RNA copies/L) με κανονικοποιηση αναστολεων	Παροχή εισόδου(m3/Day)	pH	Θερμμοκρασία λύματος (2) (C)	Χλωριούχα(mg/L)	Αγωγιμώτητα (ms/cm)	COD(mg/L)	BOD(mg/L)	Φόσφορος ολικός(mg/L)	Αζωτο αμμωνιακό(mg/L)	Ολικό άζωτο(mg/L)	Αιωρούμενα στερεά(mg/L)	Πληθυσμός που εξηπηρετείται (με βάση σταθερά στοιχεία ΜΕΛ)
677	ΗΡΑΚΛΕΙΟ	26/11/2021	26/11/2021	29/11/2021	198308,6538	208224,09	36000	7,85	19	180	14,28	685	333	16,4	52,5	89,2	245	200000
680	ΗΡΑΚΛΕΙΟ	30/11/2021	30/11/2021	31/11/2021	104353,5769	109571,26	35000	7,95	19	265	14,03	685	333	16,8	58	89,2	245	200000
688	ΗΡΑΚΛΕΙΟ	2/12/2021	2/12/2021	3/12/2021	289998,4615	304498,38	35500	7,88	15	190	1,25	561	333	16,4	56,4	89,2	255	200000
691	ΗΡΑΚΛΕΙΟ	3/12/2021	3/12/2021	6/12/2021	109562	115040,1	33500	7,81	14	225	1,292	561	333	14	44,1	89,2	225	200000
695	ΗΡΑΚΛΕΙΟ	7/12/2021	7/12/2021	7/12/2021	326595,8846	342925,68	37000	7,86	13	155	1,138	561	333	12,6	42,3	89,2	225	200000
700	ΗΡΑΚΛΕΙΟ	9/12/2021	9/12/2021	9/12/2021	317941,5385	333838,62	34500	7,62	14	155	1,234	522	333	11	36,6	89,2	230	200000
704	ΗΡΑΚΛΕΙΟ	10/12/2021	10/12/2021	13/12/2021	172767,6923	181406,08	36000	7,63	16	170	1,23	522	333	11,5	44,7	89,2	230	200000
707	ΗΡΑΚΛΕΙΟ	14/12/2021	14/12/2021	14/12/2021	220700	231735	35500	7,8	13	145	1,123	522	333	18,8	47,7	89,2	230	200000
714	ΗΡΑΚΛΕΙΟ	16/12/2021	16/12/2021	17/12/2021	254263,8462	266977,04	37500	7,6	12		0,89	574	333	9,5	27,9	89,2	160	200000

Δυναμικός πληθυσμός με βάση τα αμμωνιακά	Εκτίμηση ικού φορτίου (copies/100.000 πληθυσμό) κανονικοποιημένη ως προς την παροχή εισόδου και τον πληθυσμό (σταθερό πληθυσμό)	Εκτίμηση ικού φορτίου (copies/100.000 πληθυσμό) κανονικοποιημένη ως προς την παροχή εισόδου, τον πληθυσμό (σταθερό πληθυσμό) και τους αναστολείς	Εκτίμηση ικού φορτίου (copies/100.000 πληθυσμό) κανονικοποιημένη ως προς την παροχή εισόδου και τον πληθυσμό (δυναμικό πληθυσμό)	Εκτίμηση ικού φορτίου (copies/100.000 πληθυσμό) κανονικοποιημένη ως προς την παροχή εισόδου, τον πληθυσμό (δυναμικό πληθυσμό) και τους αναστολείς
270000	3,56956E+12	3,74803E+12	2,64412E+12	2,77632E+12
290000	1,82619E+12	1,9175E+12	1,25944E+12	1,32241E+12
286028,5714	5,14747E+12	5,40485E+12	3,59927E+12	3,77924E+12
211050	1,83516E+12	1,92692E+12	1,73908E+12	1,82603E+12
223585,7143	6,04202E+12	6,34413E+12	5,40466E+12	5,67489E+12
180385,7143	5,48449E+12	5,75872E+12	6,08085E+12	6,38489E+12
229885,7143	3,10982E+12	3,26531E+12	2,70553E+12	2,84081E+12
241907,1429	3,91743E+12	4,1133E+12	3,23878E+12	3,40072E+12
149464,2857	4,76745E+12	5,00582E+12	6,37938E+12	6,69835E+12

6.5 Indicative Sample Data for the city of Chania

Α/Α	ΔΕΥΑ	Ημερομηνία και περίοδος δειγματοληψίας (1)	Ημερομηνία παραλαβής	Ημερομηνία επεξεργασίας δείγματος	Εκτίμηση ιικού φορτίου(RNA copies/L)	Εκτίμηση ιικού φορτίου(RNA copies/L) με κανονικοποιηση αναστολεων	Παροχή εισόδου(m3/Day)	pH	Θερμμοκρασία λύματος (2) (C)	Χλωριούχα(mg/L)	Αγωγιμώτητα (ms/cm)	COD(mg/L)	BOD(mg/L)	Φόσφορος ολικός(mg/L)	Αζωτο αμμωνιακό(mg/L)	Αιωρούμενα στερεά(mg/L)	Πληθυσμός που εξηπηρετείται (με βάση σταθερά στοιχεία ΜΕΛ)
678	ΧΑΝΙΑ	26/11/2021	29/11/2021	29/11/2021	38588,30769	40517,723	15658	NLINE	ΚΑΤΑΓΡΑΦΗ ΣΤΟ ΣΗΜΕΙΟ ΔΕΙΓ	113	12,65	628	320	14	41,4	264	97000
681	ΧΑΝΙΑ	30/11/2021	1/12/2021	1/12/2021	98307,69231	103223,08	16114	7,63	ΚΑΤΑΓΡΑΦΗ ΣΤΟ ΣΗΜΕΙΟ ΔΕΙΓ	595	15,63	701	520	11,7	41,7	424	97000
685	ΧΑΝΙΑ	1/12/2021	2/12/2021	2/12/2021	40938,46154	42985,385	17100	7,55	ΚΑΤΑΓΡΑΦΗ ΣΤΟ ΣΗΜΕΙΟ ΔΕΙΓ	ΜΑΤΟΛΗΨ	19,72		360	10,6	39,3	392	97000
692	ΧΑΝΙΑ	3/12/2021	6/12/2021	6/12/2021	53321,15385	55987,212	15664	7,08	ΚΑΤΑΓΡΑΦΗ ΣΤΟ ΣΗΜΕΙΟ ΔΕΙΓ	125	0,736	604	420	13,4	36,6	404	97000
694	ΧΑΝΙΑ	6/12/2021	7/12/2021	7/12/2021	61999,80769	65099,798	16628	7,45	ΚΑΤΑΓΡΑΦΗ ΣΤΟ ΣΗΜΕΙΟ ΔΕΙΓ	235	1,238			11,8	37,2		97000
696	ΧΑΝΙΑ	7/12/2021	8/12/2021	8/12/2021	139602,6923	146582,83	16076	7,25	17,27 ONLINE ΚΑΤΑΓΡΑΦΗ ΣΤ(	215	1,27	708		13	38,7	356	97000
705	ΧΑΝΙΑ	10/12/2021	13/12/2021	13/12/2021	95118	99873,9	16000	7,09	16,68 ONLINE ΚΑΤΑΓΡΑΦΗ ΣΤ(	140	0,758	558		11	26,1	336	97000
708	ΧΑΝΙΑ	14/12/2021	15/12/2021	15/12/2021	165009,2308	173259,69	16600	7,22	16,35 ONLINE ΚΑΤΑΓΡΑΦΗ ΣΤΟ ΣΗΜΕΙΟ /		1,423	870	320	9	31,2	364	97000
711	ΧΑΝΙΑ	15/12/2021	16/12/2021	16/12/2021	190294,0385	199808,74	18120	7,34	16,03 ONLINE ΚΑΤΑΓΡΑΦΗ ΣΤΟ ΣΗΜΕΙΟ /		0,828	589	460	7,7	26,4	376	97000

Δυναμικός πληθυσμός με βάση τα αμμωνιακά	Εκτίμηση ιικού φορτίου (copies/100.000 πληθυσμό) κανονικοποιημένη ως προς την παροχή εισόδου και τον πληθυσμό (σταθερό πληθυσμό)	Εκτίμηση ιικού φορτίου (copies/100.000 πληθυσμό) κανονικοποιημένη ως προς την παροχή εισόδου, τον πληθυσμό (σταθερό πληθυσμό) και τους αναστολείς	Εκτίμηση ιικού φορτίου (copies/100.000 πληθυσμό) κανονικοποιημένη ως προς την παροχή εισόδου και τον πληθυσμό (δυναμικό πληθυσμό)	Εκτίμηση ιικού φορτίου (copies/100.000 πληθυσμό) κανονικοποιημένη ως προς την παροχή εισόδου, τον πληθυσμό (δυναμικό πληθυσμό) και τους αναστολείς
92605,88571	6,22903E+11	6,54048E+11	6,52459E+11	6,85082E+11
95993,4	1,63312E+12	1,71478E+12	1,65025E+12	1,73276E+12
96004,28571	7,21699E+11	7,57784E+11	7,29184E+11	7,65643E+11
81900,34286	8,61054E+11	9,04107E+11	1,0198E+12	1,07079E+12
88365,94286	1,06282E+12	1,11596E+12	1,16666E+12	1,225E+12
88877,31429	2,31366E+12	2,42935E+12	2,52511E+12	2,65137E+12
59657,14286	1,56896E+12	1,6474E+12	2,55106E+12	2,67861E+12
73988,57143	2,82387E+12	2,96506E+12	3,70213E+12	3,88724E+12
68338,28571	3,55477E+12	3,73251E+12	5,04568E+12	5,29796E+12

6.6 Restriction Measures Database

			Χανιά					Ηράκλειο				
	Από	Έως	Απαγόρευση Κυκλοφορίας	Σχολεία	Πανεπιστήμια	Λιανεμπόριο	Εστίαση/Νυχτερινή διασκέδαση	Απαγόρευση Κυκλοφορίας	Σχολεία	Πανεπιστήμια	Λιανεμπόριο	Εστίαση/Νυχτερινή διασκέδαση
ΕΠΙΤΗΡΗΣΗ: ΧΑΝΙΑ, ΡΕΘΥΜΝΟ, ΗΡΑΚΛΕΙΟ - ΑΥΞΗΜΕΝΟΥ ΚΙΝΔΥΝΟΥ: Α. ΝΙΚΟΛΑΟΣ	30/1/2021	6/2/2021	9 μμ - 5 πμ, έξοδος με Υ.Δ.	Δια ζώσης επαναλειτουργία	Αναστολή λειτουργίας	Λειτουργία	Αναστολή λειτουργίας	9 μμ - 5 πμ, έξοδος με Υ.Δ.	Δια ζώσης επαναλειτουργία	Αναστολή λειτουργίας	Λειτουργία	Αναστολή λειτουργίας
ΕΠΙΤΗΡΗΣΗ: ΧΑΝΙΑ, ΗΡΑΚΛΕΙΟ - ΑΥΞΗΜΕΝΟΥ ΚΙΝΔΥΝΟΥ: ΡΕΘΥΜΝΟ - ΠΟΛΥ ΑΥΞΗΜΕΝΟΥ ΚΙΝΔΥΝΟΥ: ΑΓΙΟΣ ΝΙΚΟΛΑΟΣ	6/2/2021	22/2/2021	9 μμ - 5 πμ, έξοδος με Υ.Δ.	Δια ζώσης	Αναστολή λειτουργίας	Λειτουργία	Αναστολή λειτουργίας	9 μμ - 5 πμ, έξοδος με Υ.Δ.	Δια ζώσης	Αναστολή λειτουργίας	Λειτουργία	Αναστολή λειτουργίας
ΕΠΙΤΗΡΗΣΗ: ΧΑΝΙΑ, ΑΓΙΟΣ ΝΙΚΟΛΑΟΣ - ΑΥΞΗΜΕΝΟΥ ΚΙΝΔΥΝΟΥ: ΡΕΘΥΜΝΟ, ΗΡΑΚΛΕΙΟ	22/2/2021	4/3/2021	9 μμ - 5 πμ, έξοδος με Υ.Δ.	Δια ζώσης	Αναστολή λειτουργίας	Λειτουργία	Αναστολή λειτουργίας	6 μμ - 5 πμ απαγόρευση κυκλοφορίας	Δημοτικά & Γυμνάσια: δια ζώσης Λύκεια: αναστολή λειτουργίας	Αναστολή λειτουργίας	Λειτουργία με click away	Αναστολή λειτουργίας
ΠΟΛΥ ΑΥΞΗΜΕΝΟΥ ΚΙΝΔΥΝΟΥ: ΗΡΑΚΛΕΙΟ - ΑΥΞΗΜΕΝΟΥ ΚΙΝΔΥΝΟΥ: ΧΑΝΙΑ, ΑΓΙΟΣ ΝΙΚΟΛΑΟΣ, ΡΕΘΥΜΝΟ	4/3/2021	16/3/2021	9 μμ - 5 πμ, έξοδος με Υ.Δ.	Δημοτικά & Γυμνάσια: δια ζώσης Λύκεια: αναστολή λειτουργίας	Αναστολή λειτουργίας	Λειτουργία με click away	Αναστολή λειτουργίας	7 μμ - 5 πμ απαγόρευση κυκλοφορίας	Αναστολή λειτουργίας	Αναστολή λειτουργίας	Αναστολή λειτουργίας	Αναστολή λειτουργίας
ΠΟΛΥ ΑΥΞΗΜΕΝΟΥ ΚΙΝΔΥΝΟΥ: ΗΡΑΚΛΕΙΟ, ΧΑΝΙΑ - ΑΥΞΗΜΕΝΟΥ ΚΙΝΔΥΝΟΥ: ΑΓΙΟΣ ΝΙΚΟΛΑΟΣ, ΡΕΘΥΜΝΟ	16/3/2021	20/3/2021	7 μμ - 5 πμ, έξοδος με Υ.Δ.	Αναστολή λειτουργίας	Αναστολή λειτουργίας	Αναστολή λειτουργίας	Αναστολή λειτουργίας	7 μμ - 5 πμ απαγόρευση κυκλοφορίας	Αναστολή λειτουργίας	Αναστολή λειτουργίας	Αναστολή λειτουργίας	Αναστολή λειτουργίας
ΠΟΛΥ ΑΥΞΗΜΕΝΟΥ ΚΙΝΔΥΝΟΥ: ΗΡΑΚΛΕΙΟ, ΧΑΝΙΑ - ΑΥΞΗΜΕΝΟΥ ΚΙΝΔΥΝΟΥ: ΑΓΙΟΣ ΝΙΚΟΛΑΟΣ, ΡΕΘΥΜΝΟ	20/3/2021	5/4/2021	9 μμ - 5 πμ, έξοδος με Υ.Δ.	Αναστολή λειτουργίας	Αναστολή λειτουργίας	Αναστολή λειτουργίας	Αναστολή λειτουργίας	9 μμ - 5 πμ, έξοδος με Υ.Δ.	Αναστολή λειτουργίας	Αναστολή λειτουργίας	Αναστολή λειτουργίας	Αναστολή λειτουργίας
ΠΟΛΥ ΑΥΞΗΜΕΝΟΥ ΚΙΝΔΥΝΟΥ: ΧΑΝΙΑ - ΑΥΞΗΜΕΝΟΥ ΚΙΝΔΥΝΟΥ: ΗΡΑΚΛΕΙΟ, ΑΓΙΟΣ ΝΙΚΟΛΑΟΣ, ΡΕΘΥΜΝΟ	5/4/2021	12/4/2021	9 μμ - 5 πμ, έξοδος με Υ.Δ.	Αναστολή λειτουργίας	Αναστολή λειτουργίας	Λειτουργία με click away	Αναστολή λειτουργίας	9 μμ - 5 πμ, έξοδος με Υ.Δ.	Αναστολή λειτουργίας	Αναστολή λειτουργίας	Λειτουργία με click away	Αναστολή λειτουργίας
ΠΟΛΥ ΑΥΞΗΜΕΝΟΥ ΚΙΝΔΥΝΟΥ: ΧΑΝΙΑ - ΑΥΞΗΜΕΝΟΥ ΚΙΝΔΥΝΟΥ: ΗΡΑΚΛΕΙΟ, ΑΓΙΟΣ ΝΙΚΟΛΑΟΣ, ΡΕΘΥΜΝΟ	12/4/2021	26/4/2021	9 μμ - 5 πμ, έξοδος με Υ.Δ.	Δημοτικά & Γυμνάσια: αναστολή λειτουργίας Λύκεια: δια ζώσης	Αναστολή λειτουργίας	Λειτουργία με click away	Αναστολή λειτουργίας	9 μμ - 5 πμ, έξοδος με Υ.Δ.	Δημοτικά & Γυμνάσια: αναστολή λειτουργίας Λύκεια: δια ζώσης	Αναστολή λειτουργίας	Λειτουργία με click away	Αναστολή λειτουργίας
ΠΟΛΥ ΑΥΞΗΜΕΝΟΥ ΚΙΝΔΥΝΟΥ: ΧΑΝΙΑ, ΡΕΘΥΜΝΟ - ΑΥΞΗΜΕΝΟΥ ΚΙΝΔΥΝΟΥ: ΗΡΑΚΛΕΙΟ, ΑΓΙΟΣ ΝΙΚΟΛΑΟΣ	26/4/2021	3/5/2021	10 μμ - 5 πμ, έξοδος με Υ.Δ.	Δημοτικά & Γυμνάσια: αναστολή λειτουργίας Λύκεια: δια ζώσης	Αναστολή λειτουργίας	Λειτουργία με click away	Αναστολή λειτουργίας	10 μμ - 5 πμ, έξοδος με Υ.Δ.	Δημοτικά & Γυμνάσια: αναστολή λειτουργίας Λύκεια: δια ζώσης	Αναστολή λειτουργίας	Λειτουργία με click away	Αναστολή λειτουργίας
ΠΟΛΥ ΑΥΞΗΜΕΝΟΥ ΚΙΝΔΥΝΟΥ: ΧΑΝΙΑ, ΡΕΘΥΜΝΟ - ΑΥΞΗΜΕΝΟΥ ΚΙΝΔΥΝΟΥ: ΗΡΑΚΛΕΙΟ, ΑΓΙΟΣ ΝΙΚΟΛΑΟΣ	3/5/2021	10/5/2021	11 μμ - 5 πμ, έξοδος με Υ.Δ.	Δημοτικά & Γυμνάσια: αναστολή λειτουργίας Λύκεια: δια ζώσης	Αναστολή λειτουργίας	Λειτουργία με click away	Εστίαση: λειτουργία καταστημάτων υγειονομικού ενδιαφέροντος με όρους: α) υπαίθρια, β) καθήμενοι, γ) χωρίς μουσική	11 μμ - 5 πμ, έξοδος με Υ.Δ.	Δημοτικά & Γυμνάσια: αναστολή λειτουργίας Λύκεια: δια ζώσης	Αναστολή λειτουργίας	Λειτουργία με click away	Εστίαση: λειτουργία καταστημάτων υγειονομικού ενδιαφέροντος με όρους: α) υπαίθρια, β) καθήμενοι, γ) χωρίς μουσική
ΠΟΛΥ ΑΥΞΗΜΕΝΟΥ ΚΙΝΔΥΝΟΥ: ΡΕΘΥΜΝΟ - ΑΥΞΗΜΕΝΟΥ ΚΙΝΔΥΝΟΥ: ΧΑΝΙΑ, ΗΡΑΚΛΕΙΟ, ΑΓΙΟΣ ΝΙΚΟΛΑΟΣ	10/5/2021	14/5/2021	11 μμ - 5 πμ, έξοδος με Υ.Δ.	Δια ζώσης λειτουργία όλων των σχολικών μονάδων	Αναστολή λειτουργίας	Λειτουργία με click away	Εστίαση: λειτουργία καταστημάτων υγειονομικού ενδιαφέροντος με όρους: α) υπαίθρια, β) καθήμενοι, γ) χωρίς μουσική	11 μμ - 5 πμ, έξοδος με Υ.Δ.	Δια ζώσης λειτουργία όλων των σχολικών μονάδων	Αναστολή λειτουργίας	Λειτουργία με click away	Εστίαση: λειτουργία καταστημάτων υγειονομικού ενδιαφέροντος με όρους: α) υπαίθρια, β) καθήμενοι, γ) χωρίς μουσική
ΟΡΙΖΟΝΤΙΑ ΜΕΤΡΑ	14/5/2021	14/6/2021	Απαγόρευση Κυκλοφορίας 00.30 - 5.00 πμ	Δια ζώσης	Αναστολή λειτουργίας - Επιλογή τρόπου εξέτασης από το εκάστοτε ΑΕΙ	Επαναλειτουργία - 1 πελάτης ανά 10 τ.μ.	Εστίαση με όρους από 5 μμ έως 00.15 πμ - Νυχτερινή διασκέδαση σε αναστολή	Απαγόρευση Κυκλοφορίας 00.30 - 5.00 πμ	Δια ζώσης	Αναστολή λειτουργίας - Επιλογή τρόπου εξέτασης από το εκάστοτε ΑΕΙ	Επαναλειτουργία - 1 πελάτης ανά 10 τ.μ.	Εστίαση με όρους από 5 μμ έως 00.15 πμ - Νυχτερινή διασκέδαση σε αναστολή
ΟΡΙΖΟΝΤΙΑ ΜΕΤΡΑ	14/6/2021	28/6/2021	Απαγόρευση Κυκλοφορίας 01.30 - 5.00 πμ	Δια ζώσης	Αναστολή λειτουργίας - Επιλογή τρόπου εξέτασης από το εκάστοτε ΑΕΙ	Επαναλειτουργία - 1 πελάτης ανά 10 τ.μ.	Εστίαση με όρους από 5 μμ έως 01.15 πμ - Νυχτερινή διασκέδαση σε αναστολή	Απαγόρευση Κυκλοφορίας 01.30 - 5.00 πμ	Δια ζώσης	Εστίαση με όρους από 5 μμ έως 01.15 πμ - Νυχτερινή διασκέδαση σε αναστολή	Επαναλειτουργία - 1 πελάτης ανά 10 τ.μ.	Εστίαση με όρους από 5 μμ έως 01.15 πμ - Νυχτερινή διασκέδαση σε αναστολή